THE PHYLOGENETICS AND EVOLUTIONARY HISTORY OF THE NORTHERN LATITUDE PLANT GENUS *THERORHODION* (MAXIM.) SMALL (ERICACEAE)

By

Margaret G. Oliver, B. S.

A Thesis Submitted in Partial Fulfillment of the Requirements

for the Degree of

Master of Science

in

Biological Sciences

University of Alaska Fairbanks

August 2017

APPROVED:

Stefanie M. Ickert-Bond, Committee Chair
Diana E. Wolf, Committee Member
Mary C. Stensvold, Committee Member
Kris Hundertmark, Chair
Department of Biology and Wildlife
Paul Layer, Dean
College of Natural Science and Mathematics
Michael Castellini, *Dean of the Graduate School*

Abstract

Taxonomic uncertainty in the Arctic-alpine flowering plant genus *Therorhodion* (Maxim.) Small (Ericaceae) can be attributed to two distinctly different viewpoints representing the taxonomic diversity. Russian taxonomists recognize two species, one with two subspecies, whereas three distinct species are recognized in North America following a broader species concept. *Therorhodion redowskianum* Hutch. is restricted to Asia, and is unambiguously recognized by both viewpoints. *Therorhodion camtschaticum* Small and *T. glandulosum* Standl. ex Small have an amphiberingian distribution in eastern Asia and Alaska with *T. glandulosum* sometimes recognized as a subspecies of *T. camtschaticum*. Investigating this taxonomic disagreement creates an opportunity to learn more about the diversification of Beringian taxa and how past glacial events have influenced speciation and the exchange of biota between the continents. I set out to unravel the taxonomic relationships within *Therorhodion* and the likely dispersal route/s of these amphiberingian taxa through the measurement of macromorphological characteristics from voucher specimens, phylogenetic analyses using plastid and nuclear DNA markers, and divergence time analyses. A comparison of age estimates was also performed based on secondary constraints versus fossil constraints. Although leaf length and width measurements were not reliable delimiting characters, there is strong molecular support for *Therorhodion* as the sister clade to *Rhododendron,* and within *Therorhodion* three strongly supported monophyletic clades representing three species were recovered. The use of secondary constraints in the divergence time analyses resulted in younger age estimates than when fossil constraints were applied, corroborating previous studies. Using fossil constraints I

inferred a divergence of *Therorhodion* from *Rhododendron* in the late Paleocene with the Asian-restricted species diverging first from the *T. camtschaticum*/ *T. glandulosum* clade during the middle Miocene, supporting an Asian origin for the genus. Subsequently, the remaining two species are inferred to have diverged in the middle to late Miocene and further dispersed throughout the Pliocene and Pleistocene as suitable habitat became available through a cooling climate.

Table of Contents

List of Figures

Page

List of Tables

Page

Acknowledgements

Thank you to my graduate student advisory committee members for their support and guidance: Dr. Stefanie Ickert-Bond, Dr. Diana Wolf, and Dr. Mary Stensvold; UAMN Herbarium staff and students; herbaria that loaned material (NPS, SAPS, TNS, UBC, US); those who collected/donated DNA samples and voucher specimens (Erin Alvey, Sanghoon Baek, Rachel Buxton, Olga Cherniagina, Scott Freeman, Monte Garroutte, Bombi Jin, Young-Tae Jo, Ian Jones, Robb Kaler, Daehyun Kang, Leah Kenney, Seung-Chul Kim, Yong-In Kim, Brad Krieckhaus, Heather Major, Mary Stensvold, Lisa Strecker, Stacy Studebaker, Vitaliy Teslenko, Hyosig Won, and Valentin Yakubov); Vijay Patil (UAF) for help with R; Kyoko Okano (UAF) and Akiko Soejima (Kumadai) for Japanese translations; Lisa Strecker (UAF) and Julia Mikhailova (Komarov Botanical Institute, Russian Academy of Sciences, St. Petersburg) for Russian translations; Nadja Sekretareva and Julia Mikhailova (Komarov Botanical Institute, Russian Academy of Sciences, St. Petersburg) for field support in Chukotka; Gay Sheffield (UAF) and Dan Reed for field support in Nome; Sam Coffman (UAMN) for field support in Denali National Park and Preserve; Kantishna Air Taxi; Denali National Park and Preserve (permit DENA-2016-SCI-0024). Portions of this work were performed at the Advanced Instrumentation Laboratory (AIL), University of Alaska Fairbanks. Portions of this work were also performed using UAF Life Science Informatics, which as a core research resource is supported by Grant Number RR016466 from the National Center for Research Resources (NCRR), a component of the National Institution of Health (NIH).

Funding was provided in part by a National Park Service, Shared Beringia Heritage Program and Grant (NSF-1021105), the Ted McHenry Biology Field Research Fund (UAF),

the Randy Howenstein Memorial Field Research Fund (UAF), a Thesis Completion Fellowship (UAF), the Arctic Institute of North America Grant-in-Aid Scholarship, and an Alaska Wildflower Garden Club Grant.

Chapter 1 General Introduction

The floristic disjunctions between Asia and North America have been examined by many studies, with much of the focus being on the disjunction between eastern Asia and eastern North America rather than western North America (Li, 1952; Thorne, 1972; Wen, 1999; Donoghue & Smith, 2004; Wen et al., 2010, 2016). The majority of floristic exchanges between eastern Asia and North America documented an eastward dispersal from Asia to North America (Wen et al., 2010), with the Bering land bridge in many cases providing the migration route, but also in some cases serving as a barrier (Wen, 1999; Abbott & Brochmann, 2003; Ickert-Bond et al., 2009; Wen et al., 2010, 2016).

The genus *Therorhodion* (Maxim.) Small (Ericaceae) is disjunctly distributed between eastern Asia and Alaska and comprises three species (Hutchinson, 1921). *Therorhodion camtschaticum* Small and *T. glandulosum* Standl. ex Small have an amphiberingian distribution (Ickert-Bond et al., 2009) occurring in eastern Asia and Alaska, whereas the third species *T. redowskianum* Hutch. is restricted to eastern Asia. The key to understanding disjunct distributions in Alaska concerns the time that lineages arrived in Alaska and how they attained their current biogeographic distribution.

1.1 Inferring the evolutionary history of lineages through divergence time estimation

Divergence time estimation is a tool for inferring when lineages have diverged from each other or when a particular lineage has arrived in an area. The molecular clock hypothesis posits that neutral DNA mutations are incorporated into populations at a regular rate, and has been used to date divergence among species (Zuckerkandl & Pauling, 1965). Divergence time estimation starts with measuring the genetic distance between two

sequences or taxa in an analysis. Traditionally, independent paleontological evidence (a fossil calibration) is used to assign a minimum age or age range to one of the nodes, but other means of calibration are also used (see Renner, 2005; Hipsley & Müller, 2014; Bell, 2015). Subsequently, a substitution rate is calculated by dividing the genetic distance by its known age, and lastly that rate is used to convert genetic distances between two taxa into estimates of absolute time (Fig. 0.1; Sanderson et al., 2002).

Genetic distances are calculated using nucleotide substitution models with the unit of distance being the number of nucleotide substitutions per site, which are generally correlated with time when changes are neutral (no selection; Kimura, 1983). However, many studies have demonstrated that clock-like evolution is largely absent and instead rate heterogeneity among lineages is most prevalent (Britten, 1986; Avise, 1994; Li, 1997). Incorporating rate heterogeneity into analyses has led to the development of the relaxed molecular clock approach for divergence time estimation (Sanderson, 1997; Thorne et al., 1998; Thorne & Kishino, 2002; Lepage et al., 2007; Bell, 2015).

There are a few methods that assume that evolutionary rates are somewhat inherited from ancestral lineages and so limit how much they can change (rates are auto-correlated in time). A couple of these are: non-parametric rate smoothing (NPRS; Sanderson, 1997), a Bayesian method using the Multidivtime software (Thorne et al., 1998), and a penalized likelihood method (PL; Sanderson, 2002). A commonly used relaxed molecular clock approach (without rates being auto-correlated in time) is Bayesian evolutionary analysis by sampling trees (BEAST and BEAST2; Drummond et al., 2012; Bouckaert et al., 2014). The software BEAST (Drummond et al., 2012) uses a Bayesian Markov chain Monte Carlo (B/MCMC) approach to co-estimate the topology, the

substitution rate, and node ages. It also enables for partitioning of the dataset, allowing for the ability to use separate substitution models and clock models for different partitions of the molecular dataset.

Converting genetic distances to absolute time requires a calibration method, which has often relied on fossils (Hipsley & Müller, 2014), which allow for applying a minimum age to the base of a clade but must be correctly assigned to a clade based on synapomorphies the fossil shares with either the crown group or the stem group (Forest, 2009). The crown group is composed of extant taxa, the most recent common ancestor (MRCA), and all extinct taxa within the clade (Fig. 0.1E), whereas the stem group is composed of the crown group plus all of the extinct taxa since it split from the closest living relative (Fig. 0.1E; Forest, 2009). Being a primary source, fossils are often considered the most reliable form of calibration for age estimates, assuming that the most suitable fossil is applied correctly (Marshall, 1990; Sanderson, 1998; Magallón & Sanderson, 2001; Parham et al., 2012). Incorrectly assigning fossil calibrations to nodes or applying an inaccurate age can result in errors in divergence time estimates, but consistent protocols are beginning to be followed (see Parham et al., 2012).

Although fossils may be considered the most appropriate form of calibration not all taxonomic groups are well represented in the fossil record, and so other forms of calibration are often used. Secondary constraints are frequently used and are derived from node ages that were inferred by previous studies using one or more fossil constraints (Dorn et al., 2014). Substitution rates are another form of secondary constraint taken by measuring another dated phylogeny that used different calibrations (Milne, 2004). Geological events are sometimes used to date specific nodes (Herman et al., 2014), but have

been criticized as using circular reasoning because they assume vicariance (Renner, 2005; Forest, 2009). Another constraint that is most often used with viruses and bacteria is the sampling date/ date of sequence isolation (Maree et al., 2015).

Hipsley & Müller (2014) conducted a review of the practices for calibrating trees for divergence time analyses between the years 2007 and 2013 in order to bring attention to methods that deserved more discussion and consensus on practices. They found that fossils were the most commonly used form of calibration, used in approximately 50% of the studies, followed by geological events and secondary calibrations, which were used about an equal amount of time. They also noted that the use of secondary constraints greatly increased between 2007 and 2013.

Following Hipsley & Müller's approach (2014), I reviewed calibration types used in published analyses from 2014 to 2016. In Web of Science (http://webofknowledge.com/) I searched for the same topic terms [(molecular clock* OR divergence dat*) AND (calibrat*)], and followed the same protocols for identifying relevant analyses as Hipsley & Müller (2014). My search resulted in finding 484 papers, 315 of which met the requirements (see attached file Supplemental A). Fossils were the most commonly used method of calibration, followed by secondary calibrations, substitution rates, and geological events (Fig. 0.2). The use of a sampling date for calibration was only used in one published analysis. Shown as a percentage of all of the analyses published per year, the use of fossil calibrations has remained relatively stable since 2009, but dropped from 59 to 44% in 2016 (Fig. 0.3). Secondary calibrations have continued to show an increase in use since 2013, despite concerns that have been expressed about their accuracy (Shaul & Graur, 2002; Graur &

Martin, 2004; Schenk, 2016). The use of geological events as calibrations has continued a steady decline since 2007 (Hipsley & Müller, 2014).

1.2 Taxonomic uncertainty

In addition to being able to accurately date the tenure of a lineage in a particular region, species delineation and differing taxonomies need to be reconciled to accurately describe the floristic diversity of a region. There is some taxonomic uncertainty within *Therorhodion* between *T. camtschaticum* and *T. glandulosum* in Asian descriptions as well as those put forth by Swedish botanist Eric Hultén in *Flora of Alaska and Neighboring Territories* (1968). Nevertheless, the two taxa are considered distinct species in Alaska today, where they live in allopatry, in addition to being easily distinguished based on morphology. These different taxonomic viewpoints are due to different taxonomic traditions within Asia and North America, as well as incomplete knowledge of habitat preference for *Therorhodion* in the respective regions. Russian taxonomists are more likely to use the taxon rank of subspecies rather than the rank of species when the closely related taxa occur in sympatry and the taxa have a higher chance of hybridization (Elven et al., 1999). This is the case for *T. camtschaticum* and *T. glandulosum*, although there are currently no published data on whether hybridization commonly occurs.

Whereas the Asian *T. redowskianum* is consistently recognized as a distinct species (Busch, 1915; He & Chamberlain, 2005), *T. glandulosum* is often described as a subspecies of *T. camtschaticum* in Asian descriptions (Yurtsev et al., 2010; Takahashi, 2015) and by Hultén (1968). In contrast, North American descriptions and the Panarctic Flora (http://nhm2.uio.no/paf/) separate *T. camtschaticum* and *T. glandulosum* at the species level (Viereck & Little, 2007; Kron & Judd, 2009; Elven et al., 2011). Herbarium specimens

collected from Chukotka and Kamchatka deposited at the Herbarium, University of Alaska Museum of the North (ALA) can be separated into *T. glandulosum* and *T. camtschaticum* based on their morphological characteristics.

1.3 Open access and an integrative study

Open access to molecular sequences and phylogenetic trees has increased with the creation of databases such as TreeBASE (http://treebase.org; Sanderson et al., 1994), Dryad (http://datadryad.org/), and GenBank (http://www.ncbi.nlm.nih.gov/genbank/; Benson et al., 2013), enabling users to expand their datasets and potentially answer more complex questions related to biogeography and evolutionary history of particular floristic regions. My study takes advantage of GenBank by using 205 sequences for the outgroup in order to reconstruct the phylogeny of the Ericaceae and confirm the position of *Therorhodion*. All of the newly generated sequences from this project will also be publicly available on GenBank.

This study is highly integrative by combining molecular sequencing and divergence time estimation with original field studies and examination of macromorphology from voucher specimens at the Herbarium, University of Alaska Museum of the North (ALA) and loaned specimens (NPS, SAPS, TNS, UBC, US; acronyms follow Index Herbariorum; Thiers, 2016). It aims to clarify the taxonomic relationships within *Therorhodion* as well as to unravel aspects of the evolutionary and biogeographic origins of the amphiberingian flora using *Therorhodion* as a case study.

References

Abbott RJ, Brochmann C. 2003. History and evolution of the Arctic flora: In the footsteps of Eric Hultén. *Molecular Ecology* 12: 299–313.

Avise JC. 1994. *Molecular markers, natural history and evolution*. New York: Chapman and Hall.

Bell CD. 2015. Between a rock and a hard place: Applications of the "molecular clock" in systematic biology. *Systematic Botany* 40: 6–13.

Benson DA, Cavanaugh M, Clark K, Karsch-Mizrachi I, Lipman DJ, Ostell J, Sayers EW. 2013. GenBank. *Nucleic Acids Research* 41: D36–D42.

Bouckaert R, Heled J, Kühnert D, Vaughan T, Wu CH, Xie D, Suchard MA, Rambaut A, Drummond AJ. 2014. BEAST 2: A software platform for Bayesian evolutionary analysis. *PLoS Computational Biology* 10: e1003537. doi: 10.1371/journal.pcbi.1003537.

Britten RJ. 1986. Rates of DNA-sequence evolution differ between taxonomic groups. *Science* 231: 1393–1398.

Busch E. 1915. *Therorhodion*. In: *Flora Sibiriae Et Orientis Extremi vol 2*. Saint Petersburg: Russian Academy of Sciences. 63: 35–41. (The Russian edition of *Flora of Siberia and the Far East*).

Donoghue MJ, Smith SA. 2004. Patterns in the assembly of the temperate forest around the Northern Hemisphere. *Philosophical Transactions of the Royal Society of London B: Biological Sciences* 359: 1633–1644.

Dorn A, Musilová Z, Platzer M, Reichwald K, Cellerino A. 2014. The strange case of East Africa annual fishes: Aridification correlates with diversification for a savannah aquatic group? *BMC Evolutionary Biology* 14: 210.

Drummond AJ, Suchard MA, Xie D, Rambaut A. 2012. Bayesian phylogenetics with BEAUti and the BEAST 1.7. *Molecular Biology and Evolution* 29: 1969–1973.

Elven R, Jonsell B, Murray DF, Yurtsev BA. 1999. An operational species concept for the Panarctic Flora. In: Nordal I, Razzhivin VY eds. *The species concept in the High North – A Panarctic Flora initiative*. Oslo: The Norwegian Academy of Science and Letters. 23–32.

Elven R, Murray DF, Yurtsev BA. 2011. Annotated checklist of the Panarctic Flora (PAF) vascular plants [online]. Available from http://nhm2.uio.no/paf/ [accessed 14 March 2017].

Forest F. 2009. Calibrating the Tree of Life: Fossils, molecules and evolutionary timescales. *Annals of Botany* 104: 789–794.

Graur D, Martin W. 2004. Reading the entrails of chickens: Molecular timescales of evolution and the illusion of precision. *TRENDS in Genetics* 20: 80–86.

He M, Chamberlain DF. 2005. *Rhododendron* subg. *Therorhodion* (Maximowicz). In: Wu ZY, Raven PH eds. *Flora of China, vol 14* [online]. Available from www.efloras.org [accessed 24 August 2016].

Herman JS, McDevitt AD, Kawałko A, Jaarola M, Wójcik JM, Searle JB. 2014. Land-bridge calibration of molecular clocks and the post-glacial colonization of Scandinavia by the Eurasian field vole *Microtus agrestis*. *PLoS ONE* 9: e103949. doi: 10.1371/journal.pone.0103949.

Hipsley CA, Müller J. 2014. Beyond fossil calibrations: Realities of molecular clock practices in evolutionary biology. *Frontiers in Genetics* 5: doi: 10.3389/fgene.2014.00138.

Hultén E. 1968. *Flora of Alaska and neighboring territories: A manual of the vascular plants*. Stanford: Standford University Press.

Hutchinson J. 1921. XXIII - The genus *Therorhodion*. *Bulletin of Miscellaneous Information Kew* 5: 201–205.

Ickert-Bond SM, Murray DF, DeChaine E. 2009. Contrasting patterns of plant distribution in Beringia. *Alaska Park Science* 8: 26–32.

Kron KA, Judd WS. 2009. *Therorhodion*. In: Flora of North America Editorial Committee eds. *Flora of North America north of Mexico.* 20+ vols. New York: Oxford University Press. Vol. 8, 453–543.

Kimura M. 1983. *The neutral theory of molecular evolution*. Cambridge: Cambridge University Press.

Lepage T, Bryant D, Philippe H, Lartillot N. 2007. A general comparison of relaxed molecular clock models. *Molecular Biology and Evolution* 24: 2669–2680.

Li HL. 1952. Floristic relationships between eastern Asia and eastern North America. *Transactions of the American Philosophical Society* 42: 371–429.

Li WH. 1997. *Molecular evolution*. Sunderland, Mass.: Sinauer.

Magallón S, Sanderson MJ. 2001. Absolute diversification rates in angiosperm clades. *Evolution* 55: 1762–1780.

Maree HJ, Pirie MD, Oosthuizen K, Bester R, Rees JG, Burger JT. 2015. Phylogenomic analysis reveals deep divergence and recombination in an economically important grapevine virus. *PLoS ONE* 10: e0126819. doi: 10.1371/journal.pone.0126819.

Marshall CR. 1990. The fossil record and estimating divergence times between lineages: maximum divergence times and the importance of reliable phylogenies. *Journal of Molecular Evolution* 30: 400–408.

Milne RI. 2004. Phylogeny and biogeography of *Rhododendron* subsection *Pontica*, a group with a tertiary relict distribution. *Molecular Phylogenetics and Evolution* 33: 389–401.

Parham JF, Donoghue PCJ, Bell CJ, Calway TD, Head JJ, Holroyd PA, Inoue JG, Irmis RB, Joyce WG, Ksepka DT, Patané JSL, Smith ND, Terver JE, van Tuinen M, Yang Z, Angielscyk KD, Greenwood JM, Hipsley CA, Jacobs L, Makovicky PJ, Müller J, Smith KT, Theodor JM, Warnock RCM, Benton MJ. 2012. Best practices for justifying fossil calibrations. *Systematic Biology* 61: 346–359.

Renner SS. 2005. Relaxed molecular clocks for dating historical plant dispersal events. *Trends in Plant Science* 10: 550–558.

Sanderson MJ. 1997. A nonparametric approach to estimating divergence times in the absence of rate constancy. *Molecular Biology and Evolution* 14: 1218–1231.

Sanderson MJ. 1998. Estimating rate and time in molecular phylogenies: beyond the molecular clock? In: Soltis DE, Soltis PS, Doyle JJ eds. *Molecular systematics of plants II: DNA sequencing*. New York: Springer US. 242–264.

Sanderson MJ. 2002. Estimating absolute rates of molecular evolution and divergence times: A penalized likelihood approach. *Molecular Biology and Evolution* 19: 101–109.

Sanderson MJ, Donoghue MJ, Piel W, Eriksson T. 1994. TreeBASE: A prototype database of phylogenetic analyses and an interactive tool for browsing the phylogeny of life. *American Journal of Botany* 81: 183.

Sanderson MJ, Thorne JL, Wikström N, Bremer K. 2002. Molecular evidence on plant divergence times. *American Journal of Botany* 91: 1656–1665.

Schenk JJ. 2016. Consequences of secondary calibrations on divergence time estimates. *PLoS ONE* 11: e0148228. doi: 10.1271/journal.pone.0148228.

Shaul S, Graur D. 2002. Playing chicken (*Gallus gallus*): Methodological inconsistencies of molecular divergence date estimates due to secondary calibration points. *Gene* 300: 59–61.

Takahashi H. 2015. *Plants of the Kuril Islands*. Sapporo: Hokkaido University Press. [In Japanese].

Thiers B. continuously updated. Index Herbariorum: A global directory of public herbaria and associated staff. New York Botanical Garden's Virtual Herbarium [online]. Available from http://sweetgum.nybg.org/science/ih/ [accessed 19 September 2016].

Thorne RF. 1972. Major disjunctions in the geographical ranges of seed plants. *The Quarterly Review of Biology* 47: 365–411.

Thorne JL, Kishino H. 2002. Divergence time and evolutionary rate estimation with multilocus data. *Systematic Biology* 51: 689–702.

Thorne JL, Kishino H, Painter IS. 1998. Estimating the rate of evolution of the rate of molecular evolution. *Molecular Biology and Evolution* 15: 1647–1657.

Viereck LA, Little EL Jr. 2007. *Alaska trees and shrubs*. Fairbanks, AK: University of Alaska Press.

Wen J. 1999. Evolution of eastern Asian and eastern North American disjunct distributions in flowering plants. *Annual Review of Ecology, Evolution, and Systematics* 30: 421–455.

Wen J, Ickert-Bond SM, Nie Z, Li R. 2010. Timing and modes of evolution of eastern Asian–North American biogeographic disjunctions in seed plants. In: Long, M., Gu, H., & Zhou, Z. eds. *Darwin's heritage today: Proceedings of the Darwin 20 Beijing International Conference*. Beijing: Higher Education Press. 252–269.

Wen J, Nie ZL, Ickert-Bond SM. 2016. Intercontinental disjunctions between eastern Asia and western North America in vascular plants highlight the biogeographic importance of the Bering land bridge from late Cretaceous to Neogene. *Journal of Systematics and Evolution* 54: 469–490.

Yurtsev BA, Koroleva TM, Petrovsky VV, Polozova TG, Zhukova PG, Katenin AE eds. 2010. *Checklists of flora of the Chukotkan tundra*. Saint-Petersburg: VVM Ltd. Publishing.

Zuckerkandl E, Pauling L. 1965. Evolutionary divergence and convergence in proteins. In: Bryson V, Vogel HJ eds. *Evolving genes and proteins*. New York: Academic Press. 97–166.

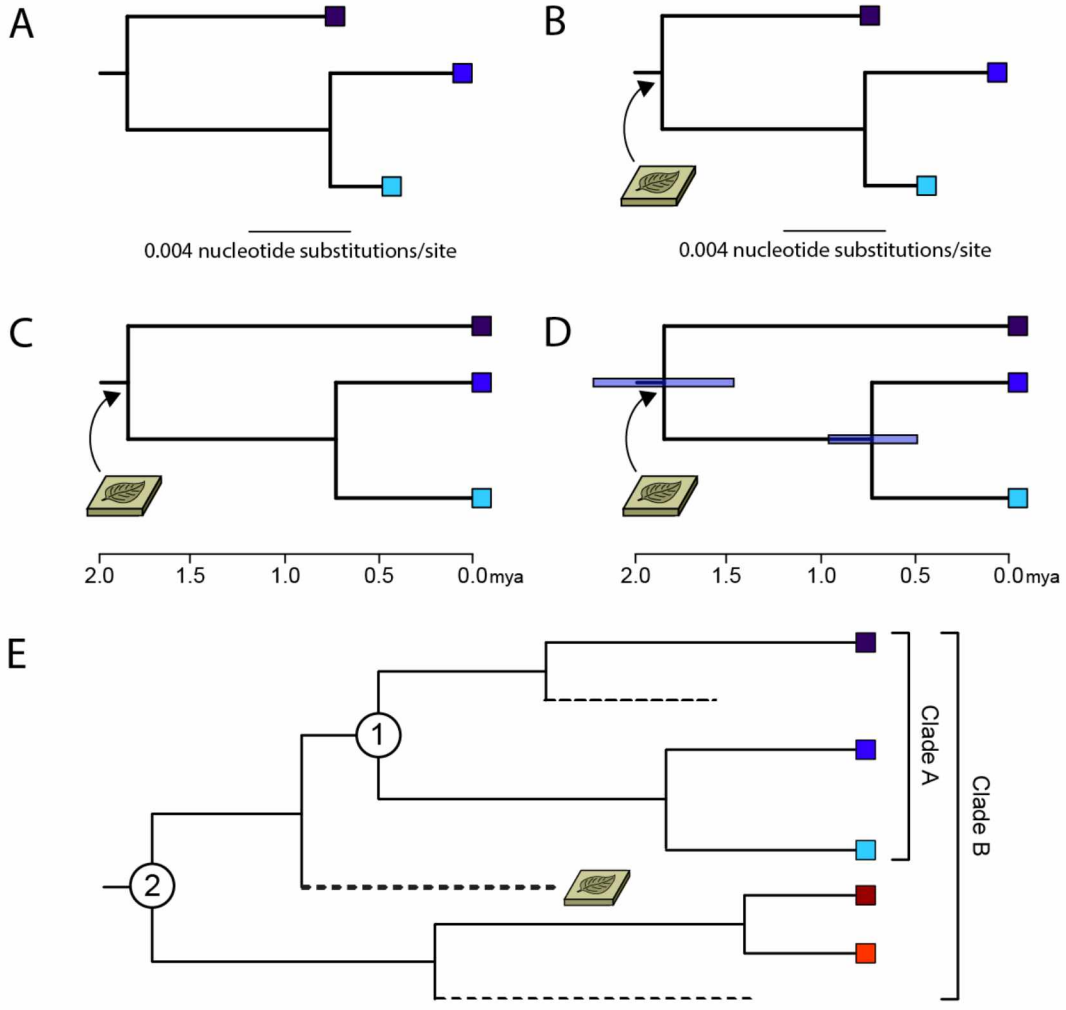

Figure 1.1 Node calibration for a divergence time analysis. A) A Phylogram with branch lengths representing the number of nucleotide substitutions per site. B) A constraint with an approximate known age, such as a fossil, is applied to the appropriate node, which adds a temporal component and converts branch length and scale to absolute time, shown in C). D) The consensus chronogram includes 95% confidence intervals as purple bars. E) Using the marked fossil (dashed lines represent extinct taxa), node 1 represents the crown group of clade A, and node 2 represents the stem group of clade A. Node 2 could also be the crown group of clade B if a different fossil constraint were used (adapted from Renner, 2005 and Forest, 2009).

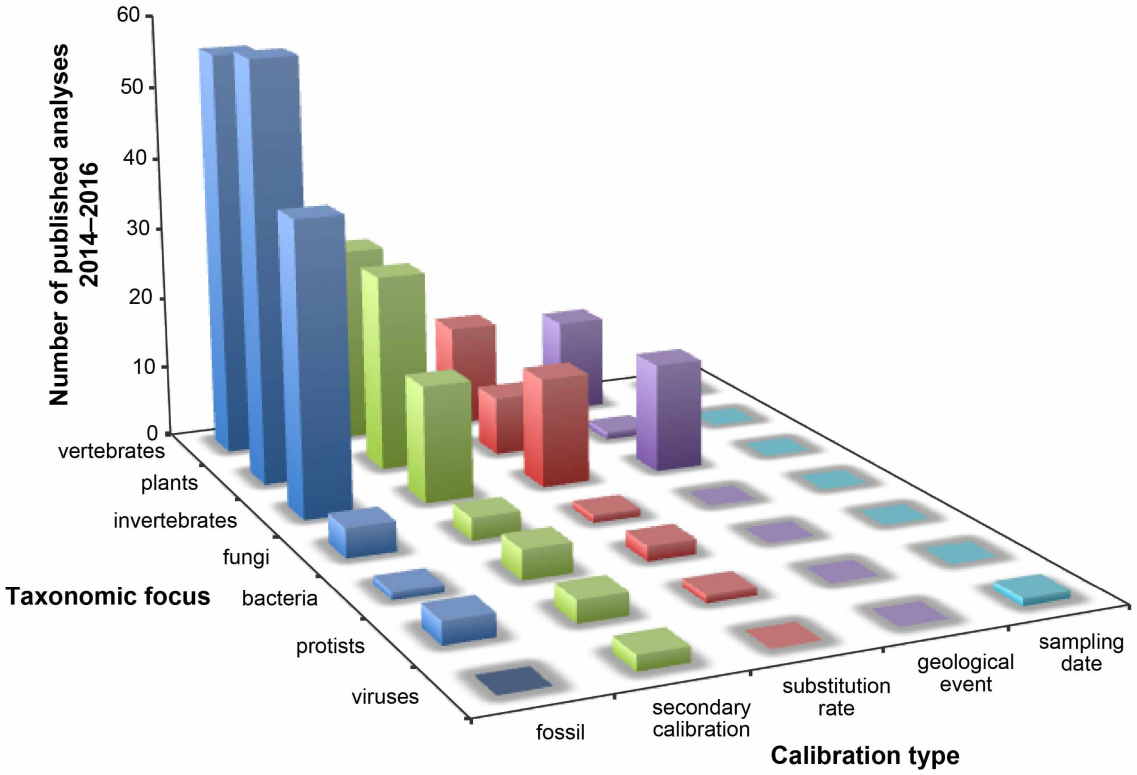

Figure 1.2 Frequency of calibration types used among different taxonomic groups. The number of published analyses from 2014 to 2016 is based on a search in Web of Science.

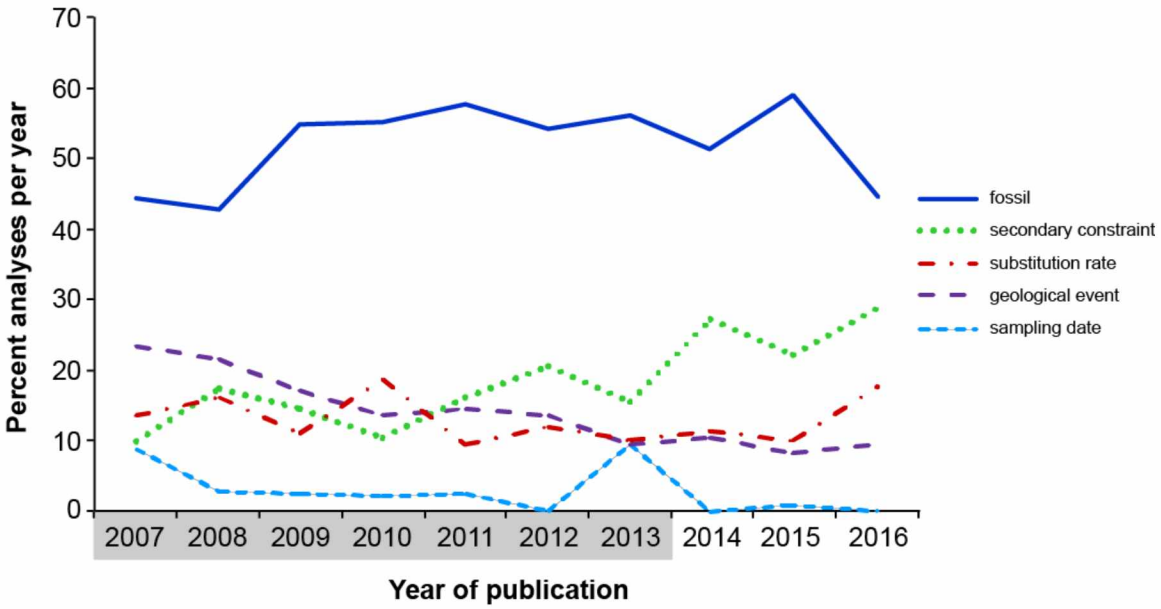

Figure 1.3 Trends in calibration methods used as percent of the total analyses published per year. Results are for the years 2007 to 2013 (years shaded in gray on the x-axis are adapted from Hipsley & Müller, 2014).

Chapter 2 Across the Bering land bridge to the New World: The evolutionary history of *Therorhodion* (Maxim.) Small (Ericaceae)[1]

2.1 Introduction

Our understanding of Arctic species and speciation was advanced by Swedish botanist Eric Hultén, who coined the term 'Beringia' (Hultén, 1937; Abbott & Brochmann, 2003) to refer to an unglaciated area during the Quaternary glaciations extending from the Lena River in Siberia (125° E. longitude) and the Mackenzie River in northwestern Canada (130 ° W. longitude), and from the Arctic Ocean (72° N. latitude) to as far south as the tip of Kamchatka (51° N. latitude; Hultén, 1937; Abbott & Brochmann, 2003). The role of Beringia as an unglaciated refuge for many plants and animals has been well studied (Hultén, 1937; Tremblay & Schoen, 1999; Abbott et al., 2000; Abbott & Brochmann, 2003; Tkach et al., 2008; Hoffmann et al., 2010; Liu et al., 2014; Hou et al., 2016a, 2016b). In addition, the 1000 km wide Bering land bridge acted as a dispersal corridor between eastern Asia and western North America for many now disjunct plant and animal taxa (Hopkins, 1967; Sanmartín et al., 2001; Donoghue & Smith, 2004; DeChaine, 2008; Ickert-Bond et al., 2009; Wen et al., 2016), with the majority of the floristic exchanges documented as being an eastward dispersal from Asia to North America (Wen et al., 2010).

---

[1] Margaret G. Oliver, Jordan S. Metzgar, and Stefanie M. Ickert-Bond. Across the Bering land bridge to the New World: The evolutionary history of *Therorhodion* (Maxim.) Small (Ericaceae). Prepared for submission in the Journal of Systematics and Evolution.

Eastern Asia and Alaska are considered to be the center of distribution for heathland plants (Bliss, 1979), which includes the Ericaceae (heather family) and Diapensiaceae (*Diapensia* family). The Ericaceae are an important part of the Arctic flora, but with relatively low species richness (Stevens et al., 2004; Schwery et al., 2015). Although the Ericaceae does contain herbs and trees, all of the representatives in Alaska are shrubs with seventeen genera and thirty species (Hultén, 1968; Viereck & Little, 2007). This includes blueberries and cranberries (*Vaccinium* L.), and Labrador tea (*Rhododendron* L.; Flora of North America Editorial Committee, 2009).

The family Ericaceae has a worldwide distribution, but is especially abundant in temperate and montane habitats with 124 recognized genera and approximately 4100 species (Stevens et al., 2004; Schwery et al., 2015). *Rhododendron* is a species-rich, mostly evergreen genus of Ericaceae with over 1000 species recognized worldwide (Stevens et al., 2004), and is well studied due to the conspicuous flowers of many of the species and as a result the genus is commonly cultivated.

Maximowicz subdivided the genus *Rhododendron* into eight sections in 1870: *Osmothamnus* Maxim., *Eurhododendron* Maxim., *Azalea* Pl. emend., *Tsusia* Pl. emend., *Keysia* Th. Nutt., *Rhodorastrum* Maxim., *Azaleastrum* Pl., and *Therorhodion* Maxim. Subsequently, following the schema by Maximowicz, Gray (1878) elevated these eight sections to subgenera including subgenus *Therorhodion* (Maxim.) Gray, which is recognized based on one or two terminal leafy shoots, bud-scales that are deciduous with the leaves, and a rotate corolla that is deeply divided close to the base on the lower side. Small in 1914 considered the morphological differences between *Therorhodion* and *Rhododendron* significant enough to raise subgenus *Therorhodion* to generic level. Hutchinson's 1921

treatment of the genus *Therorhodion* (Maxim.) Small was the first to include three species: *T. camtschaticum* Small, *T. glandulosum* Standl. ex Small and *T. redowskianum* Hutch (Fig. 1.1).

The taxonomic history of *Therorhodion* dates back to the 1780's (Table 1.1). The first taxon to be described was *T. redowskianum* by Maximowicz in 1859. He described *Therorhodion* as a section of *Rhododendron* (Maximowicz, 1870) with a distribution in the mountains of northeastern Asia. Gray (1878) expanded this distribution to include Alaska and the Aleutian Islands as well as northern Japan, where he recognized *R. kamtschaticum* (=*camtschaticum*). Small (1914), in the *North American Flora*, raised section *Therorhodion* to generic rank and described *T. glandulosum* from the Imuruk Basin of Alaska (Fig. 1.2).

Whereas the Asian *T. redowskianum* is consistently recognized as a distinct species (Busch, 1915; He & Chamberlain, 2005), *T. glandulosum* is often described as a subspecies of *T. camtschaticum* in Asian descriptions (Yurtsev et al., 2010; Takahashi, 2015) and by Hultén (1968). In contrast, today's North American descriptions and the Panarctic Flora separate *T. camtschaticum* and *T. glandulosum* at the species level (Viereck & Little, 2007; Kron & Judd, 2009; Elven et al., 2011). Herbarium specimens collected from Chukotka and Kamchatka archived at the Herbarium, University of Alaska Museum of the North (ALA) can be separated into *T. glandulosum* and *T. camtschaticum* based on their morphological characteristics.

Although *Therorhodion* has often been treated as subgenus of *Rhododendron* (e.g. He & Chamberlain, 2005), more recent genetic work within the Ericaceae has provided further support for the distinctiveness of *Therorhodion* as a closely related clade to *Rhododendron* (Kron & Judd, 1990; Kron, 1997; Kurashige et al., 1998; Kurashige et al., 2001; Kron et al.,

2002a; Gillespie & Kron, 2010). Yet we know little about the phylogenetic relationships of the taxa within *Therorhodion* and the tenure of these lineages in Beringia.

With the ubiquitous use of molecular methods for phylogeny reconstruction, and a better understanding of the fossil record of the Ericaceae (Collinson & Crane, 1978; Van der Burgh, 1978; Friis, 1979; Van der Burgh, 1987; Nixon & Crepet, 1993; Schwery et al., 2015) we are well situated to explore the evolutionary history of *Therorhodion*. Specifically we aim to test the following hypotheses (Fig. 1.3): (1) There are three reciprocally monophyletic lineages within *Therorhodion*; (2) arrival in the New World was via a northern route (Bering land bridge) to the Seward Peninsula and a southern route via the Aleutian Islands to southwest and southeast Alaska; and (3) within *T. camtschaticum* and *T. glandulosum* two distinct clades of western and eastern Beringian populations exist with an older divergence time estimation for the western Beringian population.

2.2 Materials and Methods

2.2.1 Morphological data

We reviewed 268 herbarium specimens from ALA, SAPS, TNS, UBC, and US (Thiers, continuously updated) to characterize leaf size in *Therorhodion* (Fig. 1.2). We measured leaf length (L), leaf width (W), trichome presence, and the type of trichomes (glandular or non-glandular) of herbarium specimens to better characterize the three *Therorhodion* species morphologically (see attached file Supplemental A). Ten entire leaves were randomly selected for measurements from each voucher specimen or the most leaves possible if fewer than ten leaves were available. We calculated the average leaf length, leaf width, and L:W ratio for all three taxa (Table 1.4). Analysis of Variance (ANOVA) and paired

t-tests were performed using R version 3.1.3 (R Core Team, 2015) to compare leaf length and width between taxa. Box plots depicting log-transformed measurement data were produced using R v3.1.3.

Pollen of all three taxa of *Therorhodion* were obtained from herbarium specimens at ALA (Table 1.5), and acetolyzed (Erdtman, 1960; Takahashi, 1987). Pollen samples were subsequently dehydrated in 90% ethanol, mounted on aluminum stubs with double-sided tape, sputter coated with palladium using a Ladd model 30800, and viewed with an ISI-SR-50 scanning electron microscope at approximately 20 kV at the Advanced Instrumentation Laboratory (AIL) at UAF. The diameter of pollen grains were measured using Adobe Photoshop version 13.0.4 and ANOVA was performed in R version 3.1.3 to compare the diameters among taxa.

2.2.2 Phylogeny, DNA extraction, PCR amplification, and sequencing

In order to reconstruct the phylogeny of Ericaceae and confirm the position of *Therorhodion* we assembled a large molecular dataset. We generated 80 new sequences from *Therorhodion* for four chloroplast loci (*ndhF*, *rbcL*, *matK*, and *trnL-F*) and two nuclear loci (*waxy* and *nrITS*) and used 205 sequences from GenBank (Table 1.2; http://www.ncbi.nlm.nih.gov/genbank/). This final dataset included 46 outgroup species and three ingroup species, covering four of the eight subfamilies, six of the 20 tribes, and 23 of the 124 genera in the Ericaceae (Stevens et al., 2004; Gillespie & Kron, 2010) as well as two genera from the Actinidiaceae. For the ingroup our dataset comprised 22 samples, including 20 from throughout the distributional range of *T. camtschaticum* and *T. glandulosum*. *Therorhodion redowskianum* was represented by two accessions from China (Fig 1.2; Table 1.2).

We extracted DNA from approximately 20 milligrams of silica-dried or herbarium leaf tissue per sample using the Qiagen DNeasy Plant Mini Kit (Qiagen, Valencia, California, USA). We amplified the six DNA regions mentioned previously according to protocols used in Ericaceae (Taberlet et al., 1991; Brown et al., 2005, 2006; Taberlet et al., 2006; Gillespie & Kron, 2010; Table 1.3). Amplified DNA loci were purified and sequenced at the High Throughput Genomic Center in Seattle, WA. We cleaned and assembled the sequences using Sequencher version 5.1 (Gene Codes Corporation, Ann Arbor, MI USA). Due to difficulty assembling sequencing reads, the chloroplast loci *matK* and *ndhF* were both amplified and sequenced in two parts (see Table 1.3 notes). The halves were then manually assembled into a single contig with the mindlessly join tool in Sequencher version 5.1 with a series of "N's" inserted between the halves to distinguish the unsequenced region.

2.2.3 Phylogenetic analysis

Sequence alignment was performed manually using MacClade version 4.08 (Maddison & Maddison, 2005). The chloroplast alignment was 5322 bp long (1488 bp in *ndhF*, 1431 bp in *rbcL*, 1787 bp in *matK*, and 616 bp in *trnL-F*) and the nuclear alignment was 1383 bp (651 in *waxy* and 732 bp in the *nrITS*). We excluded 451 bp out of the combined total of 6705 bp due to ambiguously aligned portions of the data matrix.

All analyses were performed on either the UAF Life Science Informatics Portal (http://biotech.inbre.alaska.edu/) or the Cipres Science Gateway (Miller et al., 2010). We used MrModeltest v2.3 to determine the best model of sequence evolution for each locus using the Akaike information criterion scores (Nylander et al., 2004). Maximum parsimony analyses with 1000 heuristic replicates were first performed using PAUP* v4.0b10 (Swofford, 2003) on all individual loci to compare topologies followed by maximum

parsimony bootstrap (MPBS) analyses with 50 heuristic replicates, to obtain bootstrap support for the most parsimonious trees. All loci were also analyzed separately using a Bayesian Markov chain Monte Carlo (B/MCMC) approach in MrBayes v 3.2 (Huelsenbeck & Ronquist, 2001; Ronquist & Huelsenbeck, 2003; Ronquist et al., 2012). To test for incongruence before combining our sequence matrices into a single, concatenated dataset we performed an incongruence length difference (ILD) test (Farris et al., 1995) in PAUP* v4.0b10 (Swofford, 2003) on our nuclear and plastid datasets using 100 heuristic replicates, three random additions per replicate, TBR swapping, and stepwise addition of taxa.

A B/MCMC approach was used to reconstruct the optimal phylogenetic tree for both the combined plastid and combined nuclear datasets in MrBayes v3.2 (Huelsenbeck & Ronquist, 2001; Ronquist & Huelsenbeck, 2003; Ronquist et al., 2012). The B/MCMC analysis used four runs, each with four chains that ran for ten million generations, sampling the trees every one thousand generations. Checks for stationarity were done using Tracer v1.6 (Drummond et al., 2012). We discarded a conservative burn-in of 2.5 million generations. The remaining 30,000 trees were pooled to calculate a 50% majority-rule consensus tree in MrBayes using the sumP and sumT commands (Drummond et al., 2012). A single combined dataset of all plastid and nuclear loci was then analyzed using a B/MCMC approach in MrBayes v3.2 (Huelsenbeck & Ronquist, 2001; Ronquist & Huelsenbeck, 2003; Ronquist et al., 2012), using settings as indicated above.

2.2.4 Divergence time analyses

In order to determine the temporal component of diversification in *Therorhodion*, divergence times were calculated in three separate analyses using different constraints

(Table 1.6). Analysis I used three secondary constraints from Schenk & Hufford (2010), analysis II used six fossil constraints (Collinson & Crane, 1978; Van der Burgh, 1978; Friis, 1979; Axelrod, 1987; Nixon & Crepet, 1993; Mai, 2001), and analysis III used a combination of secondary and fossil constraints (Table 1.6). Fossils were selected based on Schwery et al. (2015), who used the criteria set forth by Parham et al. (2012). All of the analyses were performed with the combined dataset using an uncorrelated lognormal clock in BEAST v1.7.5 (Drummond et al., 2012). We performed multiple analyses using secondary and fossil constraints because Schenk (2016) found that using secondary constraints exclusively resulted in younger divergence time estimates with narrower confidence intervals. We were interested in comparing our divergence times from analysis I to analysis II (Table 1.6) and whether a combination of the two (analysis III) would yield much different estimates from either one.

The input files for BEAST were generated using BEAUti v1.8.1 (Drummond et al., 2012). During analysis we treated each locus as a separate partition and the subsititution model and the clock model were unlinked across partitions. The HKY model (Hasegawa et al., 1985) was chosen to avoid over parameterization of the analyses associated with the more complex GTR (General Time Reversal) model (Bryson et al., 2014). Four chains were run for 50 million generations each with a 10% burn-in. Convergence between runs was assessed using Tracer v1.6 (Drummond et al., 2012). After discarding the burn-in the trees and parameters were combined in LogCombiner v1.8.1 (Drummond et al., 2012). Trees were visualized using FigTree v1.4.0 (Rambaut, http://tree.bio.ed.ac.uk/software/figtree/). The mean and 95% highest posterior densities (HPD) of age estimates were obtained from Tracer 1.6 (Drummond et al., 2012).

2.3 Results

2.3.1 Morphological measurements

We found that the average leaf length ($F_{(2, 2003)}$=164.3, p=2.2x10^{-16}) and leaf width ($F_{(2, 2003)}$=368.07, p=2.2x10^{-16}) were significantly different among taxa. Paired t-tests also revealed that all of the taxa were significantly different from each other for leaf length and leaf width (*T. camtschaticum*/ *T. glandulosum*: $t_{(12.3)}$=5.3, p=1.7x10^{-4}; *T. camtschaticum*/ *T. redowskianum*: $t_{(12.8)}$=9.8, p=2.7x10^{-7}; *T. glandulosum*/ *T. redowskianum*: $t_{(76.5)}$=22.0, p=2.2x10^{-16}). Pollen morphology appears uniform between the three taxa examined, with pollen grains found in tetrahedral tetrads, a verrucate to rugulate ornamentation, and viscin threads present in all three species (Fig. 1.5). The pollen diameter was not significantly different among taxa ($F_{(2,17)}$=0.65, p=0.53). *Therorhodion redowskianum* pollen had a mean diameter of 40.25 (±1.63) µm as compared to 43.8 (±2.21) µm and 37.02 (±1.26) µm for *T. glandulosum* and *T. camtschaticum* respectively (Table 1.5).

2.3.2 Phylogeny

The average pairwise divergence and number of parsimony informative characters (PIC) show that although *matK* has the highest number of PIC, *ndhF* has higher variability between *Therorhodion* and *Rhododendron*, and *waxy* has the highest variability between *Therorhodion* and the rest of the Ericaceae (Table 1.7). The inferred phylogeny of the plastid dataset is well resolved with 41 out of 48 nodes supported by a posterior probability (PP) ≥0.95 and 20 nodes with bootstrap support (MPBS) ≥95% (Fig. 1.6). All of the backbone nodes were supported by a PP ≥0.99. Subfamily Ericoideae is very well supported (PP 1.0 and MPBS 100%). There are four monophyletic clades within Ericoideae

with strong PP and MPBS support. The first clade represents tribe Phyllodoceae (PP 1.0, MPBS 96.7%) with the genera *Bejaria* Mutis, *Elliottia* Muhl. ex Elliott, *Epigaea* L., *Kalmiopsis* Rehder, *Phyllodoce* Salisb., *Rhodothamnus* Rchb., and *Kalmia* L. The second clade is strongly supported (PP 0.99, MPBS 83.4%) and contains the genera *Bryanthus* J.G. Gmel. and *Ledothamnus* Meisn., representing tribe Bryantheae. The third clade is also strongly supported (PP 1.0, MPBS 95.5%) and contains *Calluna* Salisb. and *Erica* L., making up tribe Ericeae, but *Daboecia* D. Don. is inferred to be basal to the rest of subfamily Ericoideae (PP 1.0, MPBS 100%). The fourth clade is well supported (PP 1.0, MPBS 89.5%) and comprises tribe Empetreae (PP 1.0, MPBS 100%) with the genera *Ceratiola* Michx., *Corema* D. Don, and *Empetrum* L., sister to tribe Rhodoreae (PP 1.0, MPBS 70.5%) that is composed of two subclades, the first consisting of a paraphyletic *Rhododendron* (with *Menziesia* Sm. nested within) and the genus *Diplarche* Hook. & Thomson as the earliest diverging lineage; this subclade is in turn sister to the *Therorhodion* subclade.

The inferred phylogeny of the nuclear dataset was not as well resolved and supported as the plastid phylogeny particulary at the backbone, but has 19 out of 28 nodes with PP ≥0.95 and seven nodes with MPBS ≥95% (Fig. 1.7). One of the backbone nodes was supported by PP 1.0 whereas the others have support of PP <0.85. Tribe Empetreae is a well-supported monophyletic clade (PP 0.99, MPBS 93.8), but there is poor resolution for the remaining tribes or they are not monophyletic. Within tribe Empetreae, *Diplarche multiflora* Hook.f. & Thomson was inferred on a much longer branch than any of the other taxa and so it was shortened for clarity indicated by hash marks on the figure (Fig. 1.7). The ILD test found that the nuclear and plastid datasets are not congruent ($p = 0.01$). However,

it has been proposed that a *p*-value between 0.01–0.001 would be a more appropriate threshold for the ILD test (Cunningham, 1997).

The inferred phylogeny of the combined nuclear and plastid dataset was well resolved with 38 out of 43 nodes supported by PP ≥0.95 and 20 nodes with MPBS ≥95% (Fig. 1.8). All backbone nodes were supported with PP ≥0.99. The subfamily Ericoideae is well supported by PP 1.0, but has weak MPBS support of 53.2%. Within Ericoideae there are four monophyletic clades with high PP, but not all with strong MPBS. The first clade has strong PP, but weak MPBS (PP 1.0, MPBS 59.6%) and contains the same genera within tribe Phyllodoceae as the plastid dataset phylogeny (Fig. 1.8). The second clade also has strong PP, but weak MPBS (PP 0.99, MPBS 71%) and contains *Bryanthus* and *Ledothamnus*, representative of tribe Bryantheae. The third clade contains *Calluna* and *Erica*, making up tribe Ericeae and has very strong PP and good MPBS support (PP 1.0, MPBS 86%). The last clade contains tribe Empetreae with moderate PP and strong MPBS support (PP 0.76, MPBS 99%) and tribe Rhodoreae is moderately suported by PP and MPBS (PP 0.76, MPBS 87.6%).

The phylogenetic results show *Therorhodion* moderately supported as a sister clade to *Rhododendron* and *Menziesia* with 87.6% MPBS support, but 0.76 PP support, and within *Therorhodion* three monophyletic clades are recovered (Fig. 1.9). The earliest diverging species is *T. redowskianum*, which is well supported (PP 1.0, MPBS 99.2%) and is sister to an unambiguously supported clade (PP 1.0, MPBS 93.9%) composed of *T. camtschaticum* and *T. glandulosum*. *Therorhodion camtschaticum* and *T. glandulosum* are each reciprocally monophyletic (both with PP 0.99). Within *T. camtschaticum* and *T. glandulosum* we cannot see distinct western and eastern Beringian clades due to poor resolution.

2.3.3 Divergence time estimation

The results of all three divergences time analyses (I, II, and III) found unambiguously supported monophyletic clades for *Therorhodion* representing the three species (Figs. 1.10, 1.11, and 1.12). Analysis I (Fig. 1.10) inferred the divergence of *Therorhodion* from *Rhododendron* during the late Oligocene to early Miocene (21.40 mya) (see Table 1.8 for 95% HPD) with *T. redowskianum* diverging first from the clade of *T. camtschaticum* and *T. glandulosum* in the late Miocene (7.49 mya). Speciation in the later clade occurred during the transition between the Miocene and Pliocene, and within-species divergences were estimated during the Pleistocene (<1.0 mya). Analysis II (Fig. 1.11) inferred *Therorhodion* and *Rhododendron* diverging in the late Paleocene (57.68 mya; Table 1.8) and *T. redowskianum* diverging from the *T. camtschaticum–T. glandulosum* clade during the Miocene (14.14 mya). *Therorhodion camtschaticum* and *T. glandulosum* are inferred to have diverged from one another in the late Miocene (9.78 mya), and further within-species divergences occurring during the Pleistocene (<0.1 mya). In analysis III (Fig. 1.12) *Rhododendron* and *Therorhodion* are inferred to have diverged from each other during the Paleocene (57.51 mya; Table 1.8) and *T. redowskianum* diverged from the *T. camtschaticum–T. glandulosum* clade during the Miocene (13.90 mya). *Therorhodion camtschaticum* and *T. glandulosum* are inferred to have diverged from each other later in the Miocene (9.58 mya) with further intraspecific divergences during the Pleistocene (<0.1 mya).

2.4 Discussion

Considering speciation is a continuous evolutionary process resulting in taxa that are found along the evolutionary spectrum of being ecologically distinct (Simpson, 1961), geographically isolated, or reproductively isolated (Dobzhansky, 1935; Mayr, 1942), it is not surprising that there has been little consensus on a single species concept. The traditional methods to delineate species have relied upon morphology, but today there are numerous species concepts taking advantage of a wider variety of available data (Mayden, 1997; Wheeler & Meier, 2000). Increasing emphasis has been placed on combining different lines of evidence for a more fully informed and powerful method for species delimitation, which has been coined the *unified species concept* or *integrative taxonomy* (see de Queiroz, 2007; Carstens et al., 2013; Andújar et al., 2014; Huang & Knowles, 2016). We have tried to follow this approach while assessing *Therorhodion* diversity.

2.4.1 Phylogenetic relationships within Ericaceae.

Our combined Bayesian phylogenetic analysis of molecular data found five well-supported tribes within Ericaceae subfamily Ericoideae, corroborating the results of Kron et al. (2002a) and Gillespie & Kron (2010) (Fig. 1.8). There have been a few taxa of contention in analyses of Ericaceae at the tribal level. Although Kron et al. (2002a), using a combination of molecular (*matK* and *rbcL*) and morphological evidence, found support for the placement of *Daboecia cantabrica* (Huds.) K.Koch in tribe Ericeae and *Diplarche multiflora* in tribe Rhodoreae, our analysis based on the combined chloroplast matrix (Fig. 1.6) and the nuclear/ chloroplast combined matrix (Fig. 1.8) found strong PP support and moderate MPBS support for *Daboecia cantabrica* as sister to the rest of subfamily

Ericoideae (PP 1.0, MPBS 59.9%; PP1.0, MPBS 53.2% respectively). Overall, our phylogeny based on the nuclear dataset was less well-resolved at deeper nodes, but *Daboecia cantabrica* fell within subfamily Ericoideae (Fig. 1.7). We found strong support for *Diplarche multiflora* belonging in tribe Empetreae both in the analysis based on the nuclear dataset as well as when analysing the combined dataset (PP 0.99, MPBS 97.9%; PP 0.76, MPBS 99% respectively; Figs. 1.7, 1.8). This corroborates results by Gillespie & Kron (2010), who also found strong support for *Diplarche multiflora* in tribe Empetreae, but inferred *Daboecia cantabrica* to belong in tribe Ericeae in agreement with Kron et al. (2002a).

2.4.2 Therorhodion sister to Rhododendron and species delineation.

Our Bayesian analysis of the combined dataset supports *Therorhodion* as a sister clade to *Rhododendron* and in turn *Rhododendron* forms a monophyletic clade together with *Menziesia pilosa* (Fig. 1.8). These results corroborate earlier findings of *Therorhodion* as a sister genus to *Rhododendron* based on analysis of morphological characters (Kron & Judd, 1990; Kron et al., 2002a) and molecular sequencing (Kron, 1997 [*matK*]; Kurashige et al., 1998 [*matK, trnK*]; Gao et al., 2002 [ITS region]; Kron et al., 2002a [*rbcL, matK*]; Goetsch et al., 2005 [six regions of the *RPB2-I* gene]; Gillespie & Kron, 2010 [*rbcL, matK, ndhF, trnS-G-G, waxy, nrITS*]). The difference in base chromosome number of *n*=12 in *Therorhodion* versus *n*=13 in the rest of tribe Rhodoreae provides further support for the recognition of *Therorhodion* as a distinct genus (Stevens, 1969; Kurashige et al., 1998). Similarly, the differences of the flowers of *Therorhodion* in comparison to those of *Rhododendron* (Fig. 1.5) support the recognition of *Therorhodion* distinct from *Rhododgendron*, as reflected in a

morphological analysis by Kron & Judd (1990), as well as the reasoning put forth by Hutchinson (1921) and Seithe (1960).

Within *Therorhodion* we recovered three distinct lineages representing *T. camtschaticum* (PP 0.99, MPBS 84.6%), *T. glandulosum* (PP 0.99, MPBS 75%), and *T. redowskianum* (PP 1.0, MPBS 95.6%) forming well-supported monophyletic clades (Fig. 1.9). This supports our first hypothesis that there are three monophyletic lineages within the genus. *Therorhodion redowskianum*, which is restricted to eastern Asia (Fig. 1.2), is the first lineage to diverge and we interpret this as support for an Asian origin of *Therorhodion* and subsequent eastward migration across Beringia.

Traditionally, characters of taxonomic importance in *Therorhodion* include the length of corolla lobes in relation to the corolla tube, whether the corolla is glabrous or pubescent, and the presence of glandular or non-glandular trichomes on the leaf margin, (Hutchinson, 1921; Rhododendron Society, 1930; Seithe, 1960; Hultén, 1968; Kron & Judd, 2009). Floristic descriptions have provided a range of leaf lengths and widths for *Therorhodion* since Small (1914) raised it to the generic level. *Therorhodion redowskianum* is consistently described as having leaves that are 0.5–1.5 cm long and 0.3–0.6 cm wide (Hutchinson, 1921; Rhododendron Society, 1930; He & Chamberlain, 2005). Because *T. redowskianum* is smaller morphologically and easily delineated, we will focus instead on *T. camtschaticum* and *T. glandulosum* in subsequent comparisons.

Historically, *T. camtschaticum* has been described as having larger leaves (~2–5 cm) than *T. glandulosum* (~1–2 cm; Hutchinson, 1921; Rhododendron Society, 1930; Ohwi, 1965; Shishkin & Bobrov, 1967). Yet newer North American descriptions have described *T. camtschaticum* and *T. glandulosum* leaves as being relatively similar in both length and

width (Viereck & Little, 2007; Kron & Judd, 2009; Fig. 1.1). Based on our leaf measurements (Table 1.4; Fig. 1.4) *T. camtschaticum* and *T. glandulosum* are significantly different in leaf length and width, although we would not consider this to be a reliable trait to distinguish the two in the field. However, the presence or absence of glandular-tipped trichomes on the leaves is a clear species delineator for *T. camtschaticum* and *T. glandulosum* (Fig. 1.1) commonly used in taxonomic keys (Small, 1914; Hutchinson, 1921; Hultén, 1968; Viereck & Little, 2007; Kron & Judd, 2009) along with differences in corolla pubescence.

The length of the corolla lobes in relation to the corolla tube has been described as a small differentiating character between *T. camtschaticum* and *T. glandulosum* (Hutchinson, 1921; Rhododendron Society, 1930). When Small (1914) described *T. glandulosum* as a new species he used the length of the corolla lobes and corolla tube of *T. camtschaticum* and *T. glandulosum* as a distinguishing character. Subsequent authors have de-emphasized this character (Kron & Judd, 2009) following Stevens' statement, "it is clear that the fusion of the corolla in the Ericaceae is not of fundamental significance" (1969, p 39). Instead, the corolla character of importance is the pubescence on the abaxial petal surface and the margin of the lobes in *T. camtschaticum* as compared to glabrous petals in *T. glandulosum.*

Pollen in *Therorhodion* is shed in tetrads held together in clumps by viscin threads (Fig. 1.5), this character is restricted to the Rhododendroideae within Ericaceae (Stevens, 1969). Sarwar & Takahashi (2013) found that the palynological similarities between *Rhododendron* and *Therorhodion* might support their sister relationship. Although they did include samples of *T. camtschaticum* and *T. redowskianum* in their study, they only reported the average pollen measurements for *T. camtschaticum* (equatorial diameter: 35.0±3.6 μm), which is comparable to our average measurement of 37.02±1.26 μm, 43.8

(±2.21) µm and 40.25 (±1.63) µm for *T. glandulosum* and *T. redowskianum* respectively (Table 1.5; Fig. 1.5). In addition, exine ornamentation is also uniform within *Therorhodion* and thus pollen morphology is of low taxonomic utility.

In addition to vegetative and reproductive characters, geographic distribution of taxa is often considered when delimiting species, particularly when categorizing a taxon at the specific or subspecific level (Nordal & Razzhivin, 1999; Stuessy, 2009). The amount of geographic overlap in addition to morphological differences is often taken into consideration when delimiting species (Stuessy, 2009). For example, Rose & Freudenstein (2014) found that an integrative approach including distributional data for the genus *Monotropsis* Schwein. (Ericaceae) strongly supports two distinct species rather than subspecies because they are geographically isolated from each other.

The distributional range of the three monophyletic lineages of *Therorhodion* is one of the main reasons why *T. glandulosum* is often considered a subspecies of *T. camtschaticum*, particularly where their ranges overlap in the Russian Far East (Fig. 1.2). This creates the possibility for hybridization, although there is no documented record of this taking place. There is a difference in taxonomic tradition between Asia and North America in regards to the use of geographical distribution for classification (Elven et al., 2011). Russian descriptions typically use the subspecific concept for taxa with partially overlapping distributions (Elven et al., 2011), describing *T. camtschaticum* subsp. *camtschaticum* and subsp. *glandulosum* (Yurtsev et al., 2010; Takahashi, 2015); American botanists instead recognize two distinct species (Viereck & Little, 2007; Kron & Judd, 2009). However, the extent that these ranges overlap in Asia is not entirely clear. The Asian range of *T. camtschaticum* is often simply described as the Kamchatka Peninsula and the

Kurile Islands (Pallas, 1784; Small, 1914; Hutchinson, 1921; Voroshilov, 1982), and that of *T. glandulosum* as the Kamchatka and Chukotka peninsulas (Busch, 1915; Komarov, 1929), which suggests that the entire Kamchatka Peninsula is an area of sympatry. Hultén (1930, 1937), as well as Phillipson & Phillipson (1986), described *T. camtschaticum* as occurring in southern and eastern Kamchatka and *T. glandulosum* in northern Kamchatka, so perhaps the area of sympatry is much smaller than typically described and thus less opportunity exists for hybridization. In North America *T. camtschaticum* and *T. glandulosum* are allopatric (Fig. 1.2) and are commonly described as distinct species (Viereck & Little, 2007; Kron & Judd, 2009).

Based on the three strongly supported monophyletic clades within *Therorhodion,* we recognize three species: *T. camtschaticum* (PP 0.99. MPBS 84.6%), *T. glandulosum* (PP 0.99, MPBS 75%), and *T. redowskianum* (PP 1.0, MPBS 95.6%; Fig. 1.9). This is consistent with other studies using strong molecular support to assist in species delimitation. The circumboreal fern genus *Cryptogramma* R.Br. has been recognized as containing as few as two species (Hultén, 1968; Tryon & Tryon, 1990) to as many as ten (Lellinger, 1985; Vaganov et al., 2010). Based on the significantly supported monophyletic clades obtained for *Cryptogramma* using six plastid loci and one nuclear locus, Metzgar et al. (2013) recognize eight species that reflect mostly allopatric reciprocally monophyletic lineages that are on independent evolutionary trajectories. Al-Shehbaz et al. (2007) recognize four North American species in the flowering genus *Parrya* R.Br. (Brassicaceae) instead of one, based on a combination of molecular and morphological support, including the amphiberingian *P. nudicaulis* (L.) Regel. In contrast to these examples, Carlsen et al. (2010)

used microsatellites, *ITS*, and a combined plastid dataset to merge three *Smelowskia* C.A.Mey. species into one, the amphiberingian *S. porsildii* (W.H.Drury & Rollins) Jurtzev.

2.4.3 Comparison of divergence times and use of constraints

The effects of applying multiple calibrations on different nodes have been tested several times using simulated and empirical datasets (Meredith et al., 2011; Sauquet et al., 2012; Paradis, 2013; Duchêne et al., 2014). Placing fossil constraints unevenly throughout the phylognetic tree (e.g. mostly on shallower or deeper nodes) can result in divergence times that are inconsistent between analyses or directly in conflict with the fossil record, whereas more evenly distributed constraints can result in more consistent age estimates (Meredith et al., 2011). Misplacing fossils as calibrations can also lead to biased divergence times. When it is unclear whether a fossil should be placed within the crown or stem group the practice is to treat it as a stem fossil, which can lead to an underestimation of divergence times (Bell & Donoghue, 2005). Parham et al. (2012) argue for the use of a specimen-based approach when applying fossil calibrations to the correct nodes. Sauquet et al. (2012) suggest that if the study group does not have appropriate fossils to use as constraints, then it would be more beneficial to expand the outgroup in order to use a single fossil calibration rather than apply a single secondary calibration to the ingroup.

Using an empirical dataset for the genus *Nothofagus* Blume (Nothofagaceae), Sauquet et al. (2012) compared the effects of different scenarios of fossil calibrations to only using secondary constraints. They found that secondary constraints resulted in much younger age estimates (age of crown group *Nothofagus* 16.7–39.5 mya), whereas fossil calibrations typically led to older estimates (age of crown group *Nothofagus* 53.4–93.2

mya). Using simulated data Schenk (2016) also showed differences in divergence estimation from analyses using fossil or secondary constraints.

When we applied only secondary constraints (analysis I), our analysis inferred younger divergence times and mostly narrower confidence intervals for all nodes compared to analysis II (fossil constraints only) and analysis III (secondary and fossil constraints) (Table 1.8). This corroborates results in Schenk (2016) from an analysis of simulated data as well as results from Sauquet et al. (2012) for an empirical dataset. Despite this overall congruence of inferring younger node ages when using only secondary constraints, the node divergence between *Rhododendron* and *Therorhodion* that was calibrated with the fossil *Paleoenkianthus sayrevillensis* Nixon & Crepet from the Late Turonian (~90 mya; Table 1.6; Nixon & Crepet, 1993) in analyses II and III was inferrred to be older in both analyses II and III than in analysis I. We observed confidence intervals that were narrower when using fossil constraints as compared to using secondary constraints.

Previous studies have included *Therorhodion* in divergence time analyses, sometimes under *Rhododendron* (Table 1.8), using different calibration methods. The oldest known estimated divergence time for *Therorhodion* from *Rhododendron* was inferred by Milne (2004) to be approximately 51.5 to 76.5 mya, spanning the Cretaceous–Paleogene extinction event. Milne's study predates the release of BEAST (Drummond et al., 2012) and he predicted divergence times using the synonymous substitution rate for the plastid locus *matK*. Liu et al. (2014), who conducted their analyses with BEAST, only used fossil constraints and found the estimated divergence time for *Therorhodion* from *Rhododendron* to be 58.33 mya (HPD 56.48–61.20). Both of these estimates span the same divergence times that analysis III (using a combination of fossil and secondary constraints)

inferred for *Therorhodion* and *Rhododendron* (57.51 mya, HPD 56.52–58.63). Merckx et al. (2015) used a substitution rate for the nuclear ITS and a secondary constraint at the root of their phylogenetic tree to infer the divergence time of *Therorhodion* and *Rhododendron* to be 36.25 mya (HPD 26.65–40.50), which is younger than our inferred times from analysis III and more comparable to our inferred times from analysis I (Fig 1.13, Table 1.8). In addition, Merckx et al. (2015) also inferred a divergence time of 11.72 mya (HPD 2.30–19.61) for *T. redowskianum* from *T. camtschaticum*, which overlaps with the age estimates we inferred in all three analyses (Table 1.8). The different types of constraints used in these different studies likely have a great deal to do with the variation in divergence time estimation. Because the use of only secondary constraints in divergence time analyses has been criticized and our age estimates between analyses II and III are so similar, we will focus our subsequent discussion on the results of analysis III.

2.4.4 Biogeographic relations between the Arctic and southern high mountains—Out of Asia?

The similarity of the Arctic flora with the flora of the southern high mountains of central Asia, Europe, and North America has led many to hypothesize that the Arctic flora has been largely recruited from high mountains in the south (Hultén, 1937; Tomalchev, 1960; Weber, 1965; Hedberg, 1992) including taxa that were pre-adapted to cooler climates (Murray, 1992, 1997; Hoffmann & Röser, 2009; Hoffmann et al., 2010). Evidence for this northward migration and origin in southerly high mountains has been shown in *Ranunculus glacialis* L. by Schönswetter et al. (2003). *In situ* diversification in the Arctic was put forth for several lineages of Arctic *Artemisia,* which diversified contemporaneously with the Arctic biome that originated approximately 2–3 mya (Murray, 1995; Abbott et al.,

2000; Abbott & Brochmann, 2003), whereas other lineages in *Artemisia* were inferred to be much older (Tkach et al., 2008).

In Asia, the Himalaya and Hengduan Mountains (HHM) and the Qinghai-Tibetan Plateau are often inferred to be a major source of Arctic taxa (Hedberg, 1992; Hou et al., 2016a). Contrary to prevailing hypotheses that a northward movement of those taxa coincided with the formation of the tundra biome some 2-3 mya (Murray, 1995; Abbott et al., 2000; Abbott & Brochmann, 2003), evidence is mounting that a split between Arctic species and those in the HHM is much more ancient, dating back to the middle Miocene to early Pleistocene as shown for *Silene acaulis* L. (Caryophyllaceae; Gussarova et al., 2015), *Cassiope* D.Don (Ericaceae; Hou et al., 2016b), and *Diapensia* L. (Diapensiaceae; Hou et al., 2016a). All three taxa are common in Beringia.

The southern Rocky Mountains in the United States are likewise thought of as a source of Arctic taxa (Weber, 1965) and Hoffmann et al. (2010) showed that *Ranunculus glacialis/ R. chamissonis* Schltdl. diverged from each other in the early Miocene and became specialized on screes and glacial moraines in Arctic and high-alpine biomes. There is also fossil evidence for the adaptation of some taxa *in situ* in the Arctic (Murray, 1992), and a Beringian origin has been supported by molecular studies for some taxa (Eidesen et al., 2007; Abbott et al., 2000; Tkach et al., 2008; Godfrey & Gillespie, 2015).

The Bering land bridge (BLB) has often been inferred as the mode of dispersal for plant taxa between eastern Asia and North America, particularly for Arctic-alpine species (Hedberg, 1992; Wen, 1999; Donoghue & Smith, 2004; Nie et al., 2006; Eidesen et al., 2007; DeChaine, 2008; Ickert-Bond et al., 2009; Xie et al., 2009; Carlsen et al., 2010; Wen et al., 2010, 2016). Based on different climatic and floristic conditions of the BLB, Sanmartín et al.

(2001) discussed three time periods when the BLB is believed to have acted as a corridor for dispersal. BLB I extended from the early Paleogene (approximately 56.0 mya) to approximately 35 mya and was characterized by warm-temperate groups associated with the boreotropical-mixed mesophytic forest (Tiffney, 1985). BLB II extended from 10–14 mya to about 3.5 mya, and was characterized by boreal groups associated with taiga-coniferous forests. BLB III extended, on and off, from about 1.5 mya to around the end of the Pleistocene (approximately 0.01 mya) and was characterized by Arctic groups associated with steppe-like treeless tundra vegetation. Even during periods of warmer climate the northern latitude of the BLB would have acted as a barrier to some taxa, especially evergreen species, due to shortened daylight during the winter months (Tiffney & Manchester, 2001). By the Neogene (23.0 mya), deciduous plants are believed to have dominated Beringia along with conifers (Wen, 1999; Sanmartín et al., 2001; Tiffney & Manchester, 2001; Wen et al., 2016).

The Ericaceae has been shown to be particularly rich near the upper margin of the montane zone worldwide (Schwery et al., 2015). Our results indicate that *Therorhodion* diverged from *Rhododendron* 57.51 mya (HPD 56.52–58.63) during the Paleocene and this split likely represents a divergence from more warm temperate ancestors with a Tertiary relictual distribution (Tiffney, 1985; Wen, 1999; Milne & Abbott, 2002). The earliest diverging lineage of *Therorhodion*, *T. redowskianum,* is restricted to the alpine-tundra of the high Changbai mountains in Jilin Province, China (2000–2600 m; He & Chamberlain, 2005), and the surrounding Manchurian region as well as central Sakhalin. A divergence age of 13.90 mya (HPD 7.57–21.54) was inferred for the split between *T. redowskianum* and the *T. camtschaticum*/ *T. glandulosum* clade during the middle Miocene (Table 1.8, Fig. 1.13)

when persistent sea ice was present (Krylov et al., 2008) and temperatures were cooling from the warmer Paleogene. Both the spatial and temporal extent of this divergence point to an out-of-Asia origin for *Therorhodion* from the treeless mountaintops in Asia as promoted by Tolmachev (1960) for many Arctic-alpine species. Then a suitable habitat in Beringia facilitated the expansion of the ranges of the *T. camtschaticum/ T. glandulosum* clade to form a classic Beringian endemic distribution (Tolmachev, 1960; Murray et al., 1994).

Although the divergence of *T. camtschaticum* and *T. glandulosum* from each other corresponds with the time that the BLB II would have been available (5.07–14.50 mya; Fig. 1.13; Table 1.8), the boreotropical-mixed mesophytic forest present during this period would not have been conducive to dispersal. However, the environment of the BLB III would have been more favorable for *Therorhodion*, which commonly occurs in an alpine-tundra environment, as *T. camtschaticum* and *T. glandulosum* continued to expand their range. The radiation of *T. glandulosum* is inferred to have begun 1.73 mya (HPD 0.35–3.62; Table 1.8), when the BLB III would have been open, and coincided with the emergence of the Arctic tundra biome, more precisely the mid-Pleistocene transition (Clark et al., 2006). Long-term sea ice volume increased during this interval and global temperatures decreased. The intraspecific diversification in *T. glandulosum* was more recent than Hultén (1937) proposed for many Arctic plants. *Therorhodion camtschaticum* began radiating 6.39 mya ago (analysis III; Table 1.8) when the BLB II would have been open. However, although the BLB III would have been a favorable environment for *T. glandulosum* to migrate from western Beringia (Chukotka) to eastern Beringia (Seward Peninsula), *T. camtschaticum*

does not occur as far north on either side of the Bering Strait today and the BLB II likely had a less suitable habitat for its eastern migration.

It has been suggested that the Aleutian Islands may have once formed a more southerly land bridge compared to the BLB (McKenna, 1983). However, there is little evidence, besides some geological, to support an Aleutian land bridge and this southerly land bridge would have likely been open from about 42–15 mya (DeLong et al., 1978; McKenna, 1983), long before *T. camtschaticum* would have been using it for dispersal. The Aleutian Islands are considered a good example of a *two-way filter bridge* (Carlquist, 1965) with some species being more prevalent in the eastern or western part of the island chain depending on their continent of origin, but it did not act as a filter for *T. camtschaticum*, which is known to occur equally across all of the Aleutians. The southern region of the BLB could have been used for dispersal by *T. camtschaticum*, but Hultén (1937) considered the flora of the Aleutian Islands to belong to the same floral region as Kamchatka rather than the Alaska Peninsula, further supporting its Asian origin. However, glaciers covered the Alaska Peninsula and much of the Aleutian Islands throughout the Quaternary, although much of the Aleutians were free of ice greater than 9000 years ago (Detterman, 1986; Thorson & Hamilton, 1986). There is also sparse evidence for glaciation on the Alaska Peninsula and the Aleutian Islands predating the Quaternary due to weathering and erosion (Detterman, 1986; Thorson & Hamilton, 1986). This makes it difficult to tell whether *T. camtschaticum* first migrated eastward across the southern region of the BLB before expanding westward across the Aleutians as glaciers retreated, or made an eastward migration across the Aleutians from Kamchatka to Alaska.

Both the spatial and temporal extent of the inferred divergences in *Therorhodion* point to an out-of-Asia origin, a pattern that has been shown for the majority of eastern Asian–North American disjunct plants (Wen 1999, 2001; Wen et al., 2016). The genus *Lysichiton* Schott (Araceae) contains two species: *L. camtschatcensis* (L.) Schott restricted to Japan and the Russian Far East, and *L. americanus* Hultén & H.St.John distributed in western and northwestern North America (Nie et al., 2006). Divergence time estimation infers the age of the split between Asia and North America to approximately 3–11 mya, when the BLB II would have been available (Nie et al., 2006). Based on a dispersal-vicariance analysis, Nie et al. (2006) found strong support for an Asian origin of *Lysichiton* and subsequent migration to North America via the BLB.

Although the BLB may have acted as a corridor for dispersal, several studies have commented on the asymmetry of the dispersal in an eastward direction (Waltari et al., 2007; Wen et al., 2010, 2016), but the New World has also been inferred as the ancestral area for several East Asian–North American disjuncts (Wen, 1999, 2001; Wen et al., 2016). Xie et al. (2009) used phylogenetic and divergence time analyses to confirm a New World origin for the flowering genus *Circaea* L. (Onagraceae). Their analyses inferred three separate dispersals from North America to Eurasia at 7.69–24.53 mya spanning the availability of BLB II, and two times from Eurasia to North America at 2.99–9.68 mya and 0.66–3.53 mya during periods that BLB II and III would have been open (Xie et al., 2009; Sanmartín et al., 2001).

2.4.5 Lack of sufficient sequence divergence prevents analysis of geographic structuring within Beringia

Geographic structuring in Beringia has been documented in small mammals (Eddingsaas et al., 2004; Hope et al., 2011; Kohli et al., 2015), birds (Zink et al., 1995; Pruett & Winker, 2005), and Arctic plants (Eidesen et al., 2007; Carlsen et al., 2010). However, intraspecific geographic structure was lacking in our analyses and accessions of *T. glandulosum* form a polytomy and thus do not support distinct western and eastern Beringian clades (Fig. 1.9). Within *T. camtschaticum* there are a few moderately supported subclades, but these also do not represent distinct western and eastern Beringian clades. Five out of seven of the Aleutian Island samples form a subclade with one of the samples from Kodiak Island. Of the two remaining Aleutian Island samples, one forms a subclade with one sample from Kamchatka and the other forms a polytomy with the second sample from Kamchatka. The three remaining samples, from Kodiak Island and Sakhalin, form another subclade (Fig. 1.9). This lack of intraspecific resolution could be a result of too little time of separation between western and eastern Beringian populations, too few samples representing populations, or perhaps enough gene flow continues to occur to prevent genetic differentiation. Additional gene regions with higher resolving power may also need to be targeted in order to decipher population divergence and infer geographic structure of *Therorhodion* within Beringia.

2.4.6 Conclusions

Our results provide further support that *Therorhodion* contains three species: *T. redowskianum, T. camtschaticum*, and *T. glandulosum*. Furthermore, they are easy to distinguish morphologically. *Therorhodion redowskianum* is easily recognized through its

smaller size in addition to the glandular trichomes on the margin of the leaves. *Therorhodion camtschaticum* has non-glandular trichomes on the margin and abaxial side of the leaves, whereas *T. glandulosum* has glandular trichomes. Leaf trichomes in addition to the described differences in pubesence on the corolla lobes of *T. camtschaticum* as compared to the glabrous corolla lobes of *T. glandulosum* make distinguishing between these two species easy. The areas of sympatry between these two species in Asia is one of the leading causes for their subspecies classification in Asian floras. It would be helpful to get a clearer picture of their distributions in the Russian Far East and whether there are clear ecological differences between the species.

Additionally, our divergence time analyses corroborated previous findings that generally showed younger age estimates when using secondary constraints exclusively (Shaul & Graur, 2002; Morrison, 2010; Schenk, 2016). When we used fossil constraints our age estimates support the out-of-Asia hypothesis and we are able to infer the BLB as the most likely route of dispersal for *Therorhodion glandulosum* during the Pleistocene (~0.35–3.74) and the strong possiblity of the Aleutians being the route of dispersal for *T. camtschaticum*, expanding current knowledge on floristic exchange between Asia and North America during periods of climatic fluctuation. However, our results did not have the resolving power to distinguish between eastern and western Beringian populations within *T. camtschaticum* and *T. glandulosum*. Targeting more variable DNA regions could help resolve these intraspecific relationships and potentially offer further support for an Asian origin and diversification within Beringia. Brown et al. (2006) were able to successfully resolve relationships at lower taxonomic levels within *Rhododendron* using the cpDNA regions *psbA-trnH* and *trnT-trnL*. Continued investigation into the habitat preferences of *T.*

camtschaticum and *T. glandulosum* throughout Beringia may also reveal what has driven the divergence.

References

Abbott RJ, Brochmann C. 2003. History and evolution of the Arctic flora: In the footsteps of Eric Hultén. *Molecular Ecology* 12: 299–313.

Abbott RJ, Smith LC, Milne RI, Crawford RMM, Wolff K, Balfour J. 2000. Molecular analysis of plant migration and refugia in the Arctic. *Science* 289: 1343–1346.

Al-Shehbaz IA, Grant JR, Lipkin R, Murray DF, Parker CL. 2007. *Parrya nauruaq* (Brassicaceae), a new species from Alaska. *Novon* 17: 275–278.

Albach DC, Soltis PS, Soltis DE, Olmstead G. 2001. Phylogenetic analysis of asterids based on sequences of four genes. *Annals of the Missouri Botanical Garden* 88: 163–212.

Albert VA, Williams SE, Chase MW. 1992. Carnivorous plants: Phylogeny and structural evolution. *Science* 257: 1491–1495.

Andújar C, Arribas P, Ruiz C, Serrano J, Gómez-Zurita J. 2014. Integration of conflict into integrative taxonomy: Fitting hybridization in species delimitation of *Mesocarabus* (Coleoptera: Carabidae). *Molecular Ecology* 23: 4344–4361.Carstens BC, Pelletier TA, Reid NM, Satler JD. 2013. How to fail at species delimitation. *Molecular Ecology* 22: 4369–4383.

Axelrod DI. 1987. *The late Oligocene Creede Flora, Colorado*. Berkeley: University of California Press.

Bell CD, Donoghue MJ. 2005. Dating the Dipsacales: Comparing models, genes, and evolutionary implications. *American Journal of Botany* 92: 284–296.

Bliss LC. 1979. Arctic heathlands. In: *Ecosystems of the world 9A: Heathlands and related shrublands*. Amsterdam: Elsevier. 415–424.

Brown GK, Craven LA, Udovicic F, Ladiges PY. 2005. Phylogeny of *Rhododendron* section Vireya (Ericaceae) based on two non-coding regions of cpDNA. *Plant Systematics and Evolution* 257: 57–93.

Brown GK, Nelson G, Ladiges PY. 2006. Historical biogeography of *Rhododendron* section Vireya and the Malesian Archipelago. *Journal of Biogeography* 33: 1929–1944.

Bryson RW Jr, Prendini L, Savary WE, Pearman PB. 2014. Caves as microrefugia: Pleistocene phylogeography of the troglophilic North American scorpion *Pseudouroctonus reddelli*. *BMC Evolutionary Biology* 14: 9.

Busch E. 1915. *Therorhodion*. In: *Flora Sibiriae Et Orientis Extremi Vol 2*. Saint Petersburg: Russian Academy of Sciences. 63: 35–41. (The Russian edition of *Flora of Siberia and the Far East*).

Bush CM, Kron KA. 2008. The phylogeny of *Bejaria* (Ericaceae; Ericoideae) based on molecular data. *Journal of the Botanical Research Institiute of Texas* 2: 1193–1205.

Carlquist S. 1965. *Island life: A natural history of the islands of the world.* New York: The Natural History Press.

Carlsen T, Elven R, Brochmann C. 2010. The evolutionary history of Beringian *Smelowskia* (Brassicaceae) inferred from combined micosatellite and DNA sequence data. *Taxon* 59: 427–438.

Carstens BC, Pelletier TA, Reid NM, Satler JD. 2013. How to fail at species delimitation. *Molecular Ecology* 22: 4369–4383.

Clark PU, Archer D, Pollard D, Blum JD, Rial JA, Brovkin V, Mix AC, Pisias NG, Roy M. 2006. The middle Pleistocene transition: Characteristics, mechanisms, and implications for long-term changes in atmospheric pCO_2. *Quaternary Science Reviews* 25: 3150–3184.

Collinson ME, Crane PR. 1978. *Rhododendron* seeds from the Palaeocene of southern England. *Botanical Journal of the Linnean Society* 76: 195–205.

Cunningham CW. 1997. Can three incongruence tests predict when data should be combined? *Molecular Biology and Evolution* 14: 733–740.

DeChaine EG. 2008. A bridge or a barrier? Beringia's influence on the distribution and diversity of tundra plants. *Plant Ecology and Diversity* 1: 197–207.

DeLong SE, Fox PJ, McDowell FW. 1978. Subduction of the Kula Ridge at the Aleutian Trench. *Geological Society of America Bulletin* 89: 83–95.

de Queiroz K. 2007. Species concepts and species delimitation. *Systematic Biology* 56: 879–886.

Detterman RL. 1986. Glaciation of the Alaska Peninsula. In: Hamilton TD, Reed KM, Thorson RM eds. *Glaciation in Alaska: The geologic record*. The Alaska Geological Society. 151–170.

Dobzhansky T. 1935. A critique of the species concept in biology. *Philosophy of Science* 2: 344–355.

Donoghue MJ, Smith SA. 2004. Patterns in the assembly of the temperate forest around the Northern Hemisphere. *Philosophical Transactions of the Royal Society of London B: Biological Sciences* 359: 1633–1644.

Drummond AJ, Suchard MA, Xie D, Rambaut A. 2012. Bayesian phylogenetics with BEAUti and the BEAST 1.7. *Molecular Biology and Evolution* 29: 1969–1973.

Duchêne S, Lanfear R, Ho SYW. 2014. The impact of calibration and clock-model choice on molecular estimates of divergence times. *Molecular Phylogenetics and Evolution* 78: 277–289.

Eddingsaas AA, Jacobsen BK, Lessa EP, Cook JA. 2004. Evolutionary history of the Arctic ground squirrel (*Spermophilus parryii*) in Nearcitic Beringia. *Journal of Mammalogy* 85: 601–610.

Eidesen PB, Carlsen T, Molau U, Brochmann C. 2007. Repeatedly out of Beringia: *Cassiope tetragona* embraces the Arctic. *Journal of Biogeography* 34: 1559–1574.

Elven R, Murray DF, Yurtsev BA. 2011. Annotated checklist of the Panarctic Flora (PAF) vascular plants [online]. Available from http://nhm2.uio.no/paf [accessed 14 March 2017].

Erdtman G. 1960. The acetolysis method: A revised description. *Svensk Botanisk Tidskrift* 54: 561–564.

Farris JS, Källersjö M, Kluge AG, Bult C. 1995. Testing significance of incongruence. *Cladistics* 10: 315–319.

Flora of North America Editorial Committee eds. 1993+. *Flora of North America north of Mexico*. 20+ vols. New York: Oxford University Press.

Floyd JW. 2002. Phylogenetic and biogeographic patterns in *Gaylussacia* (Ericaceae) based on morphological, nuclear DNA, and chloroplast DNA variation. *Systematic Botany* 27: 99–115.

Freudenstein JV. 1999. Relationships and character transformation in Pyroloideae (Ericaceae) based on ITS sequences, morphology, and development. *Systematic Botany* 24: 398–408.

Friis EM. 1979. The Damgaard flora: A new Middle Miocene flora from Denmark. *Bulletin of the Geological Society of Denmark* 27: 117–142.

Fuji N, Senni K. 2006. Phylogeography of Japanese alpine plants: Biogeographic importance of alpine region of Central Honshu in Japan. *Taxon* 55: 43–52.

Gao L, Li D, Zhang C. 2003. Phylogenetic relationships of *Rhododendron* section *Azaleastrum* (Ericaceae) based on ITS sequences. *Acta Phytotaxonomica Sinica* 41: 173–179.

Gao LM, Li DZ, Zhang CQ, Yang JB. 2002. Infrageneric and sectional relationships in the genus *Rhododendron* (Ericaceae) inferred from ITS sequence data. *Acta Botanica Sinica* 44: 1351–1356.

Gillespie E, Kron K. 2010. Molecular phylogenetic relationships and a revised classification of the subfamily Ericoideae (Ericaceae). *Molecular Phylogenetics and Evolution* 56: 343–54.

Godfrey S, Gillespie L. 2015. Systematics and phylogeography of *Parrya* (Brassicaceae) in the North American Arctic. *Botany 2015 Meetings* [online]. Available from http://2015.botanyconference.org/ [accessed 10 April 2017].

Goetsch L, Eckert AJ, Hall BD. 2005. The molecular systematics of *Rhododendron* (Ericaceae): A phylogeny based upon *rpb2* gene sequences. *Systematic Botany* 30: 616–626.

Grant ML, Toomey NH, Culham AC. 2004. Is there a such thing as *Kalmia x Rhododendron*? *Journal of the American Society of Horticultural Science* 129: 517–522.

Gray A. 1878. *Synoptical flora of North America, vol. II, part I*. New York: Ivison, Blakeman, Taylore, and Company.

Gussarova G, Allen GA, Mikhaylova Y, McCormick LJ, Mirré V, Marr KL, Hebda RJ, Brochmann C. 2015. Vicariance, long-distance dispersal, and regional extinction-recolonization dynamics explain the disjunct circumpolar distribution of the Arctic-alpine plant *Silene acaulis*. *American Journal of Botany* 102: 1703–1720.

Hasegawa M, Kishino H, Yano T. 1985. Dating of the human-ape splitting by a molecular clock of mitochondrial DNA. *Journal of Molecular Evolution* 22: 160–174.

He M, Chamberlain DF. 2005. *Rhododendron* subg. *Therorhodion* (Maximowicz). In: Wu ZY, Raven PH eds. *Flora of China, vol 14* [online]. Available from http://www.efloras.org [accessed 24 August 2016].

Hedberg KO. 1992. Taxonomic differentiation in *Saxıfraga hirculus* L. (Saxifragaceae)—A circumpolar Arctic-Boreal species of Central Asiatic origin. *Botanical Journal of the Linnean Society* 109: 377–393.

Hoffmann MH, Röser M. 2009. Taxon recruitment of the Arctic flora: An analysis of phylogenies. *The New Phytologist* 182: 774–780.

Hoffmann MH, von Hagen KB, Hörandl E, Röser M, Tkach NV. 2010. Sources of the Arctic flora: Origins of Arctic species in *Ranunculus* and related genera. *International Journal of Plant Sciences* 171: 90–106.

Hope AG, Waltari E, Fedorov VB, Goropashnaya AV, Talbot SL, Cook JA. 2011. Persistence and diversification of the Holarctic shrew, *Sorex tundrensis* (Family Soricidae), in response to climate change. *Molecular Ecology* 20: 4346–4370.

Hopkins DM ed. 1967. *The Bering land bridge*. Stanford: Stanford University Press.

Hou Y, Bjorå CS, Ikeda H, Brochmann C, Popp M. 2016a. From the north into the Himalayan-Hengduan Mountains: Fossil-calibrated phylogenetic and biogeographical inference in the Arctic-alpine genus *Diapensia* (Diapensiaceae). *Journal of Biogeography* 43: 1502–1513.

Hou Y, Nowak MD, Mirré V, Bjorå CS, Brochmann C, Popp M. 2016b. RAD-seq data point to a northern origin of the Arctic-alpine genus *Cassiope* (Ericaceae). *Molecular Phylogenetics and Evolution* 95: 152–160.

Huang JP, Knowles LL. 2016. The species versus subspecies conundrum: Quantitative delimitation from integrating multiple data types within a single Bayesian approach in Hercules beetles. *Systematic Biology* 65: 685–699.Stuessy TF. 2009. *Plant taxonomy: The systematic evaluation of comparative data.* New York: Columbia University Press.

Huelsenbeck JP, Ronquist F. 2001. MRBAYES: Bayesian inference of phylogeny. *Bioinformatics* 17: 754–755.

Hultén E. 1930. *Flora of Kamtchatka and the adjacent islands, vol. 4*. Stockholm: Almqvist and Wiksells.

Hultén E. 1937. *Flora of the Aleutian Islands and westernmost Alaska Peninsula with notes on the flora of the Commander Islands*. Stockholm: Tryckeri Aktiebolaget Thule.

Hultén E. 1968. *Flora of Alaska and neighboring territories: A manual of the vascular plants*. Stanford: Standford University Press.

Hutchinson J. 1921. XXIII - The genus *Therorhodion*. *Bulletin of Miscellaneous Information Kew* 5: 201–205.

Ickert-Bond SM, Murray DF, DeChaine E. 2009. Contrasting patterns of plant distribution in Beringia. *Alaska Park Science* 8: 26–32.

Ikeda H, Setoguchi H. 2007. Phylogeography and refugia of the Japanese endemic alpine plant, *Phyllodoce nipponica* Makino (Ericaceae). *Journal of Biogeography* 34: 169–176.

Iwatsuki K, Yamazaki T, Boufford DE, Ohba H eds. 1993. *Flora of Japan*. Tokyo: Kodansha Ltd.

Kohli BA, Fedorov VB, Waltari E, Cook JA. 2015. Phylogeography of a Holarctic rodent (*Myodes rutilus*): Testing high-latitude biogeographical hypotheses and the dynamics of range shifts. *Journal of Biogeography* 42: 377–389.

Komarov VL. 1907. *Flora Manshuriae Vol. III*. Saint Petersburg.

Komarov VL. 1929. *Flora of Kamchatka Peninsula*. Leningrad: USSR Academy of Science Publisher.

Kron K. 1997. Phylogenetic relationships of Rhododendroideae (Ericaceae). *American Journal of Botany* 84: 973–980.

Kron KA, Chase MW. 1993. Systematics of the Ericaceae, Empetraceae, Epacridaceae, and related taxa based upon *rbcL* sequence data. *Annals of the Missouri Botanical Garden* 80: 735–741.

Kron KA, Judd WS. 1990. Phylogenetic relationships within the Rhodoreae (Ericaceae) with specific comments on the placement of *Ledum*. *Systematic Botany* 15: 57–68.

Kron KA, Judd WS. 2009. *Therorhodion*. In: Flora of North America Editorial Committee eds. *Flora of North America north of Mexico.* 20+ vols. New York: Oxford University Press. Vol. 8, 453–543.

Kron KA, Judd WS, Stevens PF, Crayn DM, Anderberg AA, Gadek PA, Quinn CJ, Luteyn JL. 2002a. Phylogenetic classification of Ericaceae: Molecular and morphological evidence. *The Botanical Review* 68: 335–423.

Kron KA, King JM. 1996. Cladistic relationships of *Kalmia*, *Leiophyllum*, and *Loiseleuria* (Phyllodoceae, Ericaceae) based on *rbcL* and *nrITS* data. *Systematic Botany* 21: 17–29.

Kron KA, Powell EA, Luteyn JL. 2002b. Phylogenetic relationships within the blueberry tribe (Vaccinieae, Ericaceae) based on sequence data from *matK* and nuclear ribosomal *ITS* regions, with comments on the placement of *Satyria*. *American Journal of Botany* 89: 327–336.

Krylov AA, Andreeva IR, Vogt C, Backman J, Krupskaya VV, Grikurov GE, Moran K, Shoji H. 2008. A shift in heavy and clay mineral provenance indicates a middle Miocene onset of perennial sea ice cover in the Arctic Ocean. *Paleoceanography* 23: doi: 10.1029/2007PA001497.

Kurashige Y, Etoh J-I, Handa T, Takayanagi K, Yukawa T. 2001. Sectional relationships in the genus *Rhododendron* (Ericaceae): Evidence from *matK* and *trnK* intron sequences. *Plant Systematics and Evolution* 228: 1–14.

Kurashige Y, Mine M, Kobayashi N, Handa T, Takayanagi K, Yukawa T. 1998. Investigation of sectional relationships in the genus *Rhododendron* (Ericaceae) based on *matK* sequences. *The Journal of Japanese Botany* 73: 143–154.

Lellinger DB. 1985. *A field manual of the ferns and fern-allies of the United States and Canada*. Washington, DC: Smithsonian Institution Press.

Li J, Alexander J III, Ward T, Del Tredici P, Nicholson R. 2002. Phylogenetic relationships of Empetraceae inferred from sequences of chloroplast gene *matK* and nuclear ribosomal DNA *ITS* region. *Molecular Phylogenetics and Evolution* 25: 306–315.

Liu ZW, Jolles DD, Zhou J, Peng H, Milne RI. 2014. Multiple origins of circumboreal taxa in *Pyrola* (Ericaceae), a group with a Tertiary relict distribution. *Annals of Botany* 114: 1701–1709.

Löfstrand SD, Schönenberger J. 2015. Molecular phylogenetics and floral evolution in the sarracenioid clade (Actinidiaceae, Roridulaceae and Sarraceniaceae) of Ericales. *Taxon* 64: 1209–1224.

Maddison DR, Maddison WP. 2005. MacClade 4: Analysis of phylogeny and character evolution version 4.08. Available from http://macclade.org.

Mai HD. 2001. The Middle and Upper Miocene floras of the Meuro and Rauno sequences in the Lusatica region: Part II: Dicotyledones. *Palaeontographica Abteilung B* 257: 35–174.

Markos S, Hileman LC, Vasey MC, Parker VT. 1998. Phylogeny of the *Arctostaphylos hookeri* complex based on nrDNA data. *Madroño* 45: 187–199.

Maximowicz CJ. 1859. Primitiae Florae Amurensis: Versuch Einer Flora Des Amurlandes. *Mémoires Presentes a l'Académie Impériale des Sciences de St.-Pétersbourg par Divers Savans et lus dans ses Assemblées* 9: 189.

Maximowicz CJ. 1870. Rhododendreae Asiae Orientalis. *Mémoires de l'Académie Impériale des Sciences de Saint Pétersbourg, Septième Série (Sér. 7)* 16: 47.

Mayden RL. 1997. A hierarchy of species concepts: The denouement in the saga of the species problem. In: Claridge MF, Dawah HA, Wilson MR eds. *Species: The units of biodiversity*. London: Chapman & Hall. 381–424.

Mayr E. 1942. *Systematics and the origin of species from the viewpoint of a zoologist*. Cambridge, Mass.: Harvard University Press.

McGuire AF, Kron KA. 2005. Phylogenetic relationships of European and African *Ericas*. *International Journal of Plant Science* 166: 311–318.

McKenna MC. 1983. Holarctic landmass rearrangement, cosmic events, and Cenozoic terrestrial organisms. *Annals of the Missouri Botanical Garden* 70: 459–489.

Merckx VSFT, Hendriks KP, Beentjes KK, Mennes CB, Becking LE, Peijnenburg KTCA, Afendy A, Arumugam N, de Boer H, Biun A, Buang MM, Chen P, Chung AYC, Dow R, Feijen FAA, Feijen H, Feijen-van Soest C, Geml J, Geurts R, Fravendeel B, Hovenkamp P, Imbun P, Ipor I, Janssens SB, Jocqué M, Kappes H, Khoo E, Koomen P, Lens F, Majapun RJ, Morgado LN, Neupane S, Nieser N, Pereira JT, Rahman H, Sabran S, Sawang A, Schwallier RM, Shim PS, Smit H, Sol N, Spait M, Stech M, Stokvis F, Sugau JB, Suleiman M, Sumail S, Thomas DC, van Tol J, Tuh FYY, Yahya BE, Nais J, Repin R, Lakim M, Schilthuizen M. 2015. Evolution of endemism on a young tropical mountain. *Nature* 524: 347–350.

Meredith RW, Janečka JE, Gatesy J, Ryder OA, Fisher CA, Teeling EC, Goodbla A, Eizirik E, Simão TLL, Stadler T, Rabosky DL, Honeycutt RL, Flynn JJ, Ingram CM, Steiner C, Williams TL, Robinson TJ, Burk-Herrick A, Westerman M, Ayoub NA, Springer MS, Murphy WJ. 2011. Impacts of the Cretaceous Terrestrial Revolution and KPg extinction on mammal diversification. *Science* 334: 521–524.

Metzgar JS. Alverson ER, Chen S, Vaganov AV, Ickert-Bond SM. 2013. Diversification and reticulation in the circumboreal fern genus *Cryptogramma*. *Molecular Phylogenetics and Evolution* 67: 589–599.

Millais JG. 1917. *Rhododendrons: In which is set forth an account of all species of the genus Rhododendron (including azaleas) and the various hybrids*. London: Longmans, Green & Co.

Miller MA, Pfeiffer W, Schwartz T. 2010. Creating the CIPRES Science Gateway for inference of large phylogenetic trees. In: *Proceedings of the Gateway Computer Environments Workshop (GCE)*. New Orleans, LA. 14 Nov. 2010. 1–8.

Milne RI. 2004. Phylogeny and biogeography of *Rhododendron* subsection *Pontica*, a group with a tertiary relict distribution. *Molecular Phylogenetics and Evolution* 33: 389–401.

Milne RI, Abbott RJ. 2002. The origin and evolution of Tertiary relict floras. *Advances in Botanical Research* 38: 281–314.

Milne RI, Davies C, Prickett R, Inns LH, Chamberlain DF. 2010. Phylogeny of *Rhododendron* subgenus *Hymenanthes* based on chloroplast DNA markers: Between-lineage hybridization during adaptive radiation? *Plant Systematics and Evolution* 285: 233–244.

Morrison DA. 2010. Counting chickens before they hatch: Reciprocal consistency of calibration points for estimating divergence dates. *ArXiv e-prints*: 1001.3586.

Murray DF. 1992. Vascular plant diversity in Alaska Arctic tundra. *The Northwest Environmental Journal* 8: 29–52.

Murray DF. 1995. Causes of Arctic plant diversity: Origin and evolution. In: Chapin FS III, Körner C eds. *Arctic and alpine plant biodiversity: Patterns, causes and ecosystem consequences*. Berlin: Springer-Verlag. 21–32.

Murray DF. 1997. Regional and local vascular plant diversity in the Arctic. *Opera Botanica* 132: 9–18.

Murray DF, Kelso S, Yurtsev BA. 1994. Floristic novelites in Beringia: Patterns and questions of their origins. In: Meehan RH, Sergienko V, Weller G eds. *Bridges of science between North America and the Russian Far East*. Proceedings of the 45th Arctic Science Conference, Anchorage, AK , 25–27 August, 1994, Vladivostok, Russia, 29 August–2 September, 1994. American Association for the Advancement of Science, Arctic Division.

Nie ZL, Sun H, Li H, Wen J. 2006. Intercontinental biogeography of subfamily Orontioideae (*Symplocarpus, Lysichiton,* and *Orontium*) of Araceae in eastern Asia and North America. *Molecular Phylogenetics and Evolution* 40: 155–165.

Nixon KC, Crepet WL. 1993. Late Cretaceous fossil flowers of ericalean affinity. *American Journal of Botany* 80: 616–623.

Nordal I, Razzhivin VY eds. 1999. The species concept in the High North – A Panarctic flora initiative. *Det Norske Videnskaps-Akademi. I. Matematisk-Naturvitenskapelig Klasse. Ny Serie 38*: 1–418.

Nylander JAA, Ronquist F, Huelsenbeck JP, Nieves-Aldrey JL. 2004. Bayesian phylogenetic analysis of combined data. *Systematic Biology* 53: 47–67.

Ohwi J. 1965. *Rhododendron*. In: Meyer FG, Walker EH eds. *Flora of Japan*. Washington, D.C.: Smithsonian Institution. 696–702.

Pallas P. 1784. *Rhododendron*. In: Pallas PS ed. *Flora Rossica, Vol I*. Petropoli, E Typographia Imperiali J. J. Weitbrecht. 43–49, plate XXXIII.

Paradis E. 2013. Molecular dating phylogenies by likelihood methods: A comparison of models and a new information criterion. *Molecular Phylogenies and Evolution* 67: 436–444.

Parham JF, Donoghue PCJ, Bell CJ, Calway TD, Head JJ, Holroyd PA, Inoue JG, Irmis RB, Joyce WG, Ksepka DT, Patané JSL, Smith ND, Terver JE, van Tuinen M, Yang Z, Angielscyk KD, Greenwood JM, Hipsley CA, Jacobs L, Makovicky PJ, Müller J, Smith KT, Theodor JM, Warnock RCM, Benton MJ. 2012. Best practices for justifying fossil calibrations. *Systematic Biology* 61: 346–359.

Phillipson WR, Phillipson MN. 1986. A revision of *Rhododendron* III. subgenera *Azaleastrum, Mumeazalea, Candidastrum* and *Therorhodion*. *Notes from the Royal Botanic Garden Edinburgh* 44: 1–23.

Powell EA, Kron KA. 2002. Hawaiian blueberries and their relatives—a phylogenetic analysis of *Vaccinium* sections *Macropelma*, *Myrtillus*, and *Hemimyrtillus* (Ericaceae). *Systematic Botany* 27: 768–779.

Pruett CL, Winker K. 2005. Biological impacts of climate change on a Beringian endemic: Cryptic refugia in the establishment and differentiation of the rock sandpiper (*Calidris ptilocnemis*). *Climate Change* 68: 219–240.

R Core Team. 2015. R: A language and environment for statistical computing. R Foundation for Statistical Computing. Vienna, Austria. Available from www.R-project.org.

Rambaut A. FigTree v1.4.0. Available from http://tree.bio.ed.ac.uk/software/figtree/.

Rhododendron Society, The. 1930. *The species of* Rhododendron. Stevenson JB ed. Edinburgh: T. and A. Constable Ltd.

Ronquist F, Huelsenbeck JP. 2003. MrBayes3: Bayesian phylogenetic inference under mixed models. *Bioinformatics* 19: 1572–1574.

Ronquist F, Teslenko M, van der Mark P, Ayres DL, Darling A, Hohna S, Larget B, Liu L, Suchard MA, Huelsenbeck JP. 2012. MrBayes 3.2: Efficient Bayesian phylogenetic inference and model choice across a large model space. *Systematic Biology* 61: 539–542.

Rose JP, Freudenstein JV. 2014. Cryptic and overlooked: Species delimitation in the mycoheterotrophic *Monotropsis* (Ericaceae: Monotropoideae). *Systematic Botany* 39: 578–593.

Sanmartín I, Enghoff H, Ronquist F. 2001. Patterns of animal dispersal, vicariance and diversification in the Holarctic. *Biological Journal of the Linnean Society* 73: 345–390.

Sarwar AKM, Takahashi H. 2013. Pollen morphology of *Rhododendron* L. and related genera and its taxonomic significance. *Bangladesh Journal of Plant Taxonomy* 20: 185–199.

Sauquet H, Ho SYW, Gandolfo MA, Jordan GJ, Wilf P, Cantrill DJ, Bayly MJ, Bromham L, Brown GK, Carpenter RJ, Lee DM, Murphy DJ, Sniderman JMK, Udovicic F. 2012. Testing the impact of calibration on molecular divergence times using a fossil-rich group: The case of *Nothofagus* (Fagales). *Systematic Biology* 61: 289–313.

Schenk JJ. 2016. Consequences of secondary calibrations on divergence time estimates. *PLoS ONE* 11: e0148228. doi: 10.1271/journal.pone.0148228.

Schenk JJ, Hufford L. 2010. Effects of substitution models on divergence time estimates: Simulations and an empirical study of model uncertainty using Cornales. *Systematic Botany* 35: 578–592.

Schönswetter P, Paun O, Tribsch A, Niklfeld H. 2003. Out of the Alps: Colonization of northern Europe by East Alpine populations of the the glacier buttercup *Ranunculus glacialis*. *Molecular Ecology* 12: 3373–3381.

Schwery O, Onstein RE, Bouchenak-Khelladi Y, Xing Y, Carter RJ, Linder HP. 2015. As old as the mountains: The radiations of the Ericaceae. *New Phytologist* 207: 355–367.

Seithe A. 1960. Die Haarformen der Gattung *Rhododendron* L. und die Möglichkeit ihrer taxonomischen Verwertung. *Botanische Jahrbücher für Systematik, Pflanzengeschichte und Pflanzengegraphie* 79: 297–393.

Shaul S, Graur D. 2002. Playing chicken (*Gallus gallus*): Methodological inconsistencies of molecular divergence date estimates due to secondary calibration points. *Gene* 300: 59–61.

Shishkin BK, Bobrov EG eds. 1967. *Flora of the USSR, vol. XVIII*. Landau N trans. Moscow: USSR Academy of Sciences.

Simpson GG. 1961. *Principles of animal taxonomy*. New York: Columbia University Press.

Small JK. 1914. Ericaceae. In: *North American flora, vol 29, part I*. New York: The New York Botanical Garden. 33–102.

Soininen EM, Valentini A, Coissac E, Miquel C, Gielly L, Brochmann C, Brysting AK, Sostebo JH, Ims RA, Yoccoz NG, Taberlet P. 2009. Analysing diet of small herbivores: The efficiency of DNA barcoding coupled with high-throughput pyrosequencing for deciphering the composition of complex plant mixtures. *Frontiers In Zoology*. doi: 10.1186/1742-9994-6-16.

Stuessy TF. 2009. *Plant taxonomy: The systematic evaluation of comparative data*. New York: Columbia University Press.

Stevens PF. 1969. *Taxonomic studies in the Ericaceae*. Ph.D. Dissertation. University of Edinburgh.

Stevens PF, Luteyn J, Oliver EGH, Bell TL, Brown EA, Crowden RK, George AS, Jordan GJ, Ladd P, Lemson K, Mclean CB, Menadue Y, Pate JS, Stace HM, Weller CM. 2004. Ericaceae. In: Kubiztki K ed. *The families and genera of vascular plants, vol. 6.* Berlin: Springer Verlag. 145–194.

Swofford DL. 2003. PAUP*: *Phylogenetic analysis using parsimony (*and other methods)*, version 4. Sunderland, Mass.: Sinauer Associates.

Taberlet P, Coissa E, Pompanon F, Gielly L, Miquel C, Valentini A, Vermat T, Corthier G, Brochmann C, Willerslev E. 2006. Power and limitations of the chloroplast *trnL* (UAA) intron for plant DNA barcoding. *Nucleic Acids Research* 35: e14.

Taberlet P, Gielly L, Pautou G, Bouvet J. 1991. Universal primers for amplification of three non-coding regions of chloroplast DNA. *Plant Molecular Biology* 17: 1105–1109.

Takahashi H. 1987. Pollen morphology and its taxonomic significance of the Monotropoideae (Ericaceae). *The Botanical Magazine, Tokyo* 100: 385–405.

Takahashi H. 2015. *Plants of the Kuril Islands*. Sapporo: Hokkaido University Press. [In Japanese].

Thiers B. continuously updated. Index Herbariorum: A global directory of public herbaria and associated staff. New York Botanical Garden's Virtual Herbarium [online]. Available from http://sweetgum.nybg.org/science/ih/ [accessed 19 September 2016].

Thorson RM, Hamilton TD. 1986. Glacial geology of the Aleutian Islands. In: Hamilton TD, Reed KM, Thorson RM eds. *Glaciation in Alaska: The geologic record.* The Alaska Geological Society. 171–191.

Tiffney BH. 1985. Perspectives on the origin of the floristic similarity between eastern Asia and eastern North America. *Journal of the Arnold Arboretum* 66: 73–94.

Tiffney BH, Manchester SR. 2001. The use of geological and paleontological evidence in evaluating plant phylogeographic hypotheses in the Northern Hemisphere Tertiary. *International Journal of Plant Sciences* 162: S3–S17.

Tkach NV, Hoffmann MH, Röser M, Korobkov AA, von Hagen KB. 2008. Parallel evolutionary patterns in multiple lineages of Arctic *Artemisia* L. (Asteraceae). *Evolution* 62: 184–198.

Tolmachev AI. 1960. Der autochthone Grundstock der arktischen Flora und ihre Beziehungen zu den Hochgebirgsfloren Nord- und Zentralasiens. *Botanisk Tidsskrıft* 55: 269–276.

Tremblay NO, Schoen DJ. 1999. Molecular phylogeography of *Dryas integrıfolia*: Glacial refugia and postglacial recolonization. *Molecular Ecology* 8: 1187–1198.

Tryon RM, Tryon AF. 1990. Pteridaceae. In: Kramer KU, Green PS eds. *The families and genera of vascular plants, vol. 1, Pteridophytes and Gymnosperms*. Berlin: Springer-Verlag. 230–126.

Vaganov AV, Shmakov AI, Kuznetsov AA, Gureeva II. 2010. Spore morphology of *Cryptogramma* R. Br. ex Richards species (Cryptogrammaceae). *Turcz* 13: 50–58.

Van der Burgh J. 1978. The Pliocene flora of Fortuna-Garsdorf I. fruits and seeds of angiosperms. *Review of Palaeobotany and Palynology* 26: 173–211.

Van der Burgh J. 1987. Miocene floras in the lower Rhenish Basin and their ecological interpretation. *Review of Palaeobotany and Palynology* 52: 299–366.

Viereck LA, Little EL Jr. 2007. *Alaska trees and shrubs*. Fairbanks, AK: University of Alaska Press.

Voroshilov VN. 1982. *Plants of the Soviet Far East*. Moscow: Nauka.

Waltari E, Hoberg EP, Lessa EP, Cook JA. 2007. Eastward ho: Phylogeographical perspectives on colonization of hosts and parasites across the Beringian nexus. *Journal of Biogeography* 34: 561–574.

Weber WA. 1965. Plant geography in the southern Rocky Mountains. In: Wright HE, Frey DG eds. *The Quaternary of the United States*. Princeton: Princeton University Press. 453–468.

Wen J. 1999. Evolution of eastern Asian and eastern North American disjunct distributions in flowering plants. *Annual Review of Ecology, Evolution, and Systematics* 30: 421–455.

Wen J. 2001. Evolution of eastern Asian–eastern North American biogeographic disjunctions: A few additional issues. *International Journal of Plant Sciences* 162: S117–S122.

Wen J, Ickert-Bond S, Nie Z, Li R. 2010. Timing and modes of evolution of eastern Asian–North American biogeographic disjunctions in seed plants. In: Long, M., Gu, H., & Zhou, Z. eds. *Darwin's heritage today: Proceedings of the Darwin 20 Beijing International Conference*. Beijing: Higher Education Press. 252–269.

Wen J, Nie ZL, Ickert-Bond SM. 2016. Intercontinental disjunctions between eastern Asia and western North America in vascular plants highlight the biogeographic importance of the Bering land bridge from late Cretaceous to Neogene. *Journal of Systematics and Evolution* 54: 469–490.

Wheeler QD, Meier R eds. 2000. *Species concepts and phylogenetic theory: A debate*. New York: Columbia University Press.

Xie L, Wagner WL, Ree RH, Berry PE, Wen J. 2009. Molecular phylogeny, divergence time estimates, and historical biogeography of *Circaea* (Onagraceae) in the Northern Hemisphere. *Molecular Phylogenetics and Evolution* 53: 995–1009.

Yurtsev BA, Koroleva TM, Petrovsky VV, Polozova TG, Zhukova PG, Katenin AE eds. 2010. *Checklists of flora of the Chukotkan tundra*. Saint-Petersburg: VVM Ltd Publishing.

Zachos J, Pagani M, Sloan L, Thomas E, Billups K. 2001. Trends, rhythms, and aberrations in global climate 65 ma to present. *Science* 292: 686–693.

Zink RM, Rohwer S, Andreev AV, Dittmann DL. 1995. Trans-Beringian comparisons of mitochondrial DNA differentiation in birds. *The Condor* 97: 639–649.

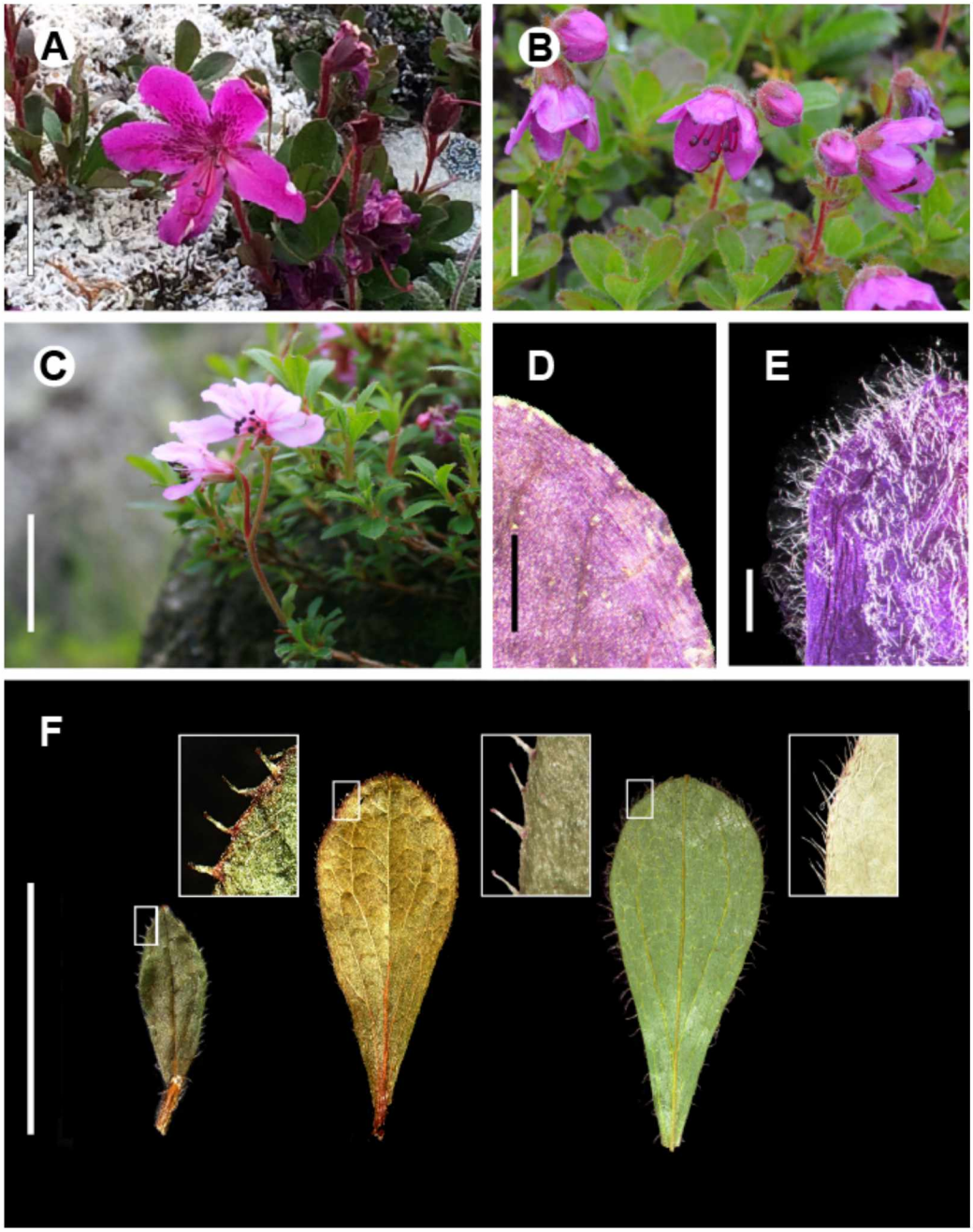

Figure 2.1 Morphological comparison of *Therorhodion*. (A) *T. glandulosum* on the Seward Peninsula, Alaska. (B) *T. camtschaticum* on Unalaska Island. (C) *T. redowskianum* on Mount Paektu, China (photo by Seung Chul Kim). (D and E) Corolla comparison of glabrous *T. glandulosum* (D) and pubescent *T. camtschaticum* (E). (F) Leaf comparison from left to right of *T. redowskianum*, *T. glandulosum*, and *T. camtschaticum.* The insets show the glandular trichomes of *T. redowskianum* and *T. glandulosum* and the non-glandular trichomes of *T. camtschaticum* respectively. Scale bars: A,B,C,F = 2 cm; D,E = 1 mm.

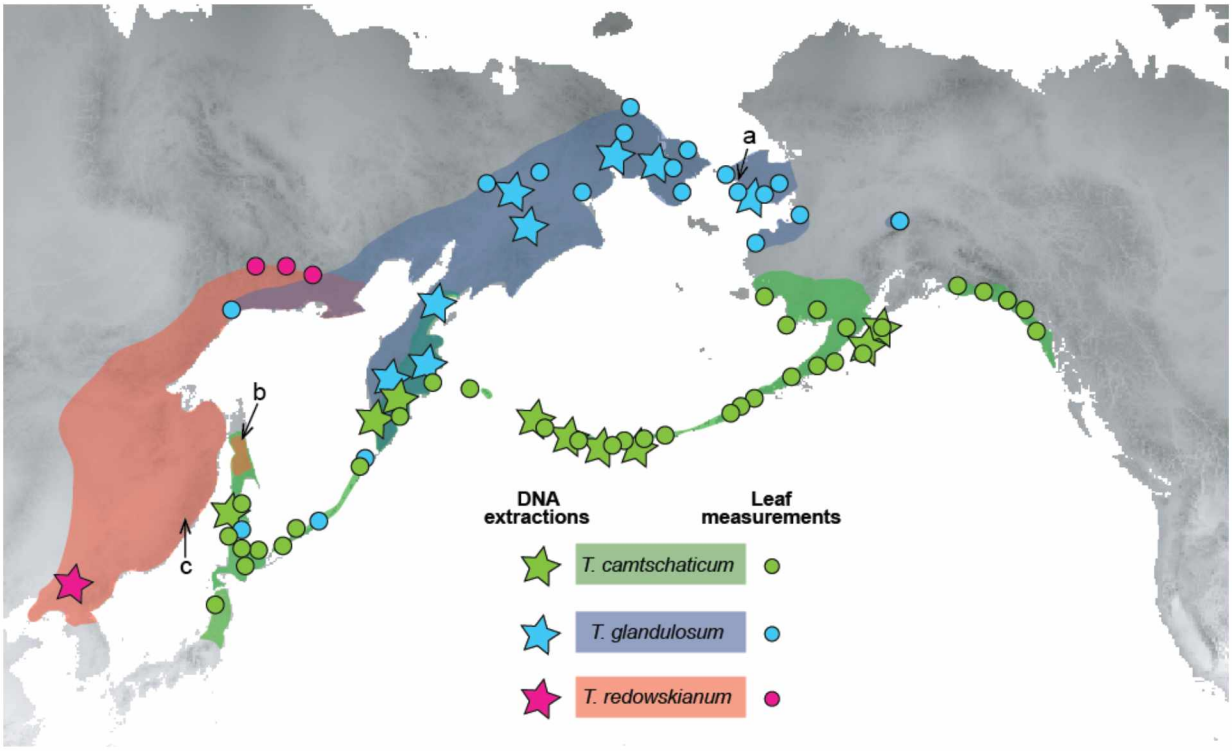

Figure 2.2 Distribution of *Therorhodion* and voucher specimen localities. The Imuruk Basin (a) is indicated on the Seward Peninsula in Alaska, Sakhalin (b) north of Japan, and the Sikhote-Alin mountain range (c) in southeast Russia. Stars indicate collection localities of DNA extractions and circles indicate collection localities of voucher specimens used for leaf measurements.

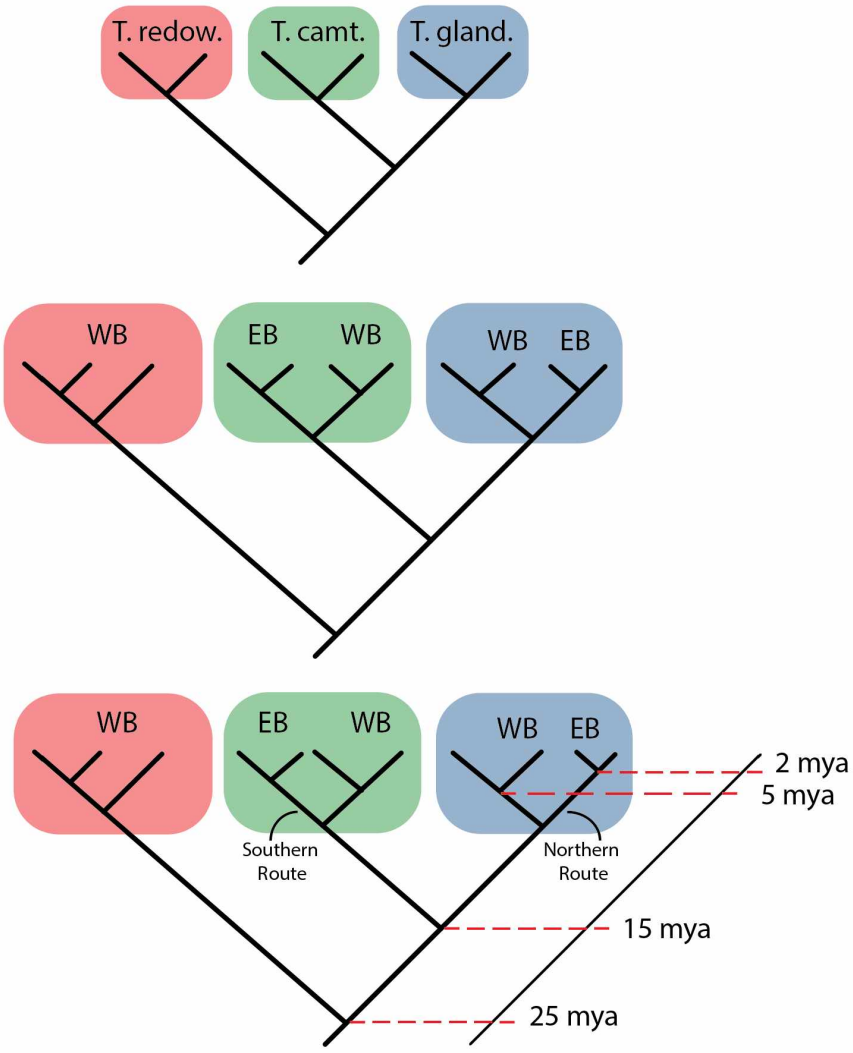

Figure 2.3 Hypothesis testing and topology expectations. A, Hypothesis 1: Three reciprocally monophyletic lineages; B, Hypothesis 2: Two distinct clades of W and E Beringian populations; C, Hypothesis 3: Lineages in eastern Beringia are younger than those in western Beringia. Arrival was via a northern route (Bering Land Bridge) to the Seward Peninsula and a southern route to the Aleutian Islands and southeast Alaska.

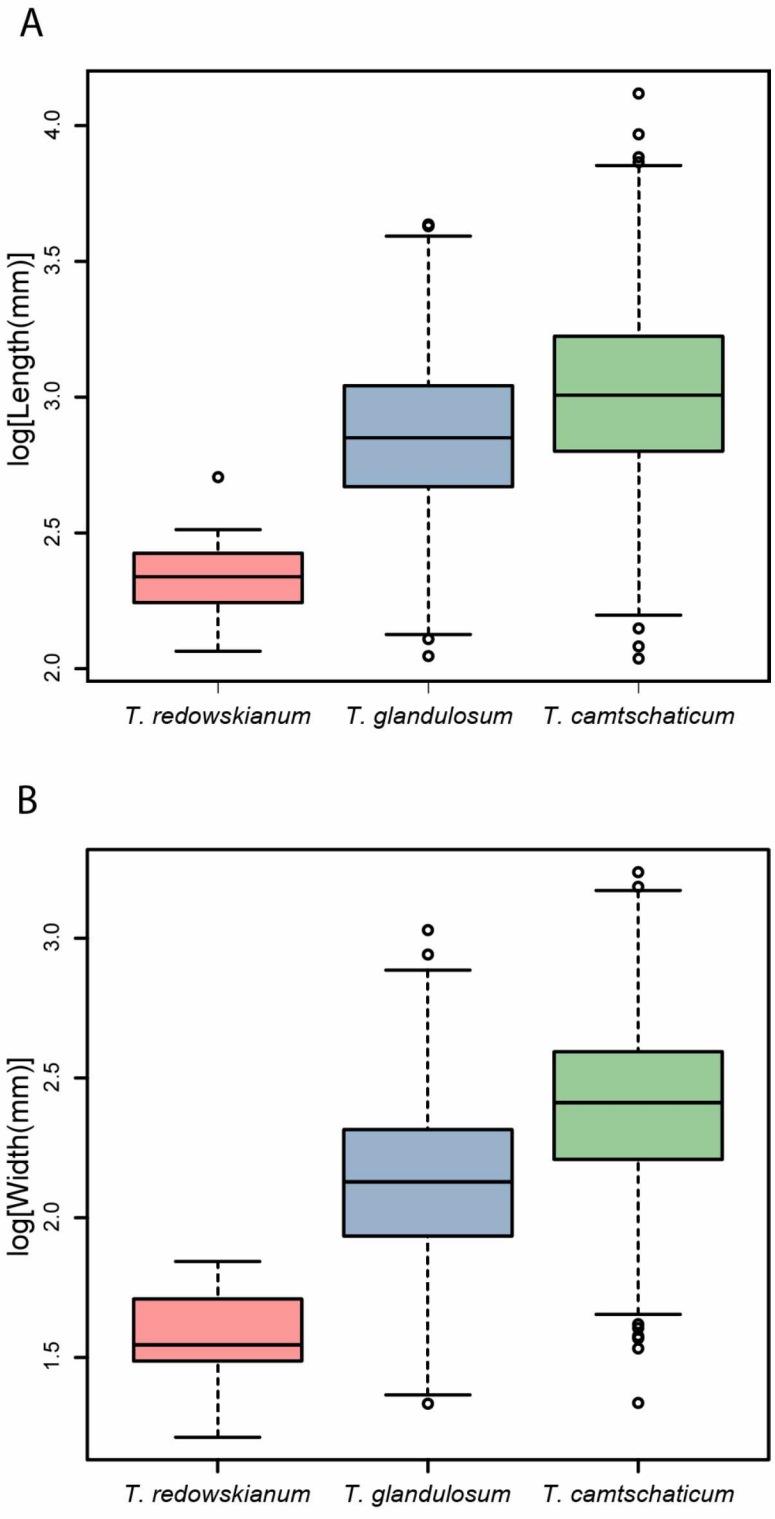

Figure 2.4 Comparison of leaf length (A) and leaf width (B) measurements of *Therorhodion*. Box plots are using log-transformed leaf measurement data.

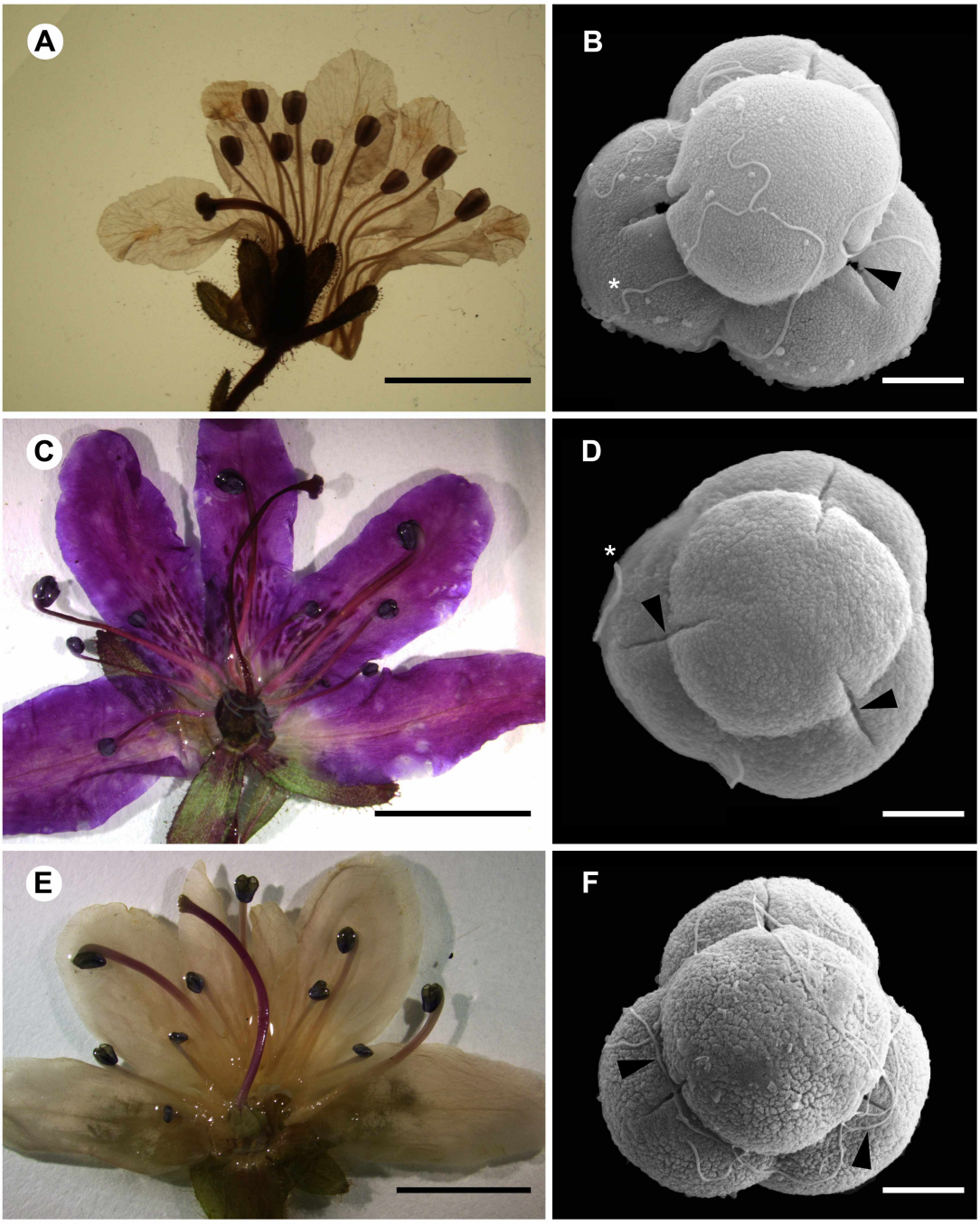

Figure 2.5 Comparison of flower and pollen morphology of *Therorhodion*. (A) *T. redowskianum* flower and (B) tetrahedral tetrad with prominent viscin threads (asterisk) and interradial colpi (arrow). (C) Flower of *T. glandulosum* and (D) *T. glandulosum* tetrahedral tetrad with interradial colpi (arrows) and remnant of viscin threads (asterisk). (E) *T. camtschaticum* flower and (F) tetrahedral tetrad with viscin threads (arrows). Scale bars: A,C,E = 1 cm; B,D,F = 10 μm.

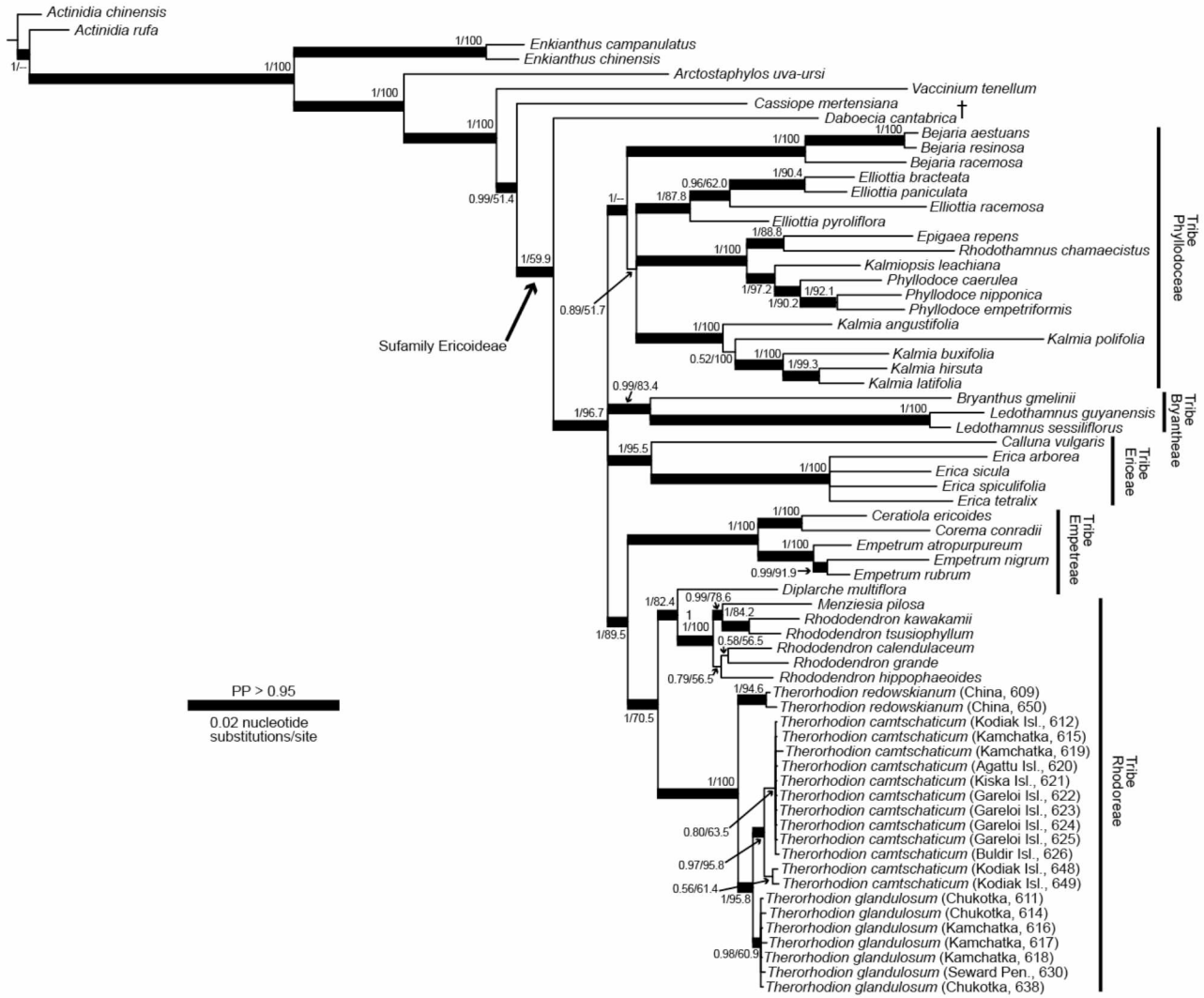

Figure 2.6 Phylogeny based on the sequencing results of the plastid dataset (*ndhF*, *rbcL*, *matK*, and *trnL-F*; 5322 bp). Thickened branches denote posterior probability (PP) of 0.95 and higher and all branches are labeled with PP/MPBS support. † *Daboecia cantabrica* is supported as a sister to subfamily Ericoideae.

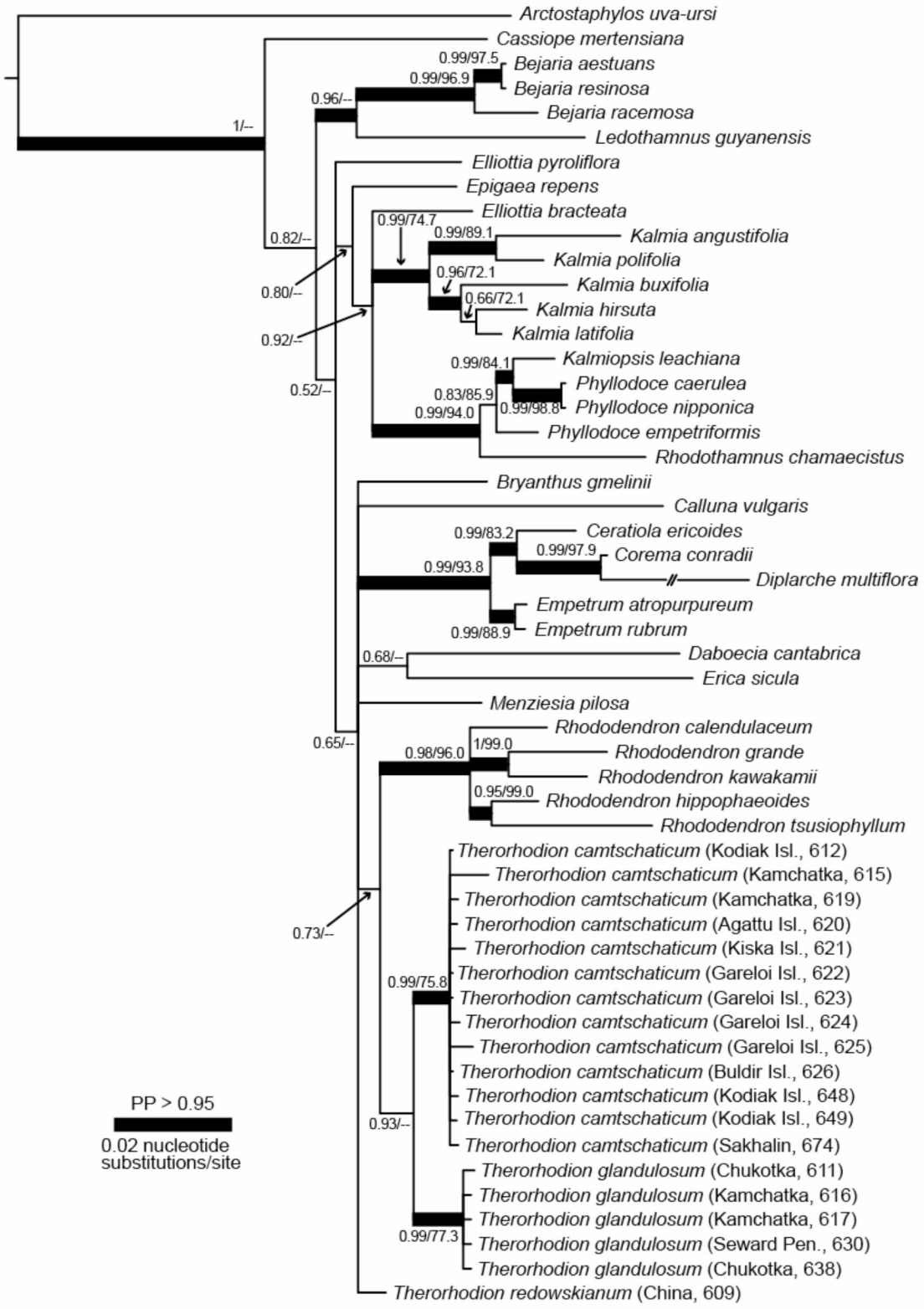

Figure 2.7 Phylogeny based on the sequencing results of the nuclear dataset (*waxy* and *nrITS*; 1383 bp). Thickened branches denote posterior probability (PP) of 0.95 and higher and all branches are labeled with PP/MPBS support.

Figure 2.8 Phylogeny based on sequencing results of the combined plastid and nuclear dataset (6705 bp). The thickest branches show posterior probability (PP) of 0.95 and higher and labels show PP/MPBS support. † *Daboecia cantabrica* is supported as a sister to subfamily Ericoideae. ‡ *Diplarche multiflora* is supported as being in tribe Empetreae.

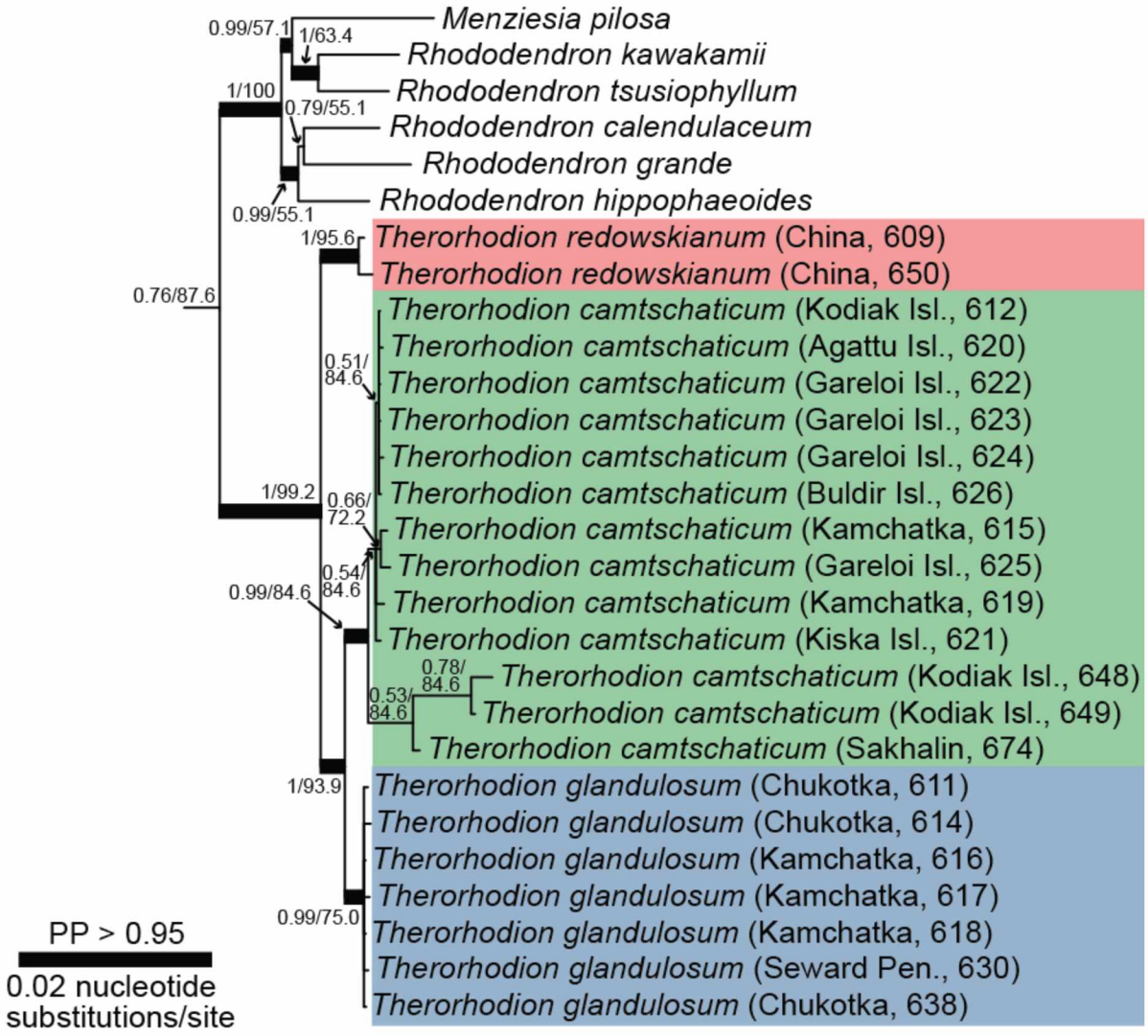

Figure 2.9 Details of tribe Rhodoreae. A close-up of the monophyletic clade containing the genus *Therorhodion* from the Bayesian analysis of the combined plastid and nuclear loci (6705 bp). The thickened branches show posterior probability (PP) of 0.95 probability and higher and node labels show PP/MPBS.

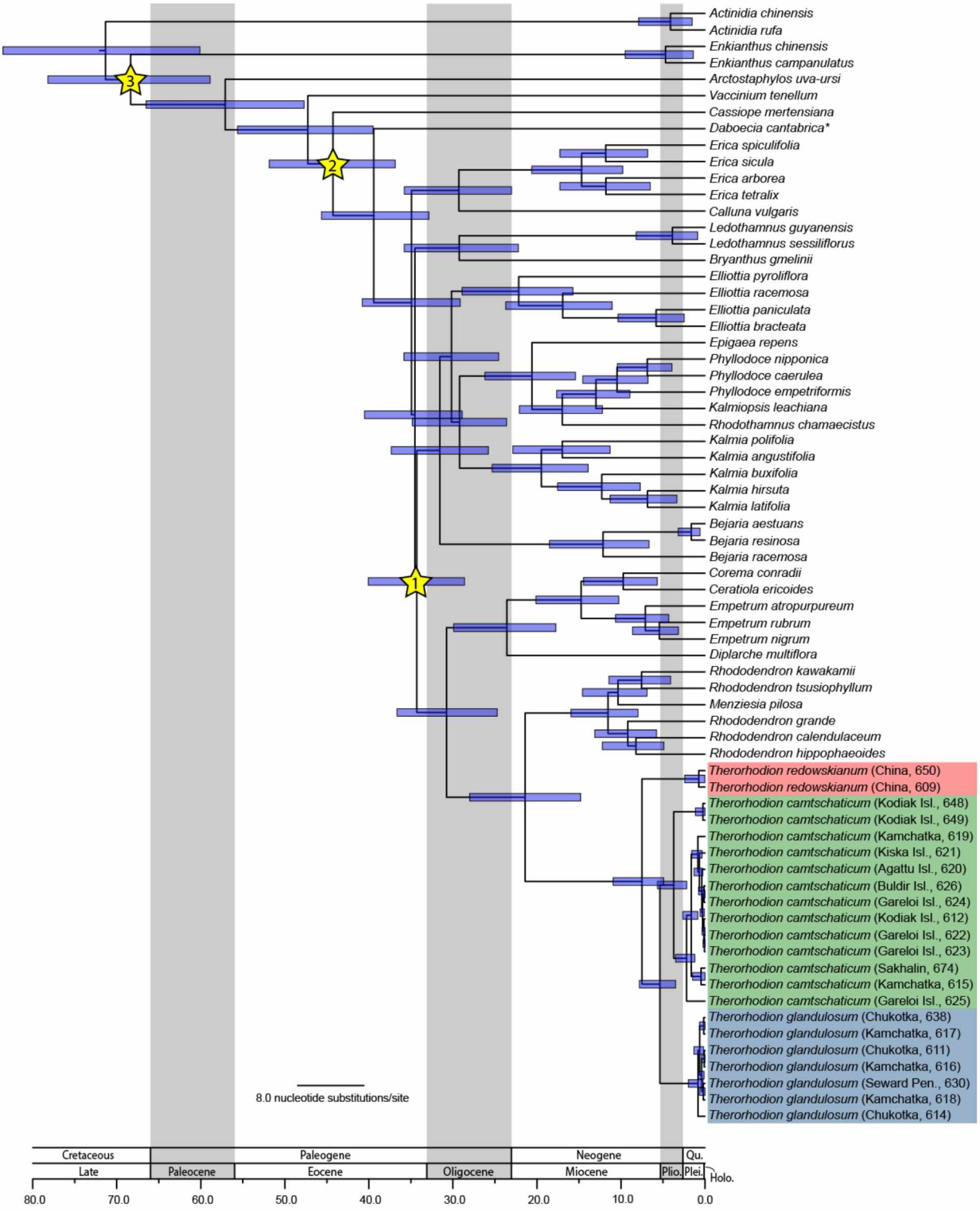

Figure 2.10 Chronogram from analysis I using secondary constraints. Chronogram based on the combined plastid and nuclear DNA matrix (6705 bp) with the secondary constraints numbered: (1) *Phyllodoce nipponica* + *Rhododendron macrophyllum*, (2) *Cassiope mertensiana* + *P. nipponica*/*R. macrophyllum*, (3) *Enkianthus campanulatus* + *C. mertensiana*/*P. nipponica*/*R. macrophyllum*. Gray bars mark every other geologic epoch.

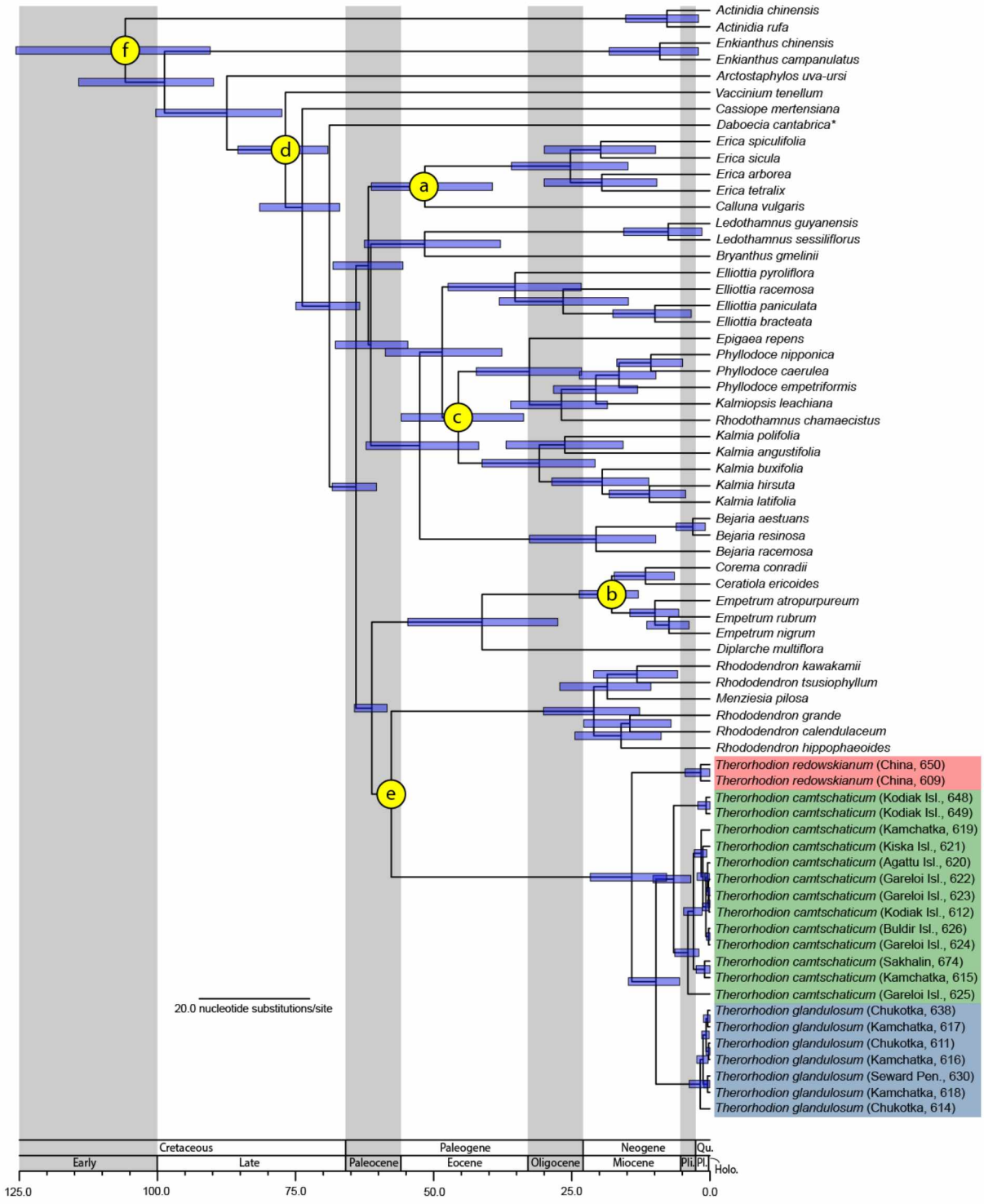

Figure 2.11 Chronogram from analysis II using fossil constraints. A chronogram based on the combined plastid and nuclear DNA matrix (6705 bp) with the fossil constraints lettered: (a) *Calluna vulgaris*, (b) *Empetrum* sp., (c) *Kalmia saxonica*, (d) *Vaccinium creedensis*, (e) *Rhododendron newburyanum*, (f) *Paleoenkianthus sayrevillensis*. Gray bars mark every other geologic epoch.

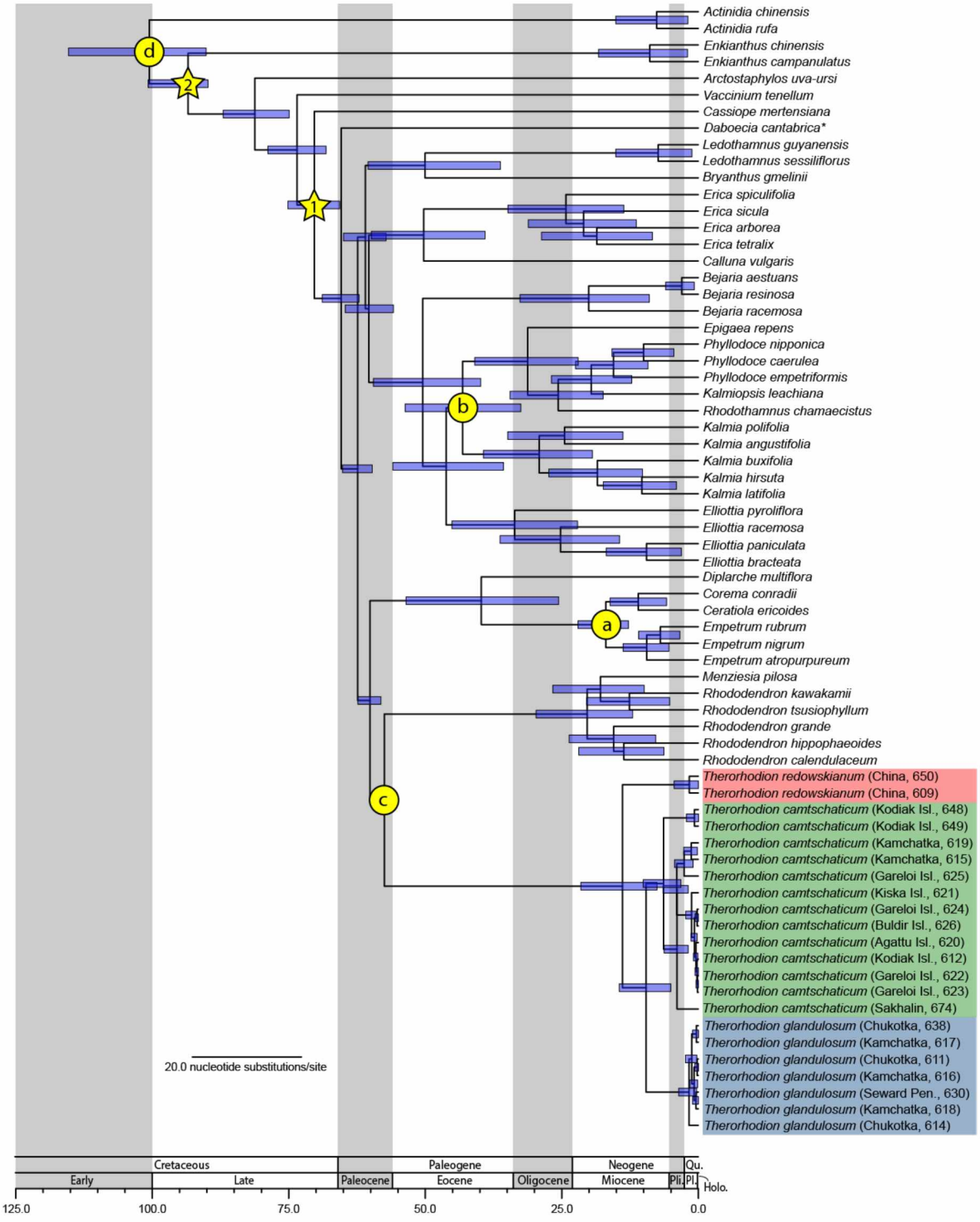

Figure 2.12 Chronogram from analysis III using a combination of secondary and fossil constraints. A chronogram based on the combined plastid and nuclear DNA matrix (6705 bp) with the secondary and fossil constraints numbered and lettered respectively: (1) *Cassiope mertensiana* + *P. nipponica*/*R. macrophyllum*, (2) *Enkianthus campanulatus* + *C. mertensiana*/*P. nipponica*/*R. macrophyllum*; (a) *Empetrum* sp. (b) *Kalmia saxonica*, (c) *Rhododendron newburyanum*, (d) *Paleoenkianthus sayrevillensis*. Gray bars mark every other geologic epoch.

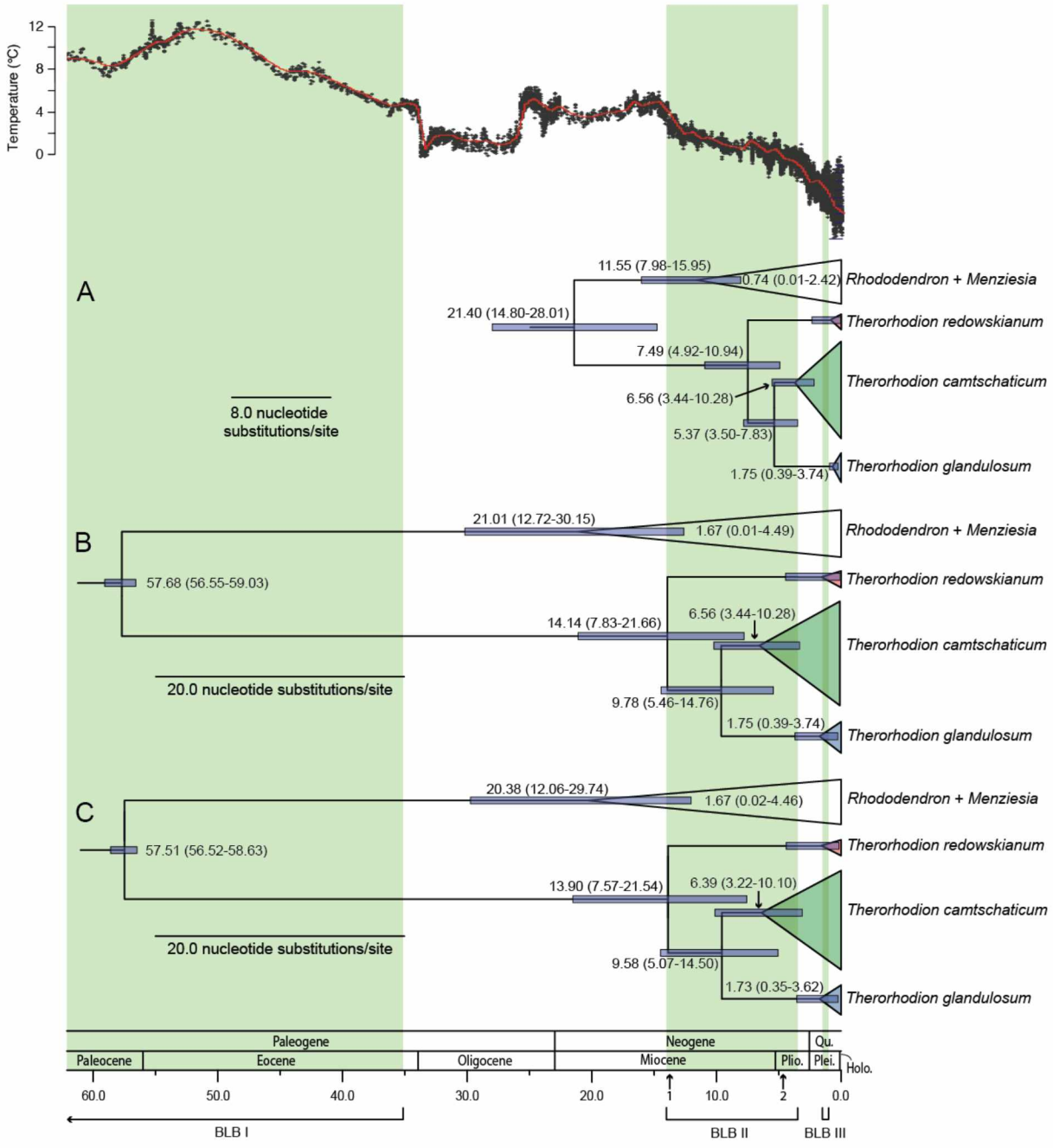

Figure 2.13 A comparison of *Therorhodion* and *Rhododendron* divergence times. A) analysis I; B) analysis II; and C) analysis III. Global temperature change is shown at the top (adapted from Zachos et al., 2001) and the green bars and brackets at the bottom mark the periods that the Bering land bridge (BLB) was available (Sanmartín et al., 2001). Arrows mark important climatological events: 1) persistent sea ice present (Krylov et al., 2008) and 2) first Arctic biomes begin to appear (Hoffmann et al., 2010).

Table 2.1 Taxonomic history of *Therorhodion*. This includes the original classification under *Rhododendron*, with morphological descriptions and geographic distribution.

Taxon	Reference	Distribution
Rhododendron kamtschaticum Pall.†	Pallas, 1784	Russia: on coast of Bering Sea and Sea of Okhotsk, Kamchatka Peninsula.
Rhododendron redowskianum Maxim.	Maximowicz, 1859	Eastern region of Siberia in alpine habitats, around the mountain range Jablonnoi Chrebét.
Rhododendron sect. *Therorhodion* Maxim.	Maximowicz, 1870	In the mountains of northeastern Asia.
		Hab. in Siberia in the east, especially in the mountains.
Rhododendron subgen. *Therorhodion* (Maxim.) Gray	Gray, 1878	Alaska and Aleutian Islands to northern Japan.
Therorhodion Small	Small, 1914	See distribution for *T. camtschaticum* and *T. glandulosum*
Therorhodion camtschaticum (Pall.) Small	Small, 1914	Distributed from Alaska, along the Aleutian Islands, to Japan. The type specimen was collected on the shore of the Sea of Okhotsk.
Therorhodion glandulosum Standl.	Small, 1914	Found at Imuruk Basin on the Seward Peninsula. The type specimen was collected at the foot of the Kigluaik Mountains near Oogluk Bay east of Port Clarence, Alaska.

Table 2.1 continued

Rhododendron kamtschaticum var. *pumilum* Busch	Busch, 1915	Found on Kamchatka and Sakhalin and described as growing in harsher habitats such as rocky tundra and mountain summits up to 64°N.
Rhododendron glandulosum (Standl. ex Small) Millais	Millais, 1917	See distribution for *T. glandulosum*.
Therorhodion redowskianum (Maxim.) Hutch.	Hutchinson, 1921	Manchuria, and cites Komarov (1907) as describing it on Kamchatka extending into Alaska (the distribution of *T. glandulosum* was likely lumped in)
Rhododendron camtschaticum subsp. *glandulosum* (Standl.ex Small) Hultén	Hultén, 1930	In northern and eastern Kamchatka, on the coast of the Sea of Okhotsk down to Ayan, on Chukotka, and northern Alaska.
Therorhodion camtschaticum var. *pumilum* (Busch) T. Yamaz.	Iwatsuki et al., 1993	See distribution for *R. camtschaticum* var. *pumilum.*
† *Rhododendron kamtschaticum* = *R. camtschaticum*		

Table 2.2 Voucher information with sampling localities and GenBank accession numbers. Herbarium acronyms in "Collector/No." field follow Index Herbariorum (Thiers, continuously updated). Vouchers are deposited at ALA unless otherwise indicated. Previous GenBank sequences are based on Albert et al. (1992), Kron & Chase (1993), Kron & King (1996), Kron (1997), Markos et al. (1998), Freudenstein (1999), Albach et al. (2001), Floyd (2002), Kron et al. (2002a), Kron et al. (2002b), Li et al. (2002), Powell & Kron (2002), Gao et al. (2003), Grant et al. (2004), Milne (2004), McGuire & Kron (2005), Fuji & Senni (2006), Ikeda & Setoguchi (2007), Bush & Kron (2008), Soininen et al. (2009), Gillespie & Kron (2010), Milne et al. (2010), Liu et al. (2014), and Löfstrand & Schönenberger (2015).

DNA Ext. No.	Taxon	Locality	Collector/No.	*trnL-F*	*rbcL*	*matK*	*ndhF*	*nrITS*	*waxy*
612	*T. camtschaticum*	USA: Alaska, Kodiak	Studebaker 12-236	MF317922	MF317902	MF317884	MF192859	MF377490	MF377466
615	*T. camtschaticum*	Russia: Kamchatka	Yakubov 9	MF317923	MF317904	MF317885	MF192861	MF377491	MF377467
619	*T. camtschaticum*	Russia: Kamchatka	Strecker 2013_08_02	MF317925	MF317908	MF317889	MF192865	MF377494	—
620	*T. camtschaticum*	US: Alaska, Agattu Island	Kenny & Kaler 026	—	MF317909	MF317890	MF192866	MF377495	MF377468
621	*T. camtschaticum.*	US: Alaska, Kiska Island	Jones Kiska2010ILI-18	MF317926	MF317910	MF317891	MF192867	MF377496	MF377469
622	*T. camtschaticum*	US: Alaska, Gareloi Island	Buxton 3	MF317927	MF317911	MF317892	MF192868	MF377497	MF377470
623	*T. camtschaticum*	US: Alaska, Gareloi Island	Buxton 4	MF317928	MF317912	MF317893	MF192869	MF377498	MF377471

Table 2.2 continued

624	*T. camtschaticum*	US: Alaska, Gareloi Island	Major & Alvey 116	MF317929	MF317913	MF317894	MF192870	MF377499	MF377472
625	*T. camtschaticum*	US: Alaska, Gareloi Island	Major & Alvey 146	—	MF317914	MF317895	MF192871	MF377500	MF377473
626	*T. camtschaticum*	US: Alaska, Buldir Island	Freeman 27	—	—	MF317896	MF192872	MF377501	MF377474
648	*T. camtschaticum*	US: Alaska, Kodiak	Studebaker 2014-028	—	MF317917	MF317898	MF192875	MF377504	—
649	*T. camtschaticum*	US: Alaska, Kodiak	Studebaker 2014-078	—	MF317918	—	MF192876	MF377505	MF377475
674	*T. camtschaticum*	Russia: Sakhalin	Hyosig Won, Bombi Jin, Vitaliy Teslenko 8085	—	—	—	—	MF377506	—
611	*T. glandulosum*	Russia: Chukotka	Ickert-Bond 1949	MF317921	MF317901	MF317883	MF192858	MF377489	MF377465
614	*T. glandulosum*	Russia: Chukotka	Ickert-Bond 1902	—	MF317903	—	MF192860	—	—
616	*T. glandulosum*	Russia: Kamchatka	Yakubov 2	—	MF317905	MF317886	MF192862	MF377492	—

Table 2.2 continued

617	*T. glandulosum*	Russia: Kamchatka	Cherniagina 5	—	MF317906	MF317887	MF192863	MF377493	—
618	*T. glandulosum*	Russia: Kamchatka	Yakubov 8	MF317924	MF317907	MF317888	MF192864	—	—
630	*T. glandulosum*	US: Alaska, Seward Peninsula	Ickert-Bond 1702	—	MF317915	MF317897	MF192873	MF377502	—
638	*T. glandulosum*	Russia: Chukotka	Ickert-Bond 1754	—	MF317916	—	MF192874	MF377503	—
609	*T. redowskianum*	China: Mt. Jang-Baek	Seung-Chul Kim 144	MF317920	MF317900	MF317882	MF192857	MF377488	—
650	*T. redowskianum*	China: Mt. Jang-Baek	Sanhoon Baek, Yon-In BSH38	—	MF317919	MF317899	MF192877	—	—
	Outgroup								
Actinidia chinensis Planch.				—	L01882	U61324	—	—	—
Actinidia rufa Franch. & Sav.				—	KR819570	AF323967	—	—	—
Arctostaphylos uva-ursi (L.) Spreng.			Anderberg 361; S	GQ244594	GU176649	AF440411	AJ236248	AF106811	GU176668

Table 2.2 continued

Bejaria aestuans L.		Luteyn 14175, NY	AF394264	GU176638	GU176669	DQ002362	AF404817	DQ000589
Bejaria racemosa Vent.		Kron 2070, IMS	—	L12600	U61327	DQ002367	U48604	DQ000594
Bejaria resinosa L.f.		Luteyn 14133, NY	—	GU176639	AF440412	DQ002368	GU176622	DQ000595
Bryanthus gmelinii D. Don		Stevens s.n., WFU	—	AF419816	AF440413	GU176715	U48612	GU176650
Calluna vulgaris (L.) Hull		1972–1443, E	GQ244671	AF419827	AF440419	GU176716	GU176623	GU176651
Cassiope mertensiana (Bong.) G. Don		Anderberg 75–83, S	EF409946	L12603	U61346	GU176745	AF419798	DQ000598
Ceratiola ericoides Michx.		Kron 2069, WFU	—	L12605	U61334	GU176717	AF519552	DQ000599
Corema conradii (Torr.) Torr.	US: Mass., cultivated	Stevens s.n., A	—	AF419820	AF440417	GU176718	AF519556	GU176653
Daboecia cantabrica (Huds.) K. Koch		1975–1770, E	—	L12611	U61349	GU176723	AY520786	GU176656
Diplarche multiflora Hook. f. & Thomson	Nepal	Suzuki et al. 8820561, A	—	AF419821	AF440418	GU176739	GU176631	GU176664

Table 2.2 continued

Elliottia bracteata (Maxim.) Benth. & Hook. f.	Chase 866, K	—	U49285	U61339	GU176725	U48609	DQ000600
Elliottia paniculata Benth. & Hook. f.	96D0097 4FRBTU11	—	GU176643	GU176671	—	GU176628	—
Elliottia pyroliflora (Bong.) Brim & P.F. Stevens	1934–009, E	—	GU176644	U61320	GU176726	GU176629	GU176658
Elliottia racemosa Muhl. ex Elliott	1967–2632, E	—	L12615	GU176672	GU176727	U48582	—
Empetrum atropurpureum Fernald & Wiegand	Chase 868, K	—	GU176641	U61355	GU176719	GU176625	DQ000601
Empetrum nigrum L.	Hills 89204, IMS	AY496911	AF419822	GU176670	GU176720	GU176626	—
Empetrum rubrum Vahl ex Willd.	Chase 865, K	—	GU176642	U61342	GU176721	U48613	GU176654
Enkianthus campanulatus G. Nicholson	Anderberg 14528, S	—	L12616	U61344	GU176746	AF133752	—
Epigaea repens L.	Kron 162, WFU	—	U49284	U61319	GU176728	U48611	GU176659
Erica arborea L.	Small s.n., Heather Soc.	—	—	AY517907	—	AY520788	—

Table 2.2 continued

Erica sicula Guss.		Chase 892, K	—	AF41923	U61341	GU176724	AY520804	GU176657
Erica spiculifolia Salisb.		Chase 873, K	—	AF419824	U61337	—	AY520785	—
Erica tetralix L.		Anderberg 195–79, S	—	AF419825	U61340	—	AY520806	—
Kalmia angustifolia L.		Kron 1895, WFU	AB247964	AF419826	U61348	GU176729	U48599	DQ000602
Kalmia buxifolia (Bergius) Gift, Kron & P.F. Stevens	US: South Carolina	Gift et al. s.n., GH	—	L12619	U61347	GU176730	U48581	GU176660
Kalmia hirsuta Walter		Judd s.n., FLAS	—	GU176645	GU176673	GU176731	U48601	GU176661
Kalmia latifolia L.		Kron 2030, WFU	AJ626917	U49294	GU176674	GU176732	U48600	GU176662
Kalmia polifolia Wangenh.		Anderberg 325–89, S	—	U49289	GU183920	GU176733	U48597	GU176663
Kalmiopsis leachiana (L.F. Hend.) Rehder.		Denton s.n.	—	U49290	U61323	GU176734	U48608	DQ000603
Ledothamnus guyanensis Meisn.		Picon & Williams 2910, WFU	—	AF419827	AF440419	GU176716	GU176623	GU176651

Table 2.2 continued

Ledothamnus sessiliflorus N.E. Br.	Clement 2468A, NY	—	GU176640	—	—	GU176624	—
Menziesia pilosa (Michx.) Juss.	Anderberg 1360–65, S	—	U49293	U61351	GU176740	AF393440	GU176665
Phyllodoce caerulea (L.) Bab.	1940–1013, E	GQ245249	AF419829	U61318	GU176735	GU176630	DQ000604
Phyllodoce empetriformis (Sm.) D. Don	Chase 871, K	—	U49291	U61333	GU176736	U48607	DQ000605
Phyllodoce nipponica Makino	Anderberg 1756–77, S	AB210057	U49292	U61325	GU176737	U48606	DQ000606
Rhododendron calendulaceium (Michx.) Torr.	Kron s.n., WFU	—	—	GU176675	GU176741	GU176632	GU176666
Rhododendron grande Wight.	1969–8606, E	EU087385	GU176646	DQ002360	DQ002383	GU176633	EU669886
Rhododendron hippophaeoides Balf. f. & W.W. Sm.	1932–1022, E	—	L01949	U61353	GU176742	GU176634	GU176667
Rhododendron kawakamii Hayata	79/026, RSF	AM296034	—	GU176676	GU176743	GU176635	—

Table 2.2 continued

Rhododendron tsusiophyllum Sugim.	76/353, RSF	AF452217	GU176647	GU176677	GU176744	GU176636	—
Rhodothamnus chamaecistus Rchb.	Chase 877, K	—	U49287	U61321	GU176738	U48605	DQ000607
Vaccinium tenellum Aiton.	Kron & Powell s.n., WFU	AF271699	GU176648	AF382818	AF419769	AF382741	—
RSF = *Rhododendron* Species Foundation							

Table 2.3 Primers and PCR protocols used.

Locus	Primer Name	Sequence (5'–3')	Protocols	Reference(s)
trnL-F	trnLc	TAC GAC GAT CTY TCT AAA CAA GC	94° C, 5:00—35 x (94° C, 1:00—50° C, 1:00—72° C, 2:00)—72° C, 10:00	Taberlet et al., 1991, 2006
	trnLd	GTC GAT AAG CYT GAG CTT GTT TAG		
rbcL	rbcL 1F	ATG TCA CCA CAA ACA GAA ACT AAA GCA AGT	94° C, 5:00—35 x (94° C, 1:00—50° C, 1:00—72° C, 2:00)—72° C, 10:00	Gillespie & Kron, 2010
	rbcL 1367R	CTT TCC AAA TTT CAC AAG CAG CAG		
	rbcL 624F†	GCG TTG GAG AGA YCG TTT CT		
	rbcL 724R†	TCR CAT GTA CCT GCA GTA GC		
matK	matK 710F‡	GTA TCG CAC TAT GTW TCA TTT GA	94° C, 5:00—35 x (94° C, 1:00—50° C, 1:00—72° C, 2:00)—72° C, 10:00	Gillespie & Kron, 2010
	matK 1600R‡	CGT GCT TGC ATT TTT CAT TGC		
	matK 1295F§	CCT CGA TAC CTA ACA TAA TGC		
	matK 1100R§	GCA TTA TGT TAG ATA TCG AGG		

Table 2.3 continued

ndhF	ndhF 1F‡	ATG GAA CAK ACA TAT SAA TAT GC	94° C, 5:00—35 x (94° C, 1:00—50° C, 1:00—72° C, 2:00)—72° C, 10:00	Gillespie & Kron, 2010
	ndhF 1955Ther R‡	AAT ATC CTT GAT CAT GRG AYA G		
	ndhF 1318R§	CGA AAC ATA TAA AAT GCR GTT AAT CC		Gillespie & Kron, 2010
	ndhF 1955Ther§	CTR TCY CATGAT CAA GGA TAT T		
waxy	waxy ex9F	GAT ACC CAA GAG TGG AAY CC	94° C, 5:00—35 x (94° C, 1:00—52° C, 1:00—72° C, 2:00)—72° C, 10:00	Gillespie & Kron, 2010
	waxy ex11R	GTT CCA TAT CGC ATR GCR TG		
nrITS	ITS 5F	GGA AGT AAA AGT CGT AAC AAG G	94° C, 5:00—35 x (94° C, 1:00—52° C, 1:00—72° C, 2:00)—72° C, 10:00	Gillespie & Kron, 2010
	ITS 4R	TCC TCC GCT TAT TGA TAT GC		

† sequencing primers; ‡ primers for first half of *matK* and *ndhF*; § primers for second half of *matK* and *ndhF*

Table 2.4 Average leaf length, width, and L:W ratio among *Therorhodion* species. Standard deviation (SD) is shown in parentheses.

	T. redowskianum (*n*=5)	*T. glandulosum* (*n*=96)	*T. camtschaticum* (*n*=167)
Average length (± SD) (mm)	10.37 (±1.40)	18.03 (±5.07)	21.42 (±6.81)
Average width (± SD) (mm)	4.84 (±0.77)	8.68 (±2.43)	11.52 (±3.28)
L:W ratio ± SD	2.18 (±0.35)	2.14 (±0.51)	1.88 (±1.12)

Table 2.5 Pollen sizes among *Therorhodion* species. Voucher specimens are from the UA Museum of the North herbarium (ALA). The average width of the pollen tetrads with standard deviation (SD) is shown.

	T. redowskianum (*n*=5)	*T. glandulosum* (*n*=5)	*T. camtschaticum* (*n*=5)
Voucher specimen	V173108	V99418	81465
Mean size (± SD) (µm)	40.25 (±1.63)	43.8 (±2.21)	37.02 (±1.26)
n = number of pollen tetrads			

Table 2.6 The constraints used in the divergence time analyses and the priors implemented in BEAUti v1.8.1 (Drummond et al., 2012).

Constraints	Analyses	Age (myr)	Priors	Reference
Phyllodoce nipponica + *Rhododendron macrophyllum*	S: I	23.11–43.5	Normal: mean = 29.3 sd = 6.0	Schenk & Hufford, 2010
Cassiope mertensiana + *P. nipponica*/*R. macrophyllum*	S: I, III	30.99–54.76	Normal: mean = 37.8 sd = 6.0	Schenk & Hufford, 2010
Enkianthus campanulatus + *C. mertensiana*/*P. nipponica*/*R. macrophyllum*	S: I, III	63.88–83.33	Normal: mean = 72.9 sd = 5.6	Schenk & Hufford, 2010
Calluna vulgaris	F: II	2.58	Lognormal: initial value = 2.58 log(mean) = 1.0 log(stdev) = 0.5 offset = 2.58	Van der Burgh, 1978
Empetrum sp.	F: II, III	11.62	Lognormal: initial value = 11.62 log(mean) = 1.0 log(stdev) = 0.5 offset = 11.62	Friis, 1979
Kalmia saxonica	F: II, III	15.97	Lognormal: inital value = 15.97 log(mean) = 1.0 log(stdev) = 0.5 offset = 15.97	Mai, 2001
Vaccinium creedensis	F: II	26.5	Lognormal: initial value = 26.5 log(mean) = 1.0 log(stdev) = 0.5 offset = 26.5	Axelrod, 1987
Rhododendron newburyanum	F: II, III	56	Lognormal: initial value = 56 log(mean) = 1.0 log(stdev) = 0.5 offset = 56	Collinson & Crane, 1978
Paleoenkianthus sayrevillensis	F: II, III	89.8	Lognormal: initial value = 89.8 log(mean) = 1.0 log(stdev) = 1.3 offset = 89.8	Nixon & Crepet, 1993
S = secondary constraint; F = fossil constraint				

Table 2.7 Average pairwise divergence. These are based on uncorrected *p*-values, percentage of parsimony informative characters, and the number of ingroup and outgroup sequences for each locus.

	trnL-F	*rbcL*	*matK*	*ndhF*	*nrITS*	*waxy*
Therorhodion–Ericaceae	0.0504 (0.0491–0.0517)	0.0271 (0.0267–0.0276)	0.0587 (0.0581–0.5940)	0.0759 (0.0750–0.0767)	—	0.0815 (0.0795–0.0835)
Therorhodion–*Rhododendron*	0.0214 (0.0251–0.0319)	0.0214 (0.0105–0.1074)	0.0303 (0.0250–0.0365)	0.0696 (0.0408–0.1163)	0.0421 (0.0339–0.0535)	0.0433 (0.0403–0.0503)
T. camtschaticum–*T. glandulosum*	0.0077 (0.0069–0.0093)	0.0104 (0.0000–0.0996)	0.0073 (0.0063–0.0120)	0.0058 (0.0031–0.1023)	0.0100 (0.0098–0.0119)	0.0356 (0.0309–0.0437)
T. camtschaticum–*T. redowskianum*	0.0091 (0.0091–0.0092)	0.0127 (0.0030–0.0996)	0.0123 (0.0120–0.0141)	0.0012 (0.0000–0.0105)	0.0156 (0.0154–0.1775)	—
T. glandulosum– *T. redowskianum*	0.0077 (0.0069–0.0093)	0.0035 (0.0030–0.0037)	0.0098 (0.0098–0.0098)	0.0031 (0.0031–0.0031)	0.0112 (0.0112–0.0112)	—
PIC	0.15 (94/617 bp)	0.14 (200/1435 bp)	0.18 (321/1803 bp)	0.19 (289/1488 bp)	—	0.27 (177/651 bp)
Ingroup	16	14	16	17	19	11
Outgroup	12	40	42	37	5	31
PIC = parsimony informative characters; bp = base pairs						

Table 2.8 Divergence times of *Therorhodion*. Time is shown in millions of years with the 95% highest posterior density (HPD) inferred for this paper and compared to previously inferred divergence times. Although substitution rates are also considered secondary methods of calibration, the category of secondary in this table strictly refers to secondary divergence times used as constraints.

Analysis	Constraints used	*Therorhodion* from *Rhododendron*	*Therorhodion redowskianum* from *T. camt. & T. gland. clade*	*Therorhodion camtschaticum* from *T. glandulosum*	Within *T. camtschaticum*	Within *T. glandulosum*
Analysis I	secondary	21.40 (14.80–28.01)	7.49 (4.92–10.94)	5.37 (3.50–7.83)	3.73 (2.17–5.65)	0.83 (0.22–1.97)
Analysis II	fossil	57.68 (56.55–59.03)	14.14 (7.83–21.66)	9.78 (5.46–14.76)	6.56 (3.44–10.28)	1.75 (0.39–3.74)
Analysis III	combination sec. & fossil	57.51 (56.52–58.63)	13.90 (7.57–21.54)	9.58 (5.07–14.50)	6.39 (3.22–10.10)	1.73 (0.35–3.62)
Milne, 2004	substitution rate (matK)	approx. 51.5–76.5	—	—	—	—
Liu et al., 2014	fossil	58.33 (56.48–61.2)	—	—	—	—
Merckx et al., 2015	substitution rate (ITS) & secondary	36.25 (26.65–40.50)	11.72 (2.30–19.61)	—	—	—

Chapter 3 General Conclusion

Taxonomy is central to exploring and understanding biodiversity. The science of taxonomy includes the characterizing, classifying, and naming of taxa. Alpha taxonomy, the naming of species, is of central importance in biology (Turrill, 1938). Species are the basic unit of many biological disciplines and the species name provides the link to the knowledge about an organism. Different taxonomic classification systems rely on varying types of data and characteristics that may be continuous or have strictly defined character states (Stuessy, 2009). Recent trends indicate an increasing use of cladistic approaches that rely only on genetic sequences for taxonomic purposes. These studies have been criticized as they can only be interpreted in the context of previous studies that have performed species delimitation using traditional methods such as morphology and ecology (Wheeler, 2004). A wider approach referred to as a *unified species concept* or *integrative taxonomy* combines multiple lines of evidence including geographical distribution, life history, in addition to genetic sequences and the more traditional methods of using morphology (see de Queiroz, 2007; Carstens et al., 2013; Andújar et al., 2014; Huang & Knowles, 2016).

The traditional method of delineating species is to present a hypothesis that outlines an exclusive set of discontinuous morphological traits (Wheeler, 2004). Yet, finding such characters can be difficult in taxa that exhibit morphological variability. Such issues have plagued plant taxonomy in particular, since plants are sessile organisms and as such, plasticity is a natural survival strategy for many plant taxa (Schlichting, 1986; Sultan, 1987). The Arctic-alpine plant genus *Therorhodion* (Maxim.) Small is a good example of morphological variability leading to uncertainty in regards to the taxonomic relationships. In particular, taxonomic concepts between Asian and North American descriptions of *T.*

camtschaticum Small and *T. glandulosum* Standl. ex Small differ in regards to the species or subspecies levels (Viereck & Little, 2007; Kron & Judd, 2009; Yurtsev et al., 2010; Takahashi, 2015).

My study set out to answer how many lineages there are within *Therorhodion* through leaf measurements, comparison of pollen morphology using scanning electron microscopy, and phylogenetic reconstruction using four chloroplast loci (*ndhF*, *rbcL*, *matK*, and *trnL-F*) and two nuclear loci (*waxy* and *nrITS*). I took advantage of nucleotide sequences available in GenBank (Benson et al., 2013) to construct a large data matrix including a large sample of outgroup taxa in order to confirm the position of *Therorhodion* within the heath family (Ericaceae subfamily Ericoideae; Table 1.2). Using these results I also investigated the timeline for the dispersal of *T. camtschaticum* and *T. glandulosum* between western and eastern Beringia using divergence time analysis. Due to the increased awareness of the effects that secondary constraints can have on estimated divergence times (Shaul & Graur, 2002; Morrison, 2010; Schenk, 2016), I compared the divergence times of *Therorhodion* using secondary constraints, fossil constraints, and a combination of these two approaches.

The morphological characteristics I examined are not all effective characters for delineating species. Although the leaves of all three taxa are significantly different in leaf length and leaf width, leaf size can really only effectively be used as a distinguishing characteristic for *T. redowskianum* in the field. Nevertheless, the presence or absence of glandular-tipped hairs on the leaves remains a clear way to delineate *T. camtschaticum* and *T. glandulosum*. Comparison of pollen morphology between the three taxa failed to provide further insight into differentiating any of the *Therorhodion* species. Sarwar & Takahashi

(2013) were also unable to delimit species of *Rhododendron* based on pollen morphology. An additional reproductive character that has been used to distinguish the three species within *Therorhodion* is the length of the style in relation to the stamens (Shishkin & Bobrov, 1967).

DNA barcoding is the use of short genetic sequences that are useful for identifying taxa at the species level (Herbert et al., 2003; Kress et al., 2015) and has been shown to be useful in delineating animals (Saitoh et al., 2014; Wilson et al., 2014; Sikes et al., 2015). The plastid markers *rbcL, matK*, and *trnH-psbA* and the nuclear internal transcriber spacer (ITS) have been shown to have a high rate of success identifying plants to the generic level (>95%), but results for using DNA barcodes at the species level has been variable (~70% to 90%) (see Kress et al., 2009; de Vere et al., 2012; Saarella et al., 2013; Kress et al., 2015). Working on the Canadian Arctic flora, Saarela et al. (2013) were able do characterize more than 95% of the generic diversity using *rbcL* and *matK,* but DNA barcodes were less suitable at the species level (42–55%). When using DNA barcodes at the intraspecific level, Saarela et al. (2013) had very little success (7%) delimiting subspecies.

Through the course of this study I generated 80 new DNA sequences for *Therorhodion* from throughout its geographic range, which are available on GenBank (http://www.ncbi.nlm.nih.gov/genbank/) (Table 1.2). In my phylogenetic analyses I found three strongly supported monophyletic clades within *Therorhodion* representing the three species. Based on the known distribution of *T. redowskianum* being restricted entirely to Asia and the first lineage to diverge in the genus, it seems plausible that the genus originated in Asia. The amphiberingian distribution of *T. camtschaticum* and *T. glandulosum* in northeastern Asia and western North America (Alaska) point toward dispersal across

Beringia to North America (Wen et al., 2016). The asymmetry in dispersal favoring an eastward dispersal from eastern Asia to North America has been documented in many plant taxa as well as animals (Walteri et al., 2004, 2007; Ickert-Bond et al., 2009; Wen et al., 2010, 2016). In contrast, in insects the number of dispersal events going either direction is believed to have been about the same (Sanmartín et al., 2001).

Glaciation events had a strong influence on the frequency of dispersals between eastern Asia and western North America by affecting the local climate and subsequently the types of habitats covering Beringia (Murray, 1992; Sanmartín et al., 2001; Brochmann & Brysting, 2008). My analyses inferred that the Asia-restricted *T. redowskianum* diverged from *T. camtschaticum*/ *T. glandulosum* during the early to middle Miocene, which supports an origin in the mountains of Asia while the climate was cooling. The subsequent divergence between *T. camtschaticum* and *T. glandulosum* (5.07–14.60 mya) took place while the BLB II would have been open and further intraspecific speciation occurred during the BLB III, driven by a cooling climate and a changing landscape that opened new habitats.

Additional analyses and more variable genetic regions are needed to help explain the diversification between *T. camtschaticum* and *T. glandulosum* as well as resolve the intraspecific relationships within each of the constituent taxa and to test the out-of-Asia hypothesis more thoroughly. For example, it is unclear whether there is a difference between the microhabitats occupied by *T. camtschaticum* and *T. glandulosum* that would have driven species divergence. A geographic information system (GIS) analysis using soil data from Alaska and the Russian Far East combined with distribution data could tell us whether or not there is a difference in soil properties throughout the range of *Therorhodion*. Resolving differences in methods for soil categorization between Russia and

North America as well as continued efforts to digitize voucher specimens from the Russian Far East, currently not available, would assist in this approach and shed more light on habitat preferences in *Therorhodion* across Beringia.

Similarly, the genetic loci that I targeted in this study were not variable enough to resolve intraspecific relationships with strong support, so I was unable to determine whether there are distinct western and eastern Beringian subclades in both *T. camtschaticum* and *T. glandulosum*. Targeting more variable loci could provide the required resolution to answer this question; which would allow testing the out-of-Asia hypothesis more thoroughly. The chloroplast DNA loci *psbA-trnH* and *trnT-trnL* have previously been used to resolve relationships at lower taxonomic levels within the Ericaceae (Brown et al., 2006).

Additionally, there are large sampling gaps in many parts of Alaska (Huettmann & Ickert-Bond, in press) that are impeding a better understanding of the state's biodiversity. Specifically, there are very few specimens in the University of Alaska Museum of the North Herbarium database (http://arctos.database.museum/home.cfm) from the area between Denali National Park and Preserve and the Seward Peninsula, including the Nulato Hills, the Kaiyuh Mountains, and the Kuskokwim Mountains (Fig. 2.1). This is of particular relevance for my study as a population of *T. glandulosum* was reported from the Kantishna Hills in Denali National Park and Preserve for the first time in 1987 by the National Park Service (Roland, 2004). This population is a range extension, approximately 500 km east from the main coastal distribution of *T. glandulosum* on the lower Yukon River depicted by Hultén (1968; Roland, 2004; Viereck & Little, 2007). National Park Service botanist Carl Roland has speculated that the crest of the Kantishna Hills have higher precipitation and increased

cloud cover, which provides a habitable landscape for otherwise coastal species like *Primula cuneifolia* Ledeb., *Phyllodoce aleutica* (Spreng.) A.Heller, and *Cassiope lycopodioides* (Pall.) D.Don (Roland, 2004). Predictive niche modeling is used to identify new ecological niches that have similar habitat conditions that a taxon is known to occupy by combining known locality information with environmental data (Heads, 2015) and has been used to identify areas for future surveys of animal and plant populations (Fleishman et al., 2001; Garza-Pérez et al., 2004; Bourg et al., 2005; Pearson et al., 2007). Applying a similar method for *T. glandulosum* could show potential habitat within this largely undersampled region of Alaska (Fig. 2.1), which could also help explain the disjunct population in the Kantishna Hills. These habitats could then be used to guide ground-truthing efforts to locate additional populations of *T. glandulosum.* Results from these additional analyses could shed more light on the diversification within Beringia and expand our knowledge on the floristic exchanges between Asia and North America, and how glacial events might have promoted such exchanges.

References

Andújar C, Arribas P, Ruiz C, Serrano J, Gómez-Zurita J. 2014. Integration of conflict into integrative taxonomy: Fitting hybridization in species delimitation of *Mesocarabus* (Coleoptera: Carabidae). *Molecular Ecology* 23: 4344–4361.

Benson DA, Cavanaugh M, Clark K, Karsch-Mizrachi I, Lipman DJ, Ostell J, Sayers EW. 2013. GenBank. *Nucleic Acids Research* 41: D36–D42.

Bourg NA, McShea WJ, Gill DE. 2005. Putting a cart before the search: Successful habitat prediction for a rare forest herb. *Ecology* 86: 2793–2804.

Brochmann C, Brystin AK. 2008. The Arctic – an evolutoinary freezer? *Plant Ecology and Diversity* 1: 181–195.

Brown GK, Craven LA, Udovicic F, Ladiges PY. 2006. Phylogeny of *Rhododendron* section *Vireya* (Ericaceae) based on two non-coding regions of cpDNA. *Plant Systematics and Evolution* 257: 57–93.

Carstens BC, Pelletier TA, Reid NM, Satler JD. 2013. How to fail at species delimitation. *Molecular Ecology* 22: 4369–4383.

de Queiroz K. 2007. Species concepts and species delimitation. *Systematic Biology* 56: 879–886.

de Vere N, Rich TCG, Ford CR, Trinder SA, Long C, Moore CW, Satterthwaite D, Davies H, Allainguillaume J, Ronca S, Tatarinova T, Garbett H, Walker K, Wilkinson MJ. 2012. DNA barcoding the native flowering plants and conifers of Wales. *PLoS ONE* 7: e37945. doi:10.1371/journal.pone.0037945.

Fleishman E, Nally RM, Fay JP, Murphy DD. 2001. Modeling and predicting species occurrence using broad-scale environmental variables: An example with butterflies of the Great Basin. *Conservation Biology* 15: 1674–1685.

Garza-Pérez JR, Lehmann A, Arias-González JE. 2004. Spatial prediction of coral reef habitats: Integrating ecology with spatial modeling and remote sensing. *Marine Ecology Progress Series* 269: 141–152.

Heads M. 2015. The relationship between biogeography and ecology: Envelopes, models, predictions. *Biological Journal of the Linnean Society* 115: 456–468.

Herbert PDN, Ratnasingham S, de Waard JR. 2003. Barcoding animal life: Cytochrome *c* oxidase subunit 1 divergences among closely related species. *Proceedings of the Royal Society B: Biological Sciences* 270: S96–S99. doi: 10.1098/rsbl.2003.0025.

Huang JP, Knowles LL. 2016. The species versus subspecies conundrum: Quantitative delimitation from integrating multiple data types within a single Bayesian approach in Hercules beetles. *Systematic Biology* 65: 685–699.

Huettmann F, Ickert-Bond SM. In press. Mining museums for conservation: An open access online data example of the Herbarium, University of Alaska Museum of the North within a circumpolar context. *Arctic Science*.

Hultén E. 1968. *Flora of Alaska and neighboring territories: A manual of the vascular plants*. Stanford: Standford University Press.

Ickert-Bond SM, Murray DF, DeChaine E. 2009. Contrasting patterns of plant distribution in Beringia. *Alaska Park Science* 8: 26–32.

Kress WJ, Erickson DL, Jones FA, Swenson NG, Perez R, Sanjur O, Bermingham E. 2009. Plant DNA barcodes and a community phylogeny of a tropical forest dynamics plot in Panama. *PNAS* 106: 18621–18626.

Kress WJ, García-Robledo C, Uriarte M, Erickson DL. 2015. DNA barcodes for ecology, evolution, and conservation. *Trends in Ecology & Evolution* 30: 25–35.

Kron KA, Judd WS. 2009. *Therorhodion*. In: Flora of North America Editorial Committee eds. *Flora of North America north of Mexico.* 20+ vols. New York: Oxford University Press. Vol. 8, 453–543.

Morrison DA. 2010. Counting chickens before they hatch: Reciprocal consistency of calibration points for estimating divergence dates. *ArXiv e-prints*: 1001.3586.

Murray DF. 1992. Vascular plant diversity in Alaskan Arctic tundra. *The Northwest Environmental Journal* 8: 29–52.

Pearson RG, Raxworthy CJ, Nakamura M, Peterson AT. 2007. Predicting species distributions from small numbers of occurrence records: A test case using cryptic geckos in Madagascar. *Journal of Biogeography* 34: 102–117.

Roland CA. 2004. *The vascular plant floristics of Denali National Park and Preserve: A summary, including the results of plant inventory fieldwork 1998–2001*. USDI-NPS. Report CAKN-04-01.

Saarela JM, Sokoloff PC, Gillespie LJ, Consaul LL, Bull RD. 2013. DNA barcoding the Canadian Arctic flora: Core plastid barcodes (*rbcL* + *matK*) for 490 vascular plant species. *PLoS ONE* 8: e77982. doi: 10.1371/journal.pone.0077982.

Saitoh T, Sugita N, Someya S, Iwami Y, Kobayashi S, Kamigaichi H, Higuchi A, Asai S, Yamamoto Y, Nishiumi I. 2014. DNA barcoding reveals 24 distinct lineages as cryptid bird species candidates in and around the Japanese Archipelago. *Molecular Ecology Resources* 15: 177–186.

Sanmartín I, Enghoff H, Ronquist F. 2001. Patterns of animal dispersal, vicariance and diversification in the Holarctic. *Biological Journal of the Linnean Society* 73: 345–390.

Sarwar AKM, Takahashi H. 2013. Pollen morphology of *Rhododendron* L. and related genera and its taxonomic significance. *Bangladesh Journal of Plant Taxonomy* 20: 185–199.

Schenk JJ. 2016. Consequences of secondary calibrations on divergence time estimates. *PLoS ONE* 11: e0148228. doi: 10.1271/journal.pone.0148228.

Schlichting CD. 1986. The evolution of phenotypic plasticity in plants. *Annual Review of Ecology and Systematics* 17: 667–693.

Shaul S, Graur D. 2002. Playing chicken (*Gallus gallus*): Methodological inconsistencies of molecular divergence date estimates due to secondary calibration points. *Gene* 300: 59–61.

Shishkin BK, Bobrov EG eds. 1967. *Flora of the USSR, vol. XVIII*. Landau N trans. Moscow: USSR Academy of Sciences.

Sikes DS, Bowser M, Morton JM, Bickford C, Meierotto S, Hildebrandt K. 2015. Building a DNA barcode library of Alaska's non-marine arthropods. *Genome* 60: 248–259.

Stuessy TF. 2009. *Plant taxonomy: The systematic evaluation of comparative data*. New York: Columbia University Press.

Sultan SE. 1987. Evolutionary implications of phenotypic plasticity in plants. In: Hecht M, Wallace B, Prance GT eds. *Evolutionary biology, vol 21*. New York: Plenum Press. 127–178.

Takahashi H. 2015. *Plants of the Kuril Islands*. Sapporo: Hokkaido University Press. [In Japanese].

Turrill WB. 1938. The expansion of taxonomy with special reference to Spermatophyta. *Biological Reviews* 13: 342–373.

Viereck LA, Little EL Jr. 2007. *Alaska trees and shrubs*. Fairbanks, AK: University of Alaska Press.

Waltari E, Demboski JR, Klein DR, Cook JA. 2004. A molecular perspective on the historical biogeography of the northern high latitudes. *Journal of Mammalogy* 85: 591–600.

Waltari E, Hoberg EP, Lessa EP, Cook JA. 2007. Eastward ho: Phylogeographical perspectives on colonization of hosts and parasites across the Beringian nexus. *Journal of Biogeography* 34: 561–574.

Wen J, Ickert-Bond SM, Nie Z, Li R. 2010. Timing and modes of evolution of eastern Asian–North American biogeographic disjunctions in seed plants. In: Long, M., Gu, H., & Zhou, Z. eds. *Darwin's heritage today: Proceedings of the Darwin 20 Beijing International Conference*. Beijing: Higher Education Press. 252–269.

Wen J, Nie ZL, Ickert-Bond. 2016. Intercontinental disjunctions between eastern Asia and western North America in vascular plants highlight the biogeographic importance of the Bering land bridge from late Cretaceous to Neogene. *Journal of Systematics and Evolution* 54: 469–490.

Wheeler QD. 2004. Taxonomic triage and the poverty of phylogeny. *Philosophical Transactions of the Royal Society B: Biological Sciences* 359: 571–583.

Wilson JJ, Sing KW, Halim MRA, Ramli R, Hashim R, Sofian-Azirun M. 2014. Utility of DNA barcoding for rapid and accurate assessment of bat diversity in Malaysia in the absence of formally described species. *Genetics and Molecular Research* 13: 920–925.

Yurtsev BA, Koroleva TM, Petrovsky VV, Polozova TG, Zhukova PG, Katenin AE eds. 2010. *Checklists of Flora of the Chukotkan Tundra*. Saint-Petersburg: VVM Ltd Publishing.

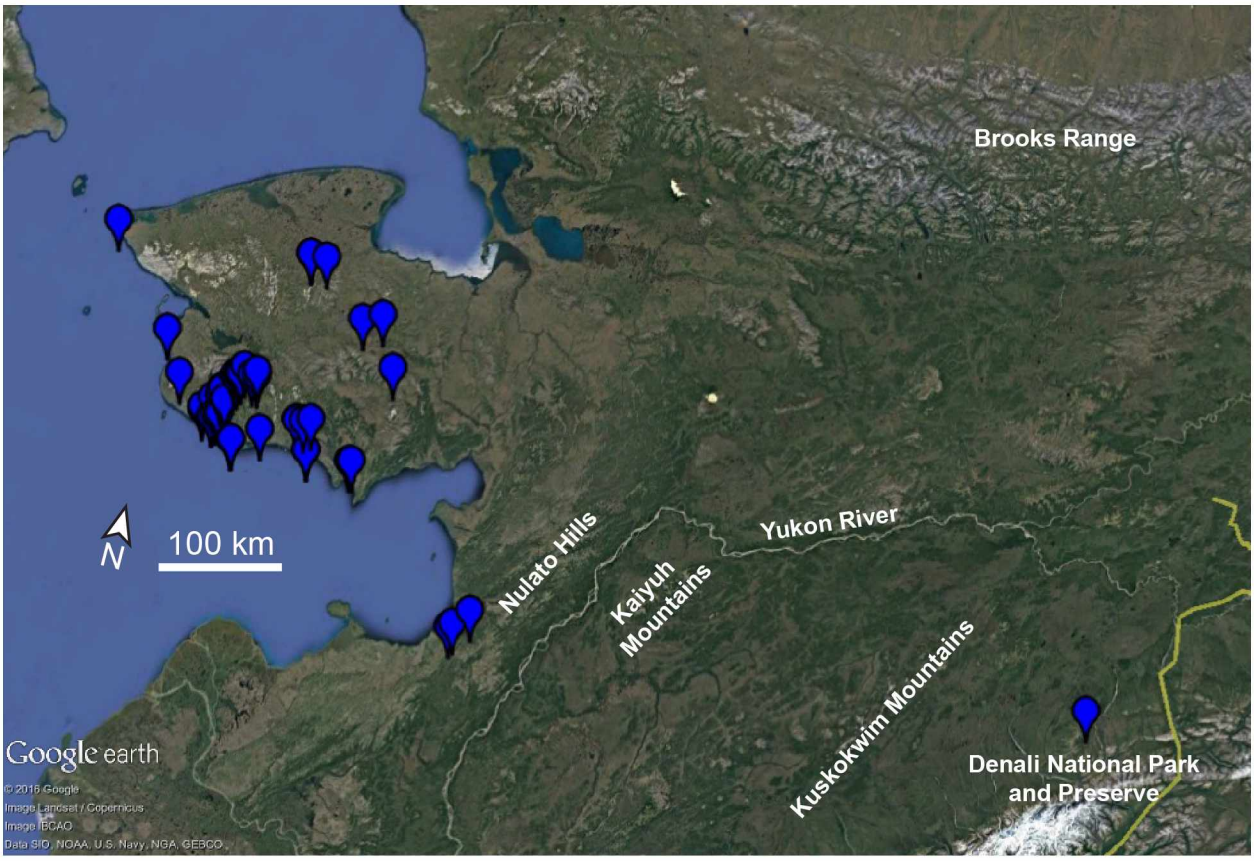

Figure 3.1 Map depicting Alaskan collection localities for *Therorhodion glandulosum* specimens (blue markers). Voucher specimens are housed at the UA Museum of the North, Herbarium (ALA).